CHAPTER III

RESULTS

1. Preliminary Investigation

The characteristics of drug-free transdermal patches prepared from casting solution technique were examined. For choosing the most promising film, their physical appearances were determined. Films were judged subjectively on their degree of flexibility and adhesive ability.

1.1 Drug-free Chitosan and Polyvinyl Derivatives Transdermal Patches Using Various Ratios of Chitosan and Polymer from 1:9 to 9:1

1.1.1 Drug-free Chitosan and Polyvinyl Alcohol Transdermal Patches

The characteristics of films were pale yellow, flexible and easy to be prepared. However there was no adhesive property. Some characteristics of films are shown in Table 8.

Higher amount of chitosan produced yellower film. Moreover, in the high ratio of chitosan caused softer film.

Plasticizers were used to increase the adhesiveness of film. The results indicated that, the variation of types and concentrations of plasticizers did not affect

the adhesiveness of films. However higher concentration of plasticizer tended to produce more flexible film.

The viscosity of the casting solution affected the disappearance of air bubbles. The high concentration of chitosan produced high viscosity solution. Therefore the disappearance of air bubbles was difficult.

1.1.2 Drug-free Chitosan and PVP K-90 Transdermal Patches

The characteristics of films were pale yellow, flexible and easy to be prepared. Films tended to show adhesiveness especially in the high concentration of PVP K-90. Some characteristics of films are shown in Table 9.

The effect of amount of chitosan on the color of film was the same as previously noted. Moreover, the high ratio of chitosan caused stronger film.

Plasticizers were used to increase the adhesiveness of film. The results indicated that, the films tended to show adhesiveness in ratio of chitosan : PVP K-90 1:9 and 2:8 when the concentration of glycerin was higher than 10 %w/w. Moreover, higher concentration of plasticizer tended to produce more flexible film.

The viscosity of the casting solution affected the disappearance of air bubbles. The high concentration of chitosan produced high viscosity solution. Therefore the disappearance of air bubbles was difficult.

Table 8 Some characteristics of drug-free chitosan and polyvinyl alcohol transdermal patches using various ratios of chitosan and polyvinyl alcohol

Formulation	Yellow Color	Glossy	Flexibility	Adhesive	Air Bubble	Easy to Prepare
CA_1	+	-	+	-	-	++
CA_2	+	-	+	-	-	++
CA_3	+	-	+	-	-	++
CA_4	+	-	+	-	-	++
CA_5	+	-	+	-	-	++
CA_6	+	-	+	-	-	++
CA_7	++	-	+	-	-	++
CA_8	++	-	+	-	-	++
CA_9	+++	-	+	-	-	++
CA_{10}	+	+	+	-	-	++
CA_{11}	+	+	+	-	-	++
CA_{12}	+	+	+	-	-	++
CA_{13}	+	+	+	-	-	++
CA_{14}	+	+	+	-	-	++
CA_{15}	+	+	+	-	-	++
CA_{16}	++	+	+	-	-	++
CA_{17}	++	+	+	-	-	++
CA_{18}	+++	+	+	-	-	++
CA_{19}	+	+	++	-	-	++
CA_{20}	+	+	++	-	-	++
CA_{21}	+	+	++	-	-	++
CA_{22}	+	+	++	-	-	++
CA_{23}	+	+	++	-	-	++
CA_{24}	+	+	++	-	-	++
CA_{25}	++	+	++	-	-	++
CA_{26}	++	+	++	-	-	++

The symbols of (+) and (-) showed the appearance and no appearance, respectively. The number of the symbol of (+) showed a degree of the appearance.

Table 8 (cont.) Some characteristics of drug-free chitosan and polyvinyl alcohol transdermal patches using various ratios of chitosan and polyvinyl alcohol

Formulation	Yellow Color	Glossy	Flexibility	Adhesive	Air Bubble	Easy to Prepare
CA_{27}	+++	+	++	-	-	++
CA_{28}	+	+	++	-	-	++
CA_{29}	+	+	++	-	-	++
CA_{30}	+	+	++	-	-	++
CA_{31}	+	+	++	-	-	++
CA_{32}	+	+	++	-	-	++
CA_{33}	+	+	++	-	-	++
CA_{34}	++	+	++	-	-	++
CA_{35}	++	+	++	-	-	++
CA_{36}	+++	+	++	-	-	++
CA_{37}	+	+	++	-	-	++
CA_{38}	+	+	++	-	-	++
CA_{39}	+	+	++	-	-	++
CA_{40}	+	+	++	-	-	++
CA_{41}	+	+	++	-	-	++
CA_{42}	+	+	++	-	-	++
CA_{43}	++	+	++	-	-	++
CA_{44}	++	+	++	-	-	++
CA_{45}	+++	+	++	-	-	++
CA_{46}	+	+	++	-	-	++
CA_{47}	+	+	++	-	-	++
CA_{48}	+	+	++	-	-	++
CA_{49}	+	+	++	-	-	++
CA_{50}	+	+	++	-	-	++
CA_{51}	+	+	++	-	-	++
CA_{52}	++	+	++	-	-	++
CA_{53}	++	+	++	-	-	++
CA_{54}	+++	+	++	-	-	++

Table 9 Some characteristics of drug-free chitosan and PVP K-90 transdermal patches using various ratios of chitosan and PVP K-90

Formulation	Yellow Color	Glossy	Flexibility	Adhesive	Air Bubble	Easy to Prepare
CP_1	+	+	+	-	-	++
CP_2	+	+	+	-	-	++
CP_3	+	+	+	-	-	++
CP_4	+	+	+	-	-	++
CP_5	+	+	+	-	-	++
CP_6	+	+	+	-	-	++
CP_7	++	+	+	-	-	++
CP_8	++	+	+	-	-	++
CP_9	+++	+	+	-	-	++
CP_{10}	+	+	+	-	-	++
CP_{11}	+	+	+	-	-	++
CP_{12}	+	+	+	-	-	++
CP_{13}	+	+	+	-	-	++
CP_{14}	+	+	+	-	-	++
CP_{15}	+	+	+	-	-	++
CP_{16}	++	+	+	-	-	++
CP_{17}	++	+	+	-	-	++
CP_{18}	+++	+	+	-	-	++
CP_{19}	+	+	++	-	-	++
CP_{20}	+	+	++	-	-	++
CP_{21}	+	+	++	-	-	++
CP_{22}	+	+	++	-	-	++
CP_{23}	+	+	++	-	-	++
CP_{24}	+	+	++	-	-	++
CP_{25}	++	+	++	-	-	++
CP_{26}	++	+	++	-	-	++
CP_{27}	+++	+	++	-	-	++
CP_{28}	+	+	++	+	-	++

Table 9 (cont.) Some characteristics of drug-free chitosan and PVP K-90 transdermal patches using various ratios of chitosan and PVP K-90

Formulation	Yellow Color	Glossy	Flexibility	Adhesive	Air Bubble	Easy to Prepare
CP_{29}	+	+	++	+	-	++
CP_{30}	+	+	++	-	-	++
CP_{31}	+	+	++	-	-	++
CP_{32}	+	+	++	-	-	++
CP_{33}	+	+	++	-	-	++
CP_{34}	++	+	++	-	-	++
CP_{35}	++	+	++	-	-	++
CP_{36}	+++	+	++	-	-	++
CP_{37}	+	+	++	+	-	++
CP_{38}	+	+	++	+	-	++
CP_{39}	+	+	++	-	-	++
CP_{40}	+	+	++	-	-	++
CP_{41}	+	+	++	-	-	++
CP_{42}	+	+	++	-	-	++
CP_{43}	++	+	++	-	-	++
CP_{44}	++	+	++	-	-	++
CP_{45}	+++	+	++	-	-	++
CP_{46}	+	+	++	+	-	++
CP_{47}	+	+	++	+	-	++
CP_{48}	+	+	++	-	-	++
CP_{49}	+	+	++	-	-	++
CP_{50}	+	+	++	-	-	++
CP_{51}	+	+	++	-	-	++
CP_{52}	++	+	++	-	-	++
CP_{53}	++	+	++	-	-	++
CP_{54}	+++	+	++	-	-	++

1.2 Drug-free Chitosan and Polyvinyl Derivatives Transdermal Patches Using Various Amounts of Polyvinyl Derivatives from 9 to 20 %w/w

1.2.1 Drug-free Chitosan and Polyvinyl Alcohol Transdermal Patches

The effect of amount of chitosan on the color of film was the same as previously described. Some characteristics of films are presented in Table 10.

The results were notable that stiffer and tougher films were found when increasing the amount of polyvinyl alcohol in the formulation. All films did not show adhesive property. Thus, polyvinyl alcohol was not used for further study.

1.2.2 Drug-free Chitosan and PVP K-90 Transdermal patches

The films were pale yellow, flexible and adhesive. Some characteristics of films are tabulated in Table 11.

Using higher amount of PVP K-90 exhibited air bubbles in the obtained casting solution and did not disappear when left to stand for a long time. Therefore, the amount of PVP K-90 suited for preparing the adhesive film was up to 15 %w/w.

Chitosan was used in a concentrations of 0.5 and 1.0 %w/w. When the concentration of chitosan was fixed at 1.0 %w/w. The results indicated that the viscosities of prepared casting solutions were very high and difficult to prepare for all concentrations of PVP K-90.

Table 10 Some characteristics of drug-free chitosan and polyvinyl alcohol transdermal patches using various amounts of polyvinyl alcohol

Formulation	Yellow Color	Glossy	Flexibility	Adhesive	Air Bubble	Easy to Prepare
FCA_1	+	+	++	-	-	++
FCA_2	+	+	++	-	-	++
FCA_3	+	+	++	-	-	++
FCA_4	+	+	++	-	-	++
FCA_5	+	+	++	-	-	++
FCA_6	+	+	++	-	-	++
FCA_7	+	+	++	-	-	+
FCA_8	+	+	++	-	-	+
FCA_9	+	+	+	-	-	+
FCA_{10}	+	+	+	-	+	+
FCA_{11}	+	+	+	-	+	+
FCA_{12}	+	+	+	-	+	+
FCA_{13}	++	+	+	-	+	+
FCA_{14}	++	+	+	-	+	+
FCA_{15}	++	+	+	-	+	+
FCA_{16}	++	+	+	-	+	+
FCA_{17}	++	+	+	-	+	+
FCA_{18}	++	+	+	-	+	+
FCA_{19}	++	+	+	-	+	+
FCA_{20}	++	+	+	-	+	+
FCA_{21}	++	+	+	-	+	+
FCA_{22}	++	+	+	-	+	+
FCA_{23}	++	+	+	-	++	+
FCA_{24}	++	+	+	-	++	+

Table 11 Some characteristics of drug-free chitosan and PVP K-90 transdermal patches using various amounts of PVP K-90

Formulation	Yellow Color	Glossy	Flexibility	Adhesive	Air Bubble	Easy to Prepare
FCP_1	+	+	++	+	-	++
FCP_2	+	+	++	+	-	++
FCP_3	+	+	++	+	-	++
FCP_4	+	+	++	+	-	++
FCP_5	+	+	++	+	-	++
FCP_6	+	+	++	+	-	++
FCP_7	+	+	++	+	-	+
FCP_8	+	+	++	+	-	+
FCP_9	+	+	+	+	-	+
FCP_{10}	+	+	+	+	+	+
FCP_{11}	+	+	+	+	+	+
FCP_{12}	+	+	+	+	+	+
FCP_{13}	++	+	+	+	+	+
FCP_{14}	++	+	+	+	+	+
FCP_{15}	++	+	+	+	+	+
FCP_{16}	++	+	+	+	+	+
FCP_{17}	++	+	+	+	+	+
FCP_{18}	++	+	+	+	+	+
FCP_{19}	++	+	+	+	+	+
FCP_{20}	++	+	+	+	+	+
FCP_{21}	++	+	+	+	+	+
FCP_{22}	++	+	+	+	+	+
FCP_{23}	++	+	+	+	++	+
FCP_{24}	++	+	+	+	++	+

1.3 Drug-free Chitosan and PVP K-90 Transdermal Patches Using Three Grades of Chitosan

All the transdermal films showed good characteristics. The characteristics of films were pale yellow, glossy, flexible and adhesive. Some characteristics of films are presented in Table 12.

Three grades, different in molecular weight, of chitosan were used in this experiment. The viscosity of prepared chitosan and PVP K-90 casting solution at the same concentration of chitosan using SEACURE 343 was higher than SEACURE 243 and SEACURE 143 respectively. Moreover, increasing the amounts of chitosan and PVP K-90 increased the viscosities of the casting solutions. It could be seen that the molecular weight of chitosan and the amounts of chitosan and PVP K-90 affected the viscosities of prepared chitosan and PVP K-90 casting solutions.

2. Evaluation of Physicochemical Properties of Terbutaline Sulfate Transdermal Patches

2.1 Characteristic of Films

When terbutaline sulfate was incorporated into the films, the obtained casting mixtures were more viscous and turbid. Some characteristics of terbutaline sulfate transdermal patches are shown in Table 13.

The amount of plasticizer affected the adhesiveness of the film. When glycerin was used in a concentration of 5 %w/w it was found that the films did not show improved adhesiveness.

Table 12 Some characteristics of drug-free chitosan and PVP K-90 transdermal patches using three grades of chitosan

Formulation	Yellow Color	Glossy	Flexibility	Adhesive	Air Bubble	Easy to Prepare
VCP_1	+	+	++	+	-	+++
VCP_2	+	+	++	+	-	+++
VCP_3	+	+	++	+	-	++
VCP_4	++	+	++	+	-	++
VCP_5	+	+	++	+	-	+++
VCP_6	+	+	++	+	-	+++
VCP_7	+	+	++	+	-	++
VCP_8	++	+	++	+	-	++
VCP_9	+	+	++	+	-	+++
VCP_{10}	+	+	++	+	-	+++
VCP_{11}	+	+	++	+	-	++
VCP_{12}	++	+	++	+	-	++
VCP_{13}	+	+	++	+	-	+++
VCP_{14}	+	+	++	+	-	+++
VCP_{15}	+	+	++	+	-	++
VCP_{16}	++	+	++	+	-	++
VCP_{17}	+	+	++	+	-	+++
VCP_{18}	+	+	++	+	-	+++
VCP_{19}	+	+	++	+	-	++
VCP_{20}	++	+	++	+	-	++
VCP_{21}	+	+	++	+	-	+++
VCP_{22}	+	+	++	+	-	+++
VCP_{23}	+	+	++	+	-	++
VCP_{24}	++	+	++	+	-	++

Table 13 Some characteristics of terbutaline sulfate transdermal patches

Formulation	Yellow Color	Glossy	Flexibility	Adhesive	Air Bubble	Easy to Prepare
A_1	+	+	+	+	-	++
A_2	+	+	+	+	-	++
A_3	+	+	+	+	-	+
A_4	++	+	+	+	-	+
A_5	+	+	+	-	-	++
A_6	+	+	+	-	-	++
A_7	+	+	+	-	-	+
A_8	++	+	+	-	-	+
B_1	+	+	+	+	-	++
B_2	+	+	+	+	-	++
B_3	+	+	+	+	-	+
B_4	++	+	+	+	-	+
B_5	+	+	+	-	-	++
B_6	+	+	+	-	-	++
B_7	+	+	+	-	-	+
B_8	++	+	+	-	-	+
C_1	+	+	+	+	-	++
C_2	+	+	+	+	-	++
C_3	+	+	+	+	-	+
C_4	++	+	+	+	-	+
C_5	+	+	+	-	-	++
C_6	+	+	+	-	-	++
C_7	+	+	+	-	-	+
C_8	++	+	+	-	-	+
AA_1	+	+	+	+	-	++
AA_2	+	+	+	+	-	++

Table 13 (cont.) Some characteristics of terbutaline sulfate transdermal patches

Formulation	Yellow Color	Glossy	Flexibility	Adhesive	Air Bubble	Easy to Prepare
AA_3	+	+	+	+	-	+
AA_4	++	+	+	+	-	+
BB_1	+	+	+	+	-	+
BB_2	+	+	+	+	-	+
BB_3	+	+	+	+	-	+
BB_4	++	+	+	+	-	+
CC_1	+	+	+	+	-	+
CC_2	+	+	+	+	-	+
CC_3	+	+	+	+	-	+
CC_4	++	+	+	+	-	+

2.2 Thickness

The mean thickness of terbutaline sulfate transdermal patches (including backing material) is presented in Table 14.

In each formulation the amount of the casting mixture which was poured into the petri dish was the same. So, the thickness of films prepared from higher concentration of chitosan and PVP K-90 was higher than that of films prepared from lower concentration of chitosan and PVP K-90. It was found that the standard deviation of the mean thickness was high when the viscosity of casting mixture increased. The results indicated that the thickness of terbutaline sulfate transdermal patches varied from 210 to 270 μm.

Table 14 Mean thickness of terbutaline sulfate transdermal patches

Formulation	Mean thickness (μm) ± SD		
	Sample 1	Sample 2	Sample 3
A_1	207 ± 2.74	208 ± 4.47	208 ± 4.47
A_2	220 ± 3.54	219 ± 2.24	216 ± 4.18
A_3	214 ± 5.48	218 ± 2.74	219 ± 5.48
A_4	229 ± 4.18	227 ± 4.47	227 ± 9.75
B_1	210 ± 3.54	213 ± 4.47	208 ± 5.70
B_2	212 ± 2.74	207 ± 6.71	210 ± 6.12
B_3	229 ± 8.94	230 ± 10.00	228 ± 10.95
B_4	229 ± 7.42	230 ± 6.12	229 ± 5.48
C_1	225 ± 5.48	225 ± 5.00	226 ± 4.18
C_2	231 ± 4.18	225 ± 5.00	225 ± 5.00
C_3	240 ± 7.07	241 ± 5.48	234 ± 5.48
C_4	238 ± 7.58	241 ± 6.52	246 ± 6.52
AA_1	246 ± 5.47	247 ± 4.47	253 ± 4.47
AA_2	248 ± 8.37	257 ± 4.47	246 ± 5.47
AA_3	247 ± 4.47	245 ± 5.00	248 ± 8.37
AA_4	256 ± 8.94	248 ± 8.37	253 ± 8.37
BB_1	265 ± 5.00	259 ± 7.42	264 ± 5.48
BB_2	264 ± 8.94	264 ± 8.37	258 ± 5.48
BB_3	265 ± 5.00	258 ± 8.37	265 ± 7.07
BB_4	267 ± 4.47	263 ± 9.75	261 ± 7.42
CC_1	240 ± 3.54	246 ± 4.18	244 ± 5.48
CC_2	252 ± 4.47	258 ± 4.47	261 ± 2.24
CC_3	269 ± 5.48	268 ± 4.47	265 ± 7.07
CC_4	267 ± 5.16	263 ± 8.37	268 ± 5.70

2.3 Moisture Absorption/Loss

Selected terbutaline sulfate transdermal patches which showed good characteristics; glossy, flexible, easy to prepare and adhesive were further studied. After exposed to the low relative humidities of 0 and 20 %RH, these films loosed moisture. After exposed to higher relative humidities at 52 and 93 %RH, it was found that those films absorbed moisture from the environment. The results of moisture absorption/loss are shown in Tables 15 and 16 and Figures 12-19.

After stored at 0 %RH for one week. The results indicated that, an increased in chitosan concentration from 0.1 to 0.7 %w/w clearly increased the moisture loss of film. The effect of molecular weight of chitosan on the moisture loss of film was examined. It was found that the films prepared using different molecular weights of chitosan and 15 % w/w PVP K-90 could be arranged in the following increasing order according to their moisture loss; SEACURE 243 < SEACURE 143 < SEACURE 343 respectively. When stored for four weeks, the results were the same as stored for one week but decreased the moisture loss of films.

When exposed to 20 %RH, the moisture loss of films was lower than that of films stored at 0 %RH. The effects of concentration and molecular weight of chitosan on the moisture loss of film were the same as previously noted. Increasing PVP K-90 concentration affected the moisture loss of films. The results indicated that the moisture loss of films increased when increased PVP K-90 concentration. The pattern of moisture loss of films stored for four weeks was not apparently different from that of films stored for one week but decreasing percent moisture loss.

The results when stored at 52 %RH for one week indicated that, the moisture absorption of films decreased when chitosan concentration increased. It was found that the films prepared using different molecular weights of chitosan could be arranged in the following increasing order according to their moisture absorption; SEACURE 343 < SEACURE 143 < SEACURE 243 respectively. Increasing PVP K-90 concentration affected the moisture absorption of films. The moisture absorption of prepared films decreased when PVP K-90 concentration increased. The pattern of moisture absorption of films stored for four weeks was not apparently different from that of films stored for one week but increasing percent moisture absorption.

When exposed to 93 %RH for one week, those films extremely absorbed moisture. The effect of chitosan concentration on the moisture absorption of film was the same as previously described. It was found that films prepared using different molecular weights of chitosan could be arranged in the following increasing order according to their moisture absorption; SEACURE 343 < SEACURE 143 < SEACURE 243 respectively. In addition, it could be seen that moisture absorption slightly decreased when increased PVP K-90 concentration. When stored for four weeks, films absorbed higher moisture content. The obtained films prepared using chitosan in a concentration of 0.1 %w/w (formulations A_1, B_1, C_1 and AA_1) seemed to be soft and viscous liquid when stored for four weeks. Thus, percent moisture absorption of these formulations could not be examined.

2.4 Mechanical Properties

The mechanical properties of terbutaline sulfate transdermal patches were examined by measuring the ultimate tensile strength and percent elongation at break.

Table 15 Percent moisture absorption/loss of terbutaline sulfate transdermal patches stored at various relative humidities for 1 week (n=3)

Formulation	%moisture loss ± SD		%moisture absorption ± SD	
	0 %RH	20 %RH	52 %RH	93 %RH
A_1	0.86 ± 0.10	0.42 ± 0.33	5.06 ± 0.64	44.55 ± 2.76
A_2	1.05 ± 0.54	0.86 ± 0.70	3.37 ± 0.78	42.05 ± 1.68
A_3	1.28 ± 0.12	0.94 ± 1.13	2.28 ± 0.23	36.66 ± 0.46
A_4	1.99 ± 0.76	1.95 ± 0.04	1.97 ± 1.57	28.70 ± 5.15
B_1	0.90 ± 0.35	0.84 ± 0.52	7.77 ± 0.26	56.93 ± 2.84
B_2	0.94 ± 0.28	0.87 ± 0.39	6.92 ± 1.26	51.04 ± 3.58
B_3	2.90 ± 0.52	1.23 ± 1.01	4.48 ± 1.32	42.98 ± 2.01
B_4	4.46 ± 0.49	3.62 ± 2.26	2.72 ± 1.29	39.22 ± 5.91
C_1	5.62 ± 0.46	3.24 ± 0.82	3.32 ± 1.01	44.48 ± 2.00
C_2	6.03 ± 0.17	3.30 ± 0.92	3.32 ± 0.75	41.93 ± 2.14
C_3	6.41 ± 0.27	3.98 ± 0.28	2.16 ± 0.88	36.59 ± 1.46
C_4	6.76 ± 0.42	6.17 ± 0.54	1.01 ± 0.26	25.21 ± 1.90
AA_1	1.26 ± 0.35	1.04 ± 0.82	5.00 ± 0.92	42.96 ± 0.57
AA_2	4.86 ± 0.40	2.86 ± 1.31	2.97 ± 0.84	40.70 ± 1.25
AA_3	5.32 ± 0.32	3.26 ± 0.42	2.15 ± 0.25	34.46 ± 1.89
AA_4	5.81 ± 0.46	4.26 ± 0.67	1.58 ± 0.16	28.11 ± 1.11
BB_1	3.94 ± 0.21	1.50 ± 0.77	6.90 ± 1.27	47.53 ± 1.39
BB_2	4.06 ± 1.16	2.82 ± 0.17	6.32 ± 0.46	40.51 ± 0.60
BB_3	4.22 ± 0.12	3.54 ± 0.52	4.47 ± 0.04	37.81 ± 3.34
BB_4	4.76 ± 0.08	4.76 ± 0.95	2.59 ± 0.60	32.29 ± 6.17
CC_1	8.49 ± 0.61	5.95 ± 0.10	3.28 ± 0.73	41.78 ± 2.34
CC_2	8.74 ± 0.57	6.68 ± 0.46	3.17 ± 0.58	39.99 ± 0.15
CC_3	9.25 ± 0.19	6.87 ± 0.43	2.07 ± 0.29	34.84 ± 2.63
CC_4	11.09 ± 1.02	8.82 ± 1.03	0.99 ± 0.03	25.66 ± 0.77

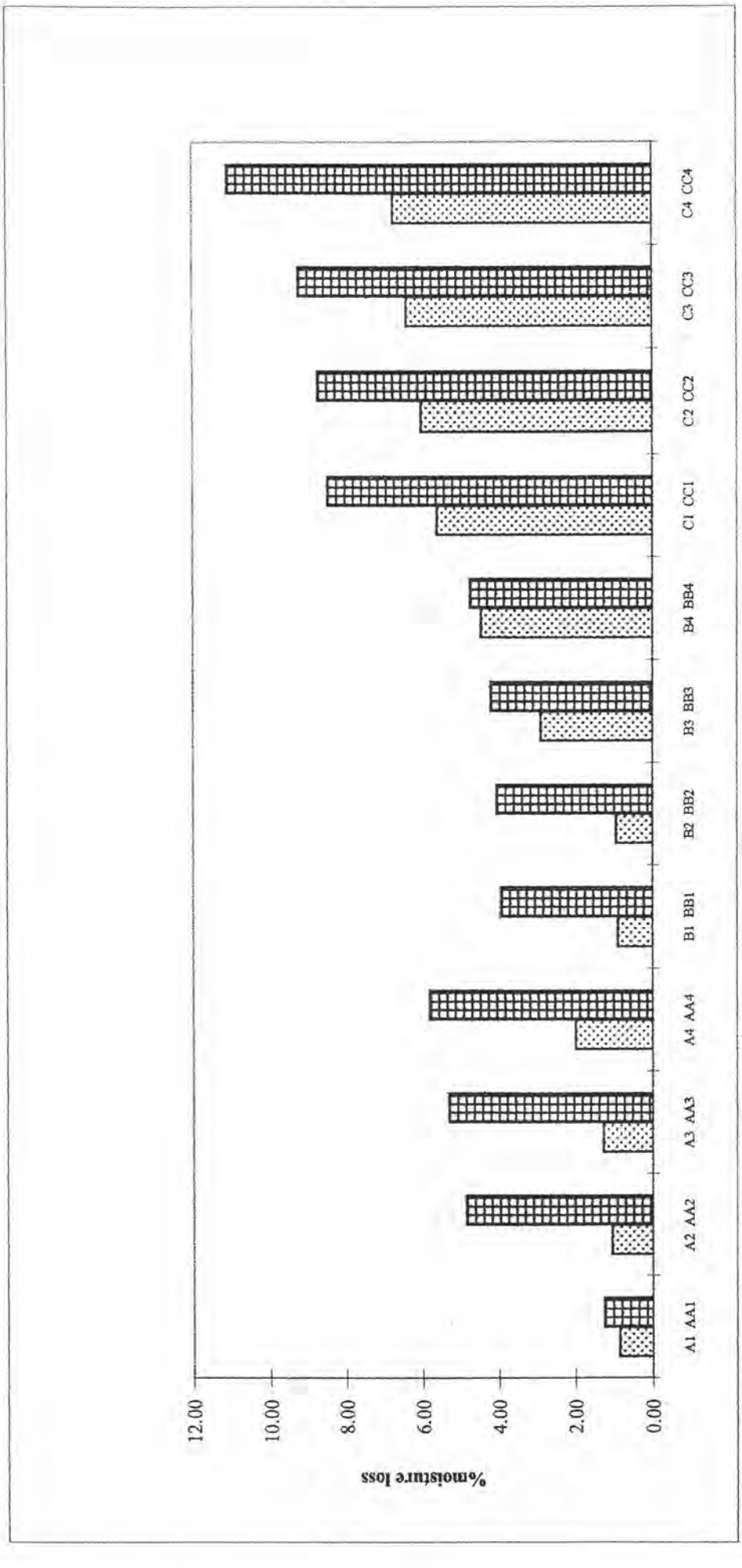

Figure 12 Percent moisture loss of terbutaline sulfate transdermal patches stored at 0 %RH for 1week

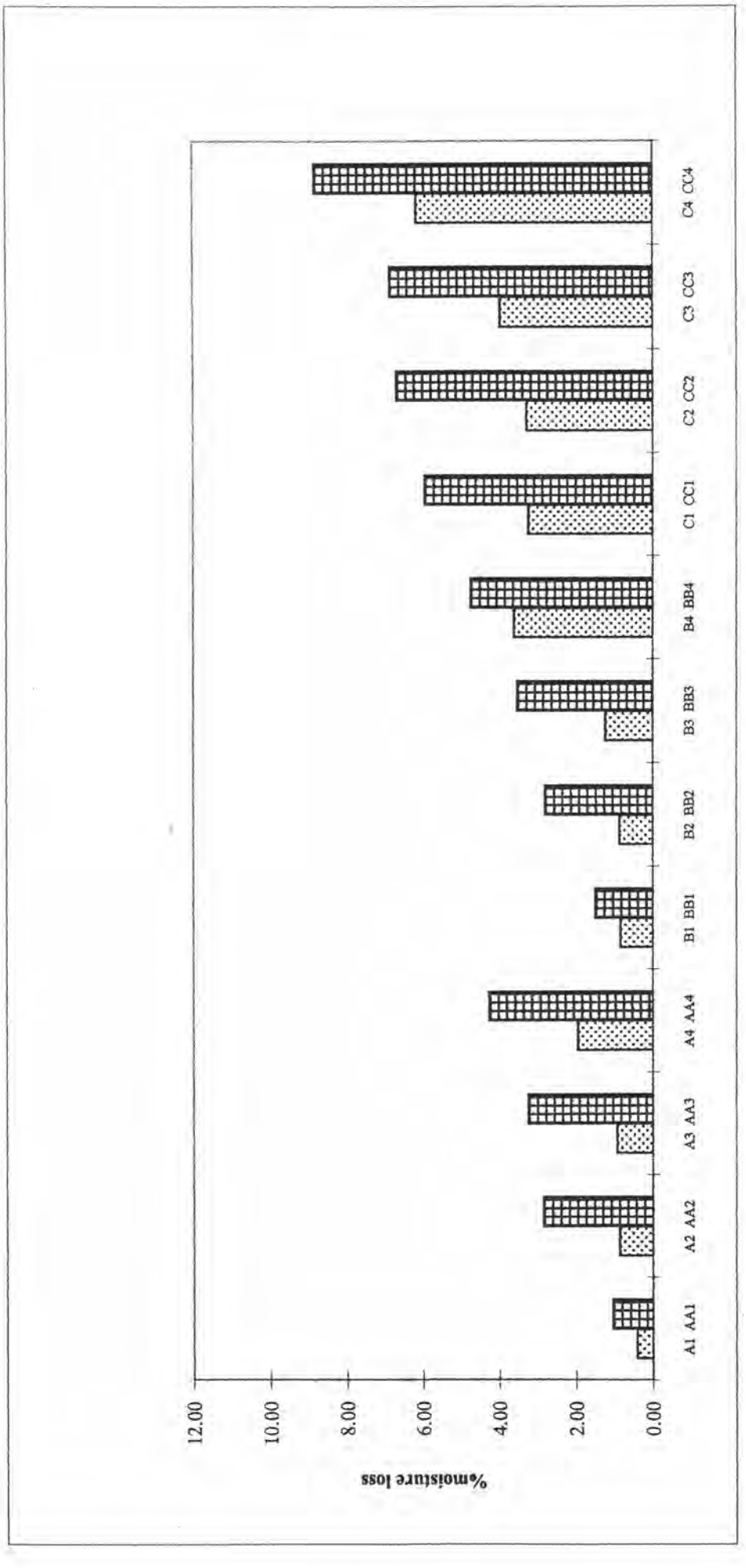

Figure 13 Percent moisture loss of terbutaline sulfate transdermal patches stored at 20 %RH for 1 week

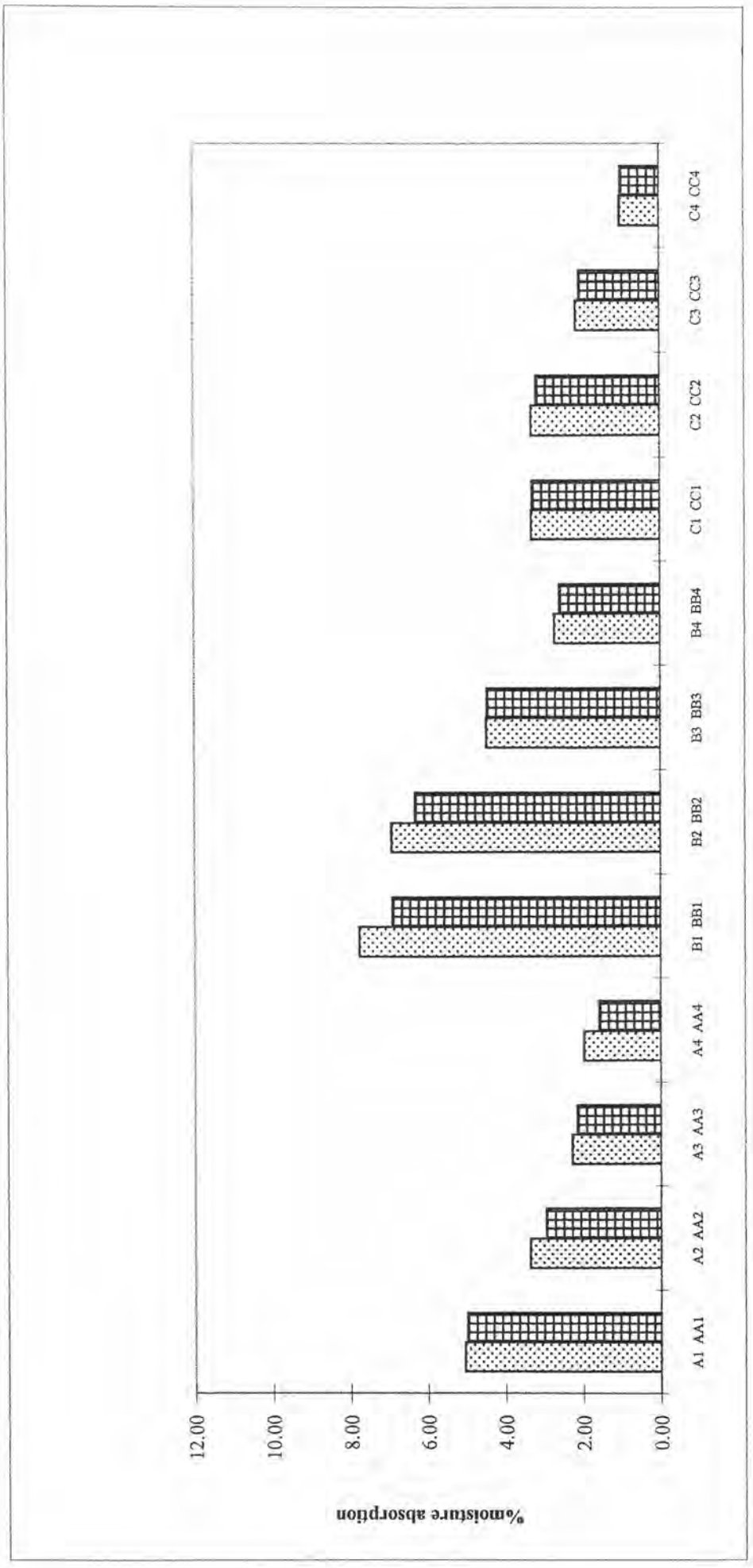

Figure 14 Percent moisture absorption of terbutaline sulfate transdermal patches stored at 52 %RH for 1 week

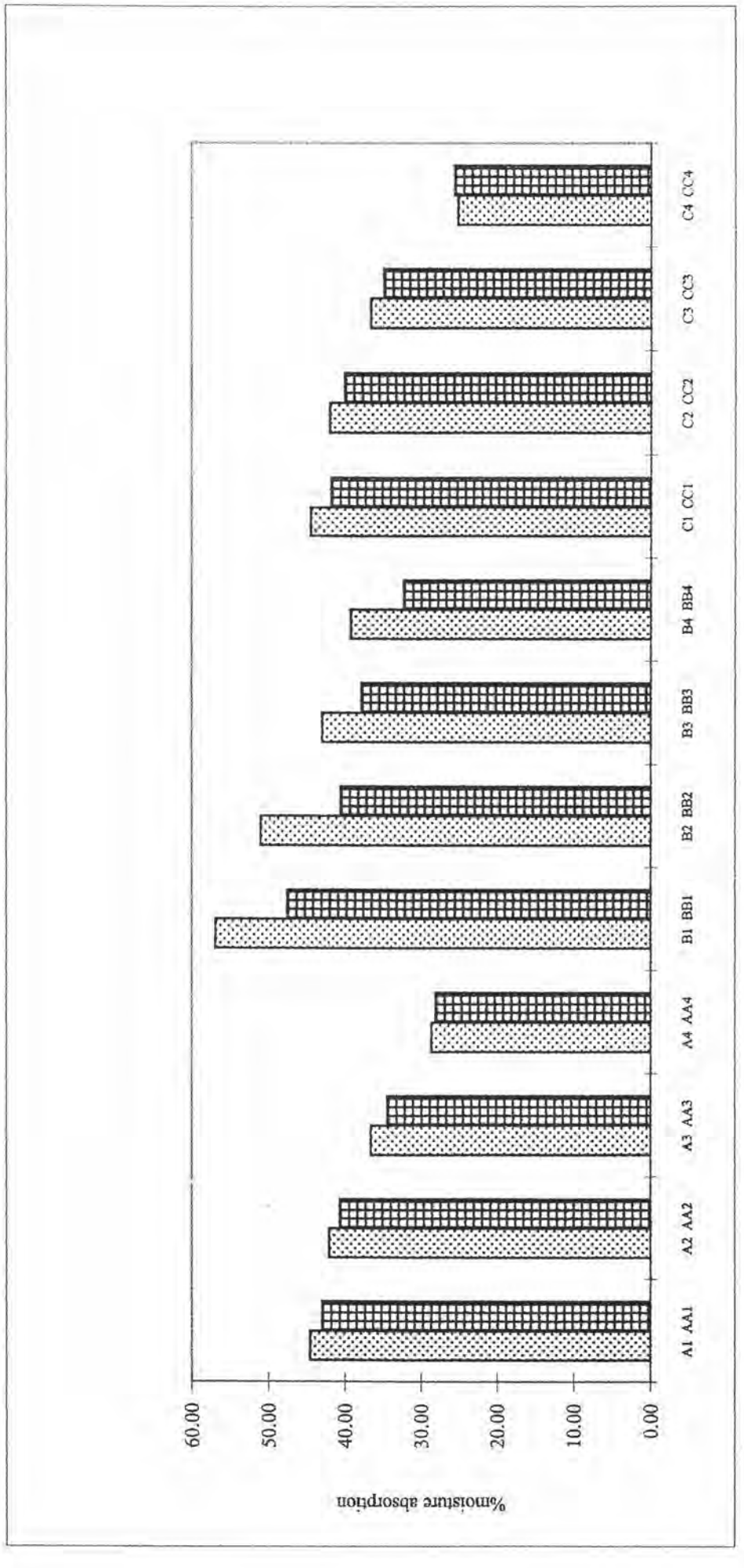

Figure 15 Percent moisture absorption of terbutaline sulfate transdermal patches stored at 93 %RH for 1 week

Table 16 Percent moisture absorption/loss of terbutaline sulfate transdermal patches stored at various relative humidities for 4 weeks (n=3)

Formulation	%moisture loss ± SD		%moisture absorption ± SD	
	0 %RH	20 %RH	52 %RH	93 %RH
A_1	0.54 ± 0.11	0.15 ± 0.03	5.13 ± 0.92	-*
A_2	0.57 ± 0.19	0.42 ± 0.27	3.68 ± 0.20	43.39 ± 2.31
A_3	0.74 ± 0.06	0.44 ± 0.09	2.73 ± 0.18	41.56 ± 2.86
A_4	1.53 ± 0.19	1.51 ± 0.30	2.53 ± 1.82	36.43± 5.03
B_1	0.86 ± 0.45	0.78 ± 0.69	9.25 ± 1.38	-*
B_2	0.87 ± 0.19	0.85 ± 0.57	7.96 ± 1.12	53.54 ± 2.26
B_3	2.70 ± 0.62	1.19 ± 0.27	5.04 ± 1.48	47.40 ± 0.71
B_4	3.98 ± 0.77	2.60 ± 1.83	3.83 ± 0.85	46.34 ± 2.25
C_1	5.60 ± 0.34	3.20 ± 0.56	3.66 ± 1.07	-*
C_2	5.79 ± 0.67	3.47 ± 0.41	3.51 ± 0.67	45.26 ± 2.14
C_3	5.92 ± 0.37	3.86 ± 0.42	2.39 ± 0.76	38.93 ± 1.54
C_4	6.26 ± 0.47	5.88 ± 0.65	1.16 ± 0.43	32.52 ± 0.45
AA_1	1.22 ± 0.31	1.00 ± 0.52	5.12 ± 0.84	-*
AA_2	4.69 ± 0.36	2.47 ± 0.17	3.32 ± 0.78	42.96 ± 2.33
AA_3	5.19 ± 0.33	2.94 ± 0.99	2.57 ± 0.27	38.91 ± 1.93
AA_4	5.78 ± 0.40	3.58 ± 0.23	2.25 ± 0.24	35.50 ± 1.82
BB_1	2.89 ± 1.09	0.94 ± 0.82	7.33 ± 1.34	51.74 ± 2.62
BB_2	3.13 ± 0.84	2.43 ± 1.47	6.96 ± 0.16	44.45 ± 2.69
BB_3	3.48 ±0.19	3.02 ±0.52	4.70 ± 0.15	41.92± 3.77
BB_4	3.51 ± 0.13	3.41 ± 0.46	3.11 ± 0.82	37.60 ± 3.58
CC_1	8.03 ± 0.59	5.52 ± 1.23	3.61 ± 0.46	48.08 ± 0.95
CC_2	8.16 ± 0.61	6.23 ± 0.81	3.38 ± 0.74	44.16 ± 0.94
CC_3	8.27 ± 0.25	6.26 ± 0.20	2.25 ± 0.19	36.51 ± 2.44
CC_4	10.08 ± 0.21	7.36 ± 1.28	1.40 ± 0.28	31.96 ± 1.89

* = Film seemed to be soft and viscous liquid.

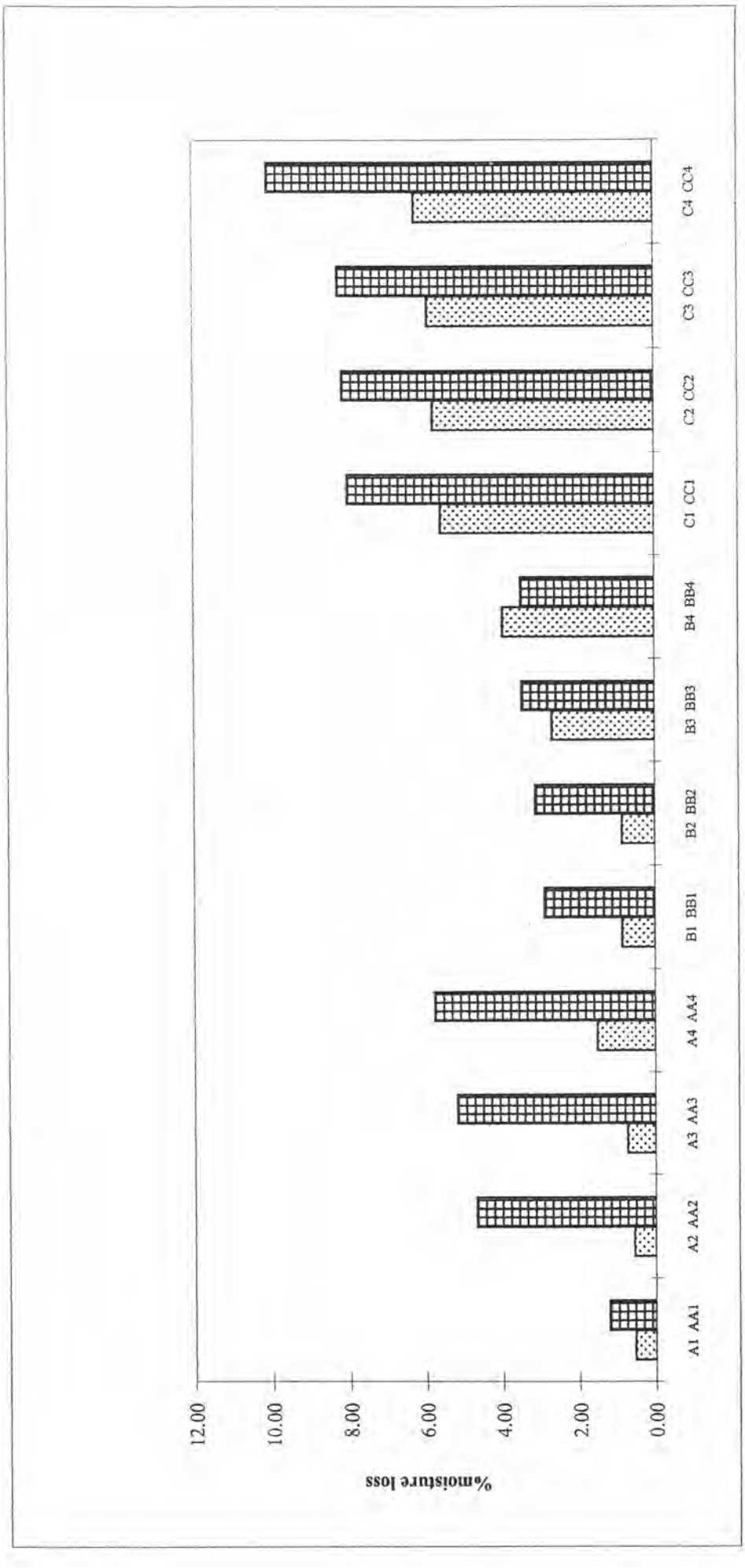

Figure 16 Percent moisture loss of terbutaline sulfate transdermal patches stored at 0 %RH for 4 weeks

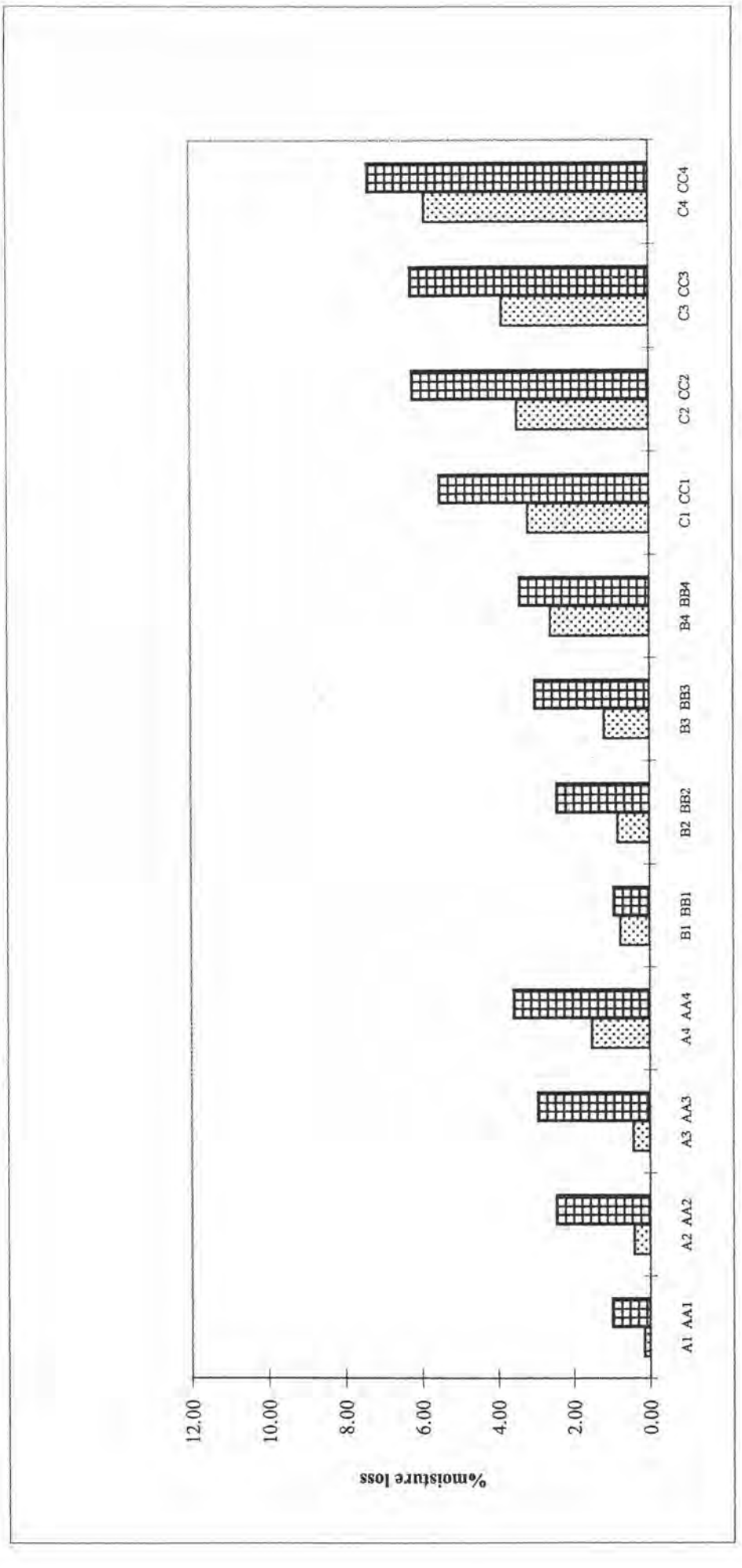

Figure 17 Percent moisture loss of terbutaline sulfate transdermal patches stored at 20 %RH for 4 weeks

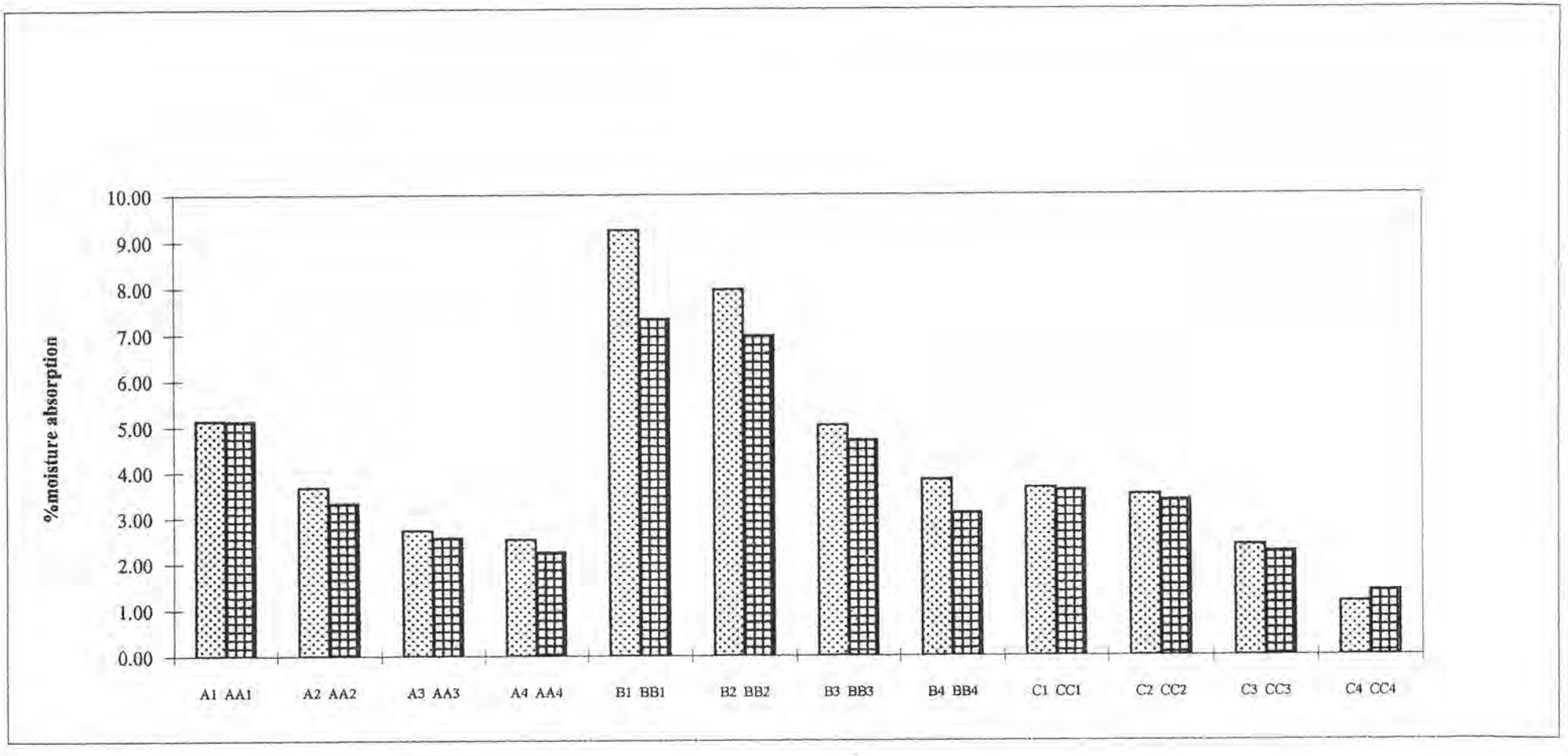

Figure 18 Percent moisture absorption of terbutaline sulfate transdermal patches stored at 52 %RH for 4 weeks

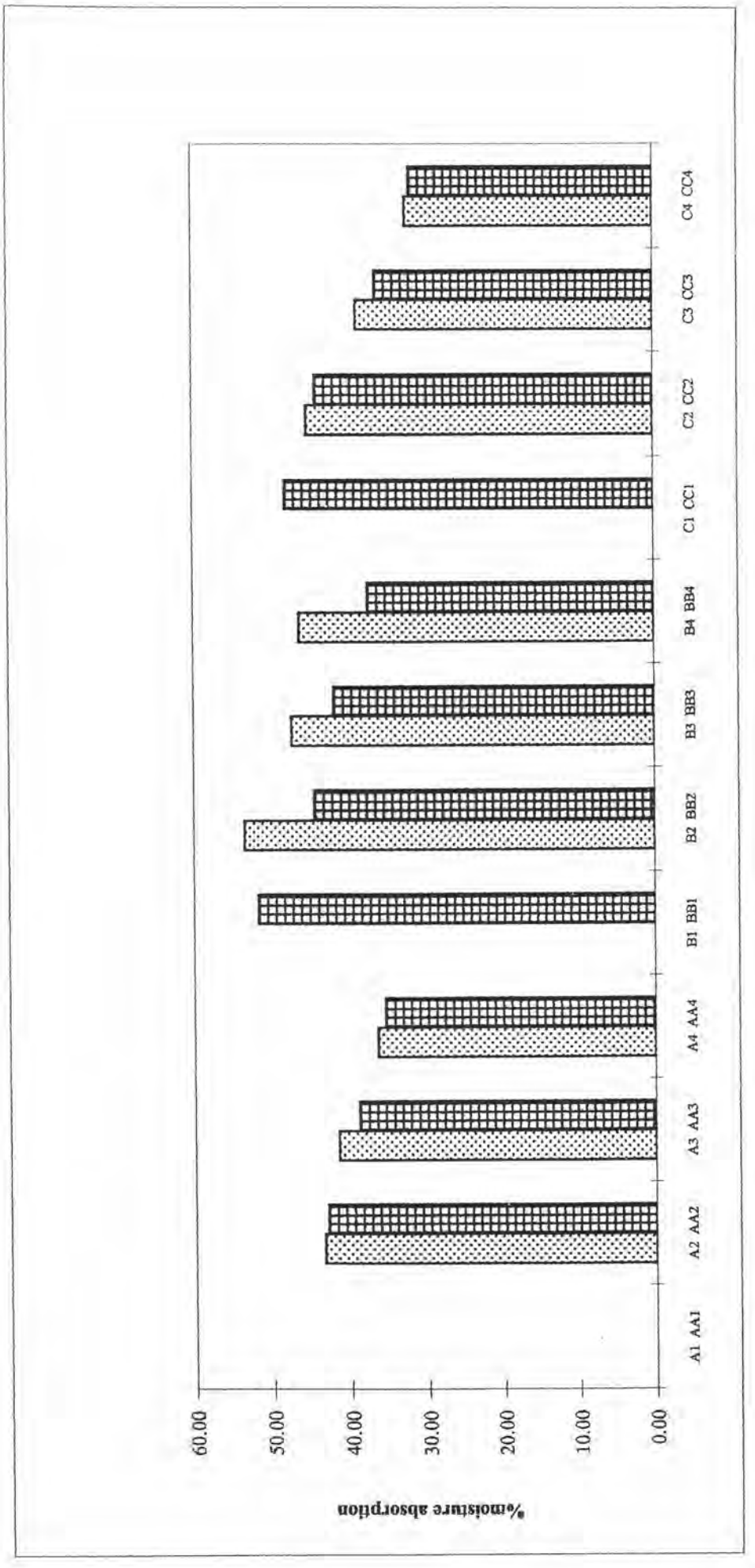

Figure 19 Percent moisture absorption of terbutaline sulfate transdermal patches stored at 93 %RH for 4 weeks

The ultimate tensile strength and percent elongation at break are shown in Table 17 and Figures 20 and 21.

The results indicated that, higher concentration of chitosan increased the ultimate tensile strength. The ultimate tensile strength of three grades of chitosan could be ranked in the following manner: SEACURE 143 < SEACURE 243 < SEACURE 343. The effect of PVP K-90 concentration on ultimate tensile strength of films showed that, increasing the PVP K-90 concentration increased ultimate tensile strength.

Focused on percent elongation at break, the obtained film using low amount of chitosan showed higher percent elongation at break than the obtained film using high amount of chitosan. Considering the effect of molecular weight of chitosan on percent elongation at break of film, it was found that percent elongation at break of samples with a high molecular weight of chitosan was higher than that of samples with a lower molecular weight. In formulation which composed of the same molecular weight of chitosan, increasing amount of PVP K-90 led to high percent elongation at break.

2.5 Peel Adhesion Property

The peel adhesion property of terbutaline sulfate transdermal patches was examined by measuring peel stress. Peel stress is shown in Table 18 and Figure 22. The effect of concentration of chitosan on adhesiveness was not obviously different. It was interesting to note that molecular weight of chitosan affected the adhesiveness of the films. Increasing the molecular weight of chitosan increased the adhesiveness of the films. The amount of PVP K-90 affected the adhesiveness of film. Higher concentration of PVP K-90 produced less adhesive film.

Table 17 Mechanical properties of terbutaline sulfate transdermal patches (n=6)

Formulation	Ultimate tensile strength ± SD (kg/mm^2)	% Elongation at break ± SD
A_1	0.122 ± 0.011	17.180 ± 1.720
A_2	0.150 ± 0.009	11.333 ± 1.287
A_3	0.163 ± 0.006	11.163 ± 1.695
A_4	0.164 ± 0.014	10.144 ± 2.458
B_1	0.135 ± 0.006	17.252 ± 1.005
B_2	0.155 ± 0.014	14.217 ± 2.304
B_3	0.165 ± 0.015	11.938 ± 3.132
B_4	0.201 ± 0.014	10.219 ± 8.553
C_1	0.171 ± 0.006	17.359 ± 14.512
C_2	0.175 ± 0.014	14.358 ± 11.501
C_3	0.197 ± 0.015	13.578 ± 10.696
C_4	0.221 ± 0.010	11.053 ± 0.440
AA_1	0.150 ± 0.027	17.912 ± 2.035
AA_2	0.172 ± 0.005	13.540 ± 3.343
AA_3	0.190 ± 0.004	11.736 ± 0.976
AA_4	0.218 ± 0.008	10.853 ± 1.009
BB_1	0.155 ± 0.014	17.969 ± 0.873
BB_2	0.172 ± 0.016	14.861 ± 1.633
BB_3	0.222 ± 0.009	13.928 ± 3.982
BB_4	0.240 ± 0.007	11.484 ± 0.928
CC_1	0.180 ± 0.022	19.739 ± 1.754
CC_2	0.202 ± 0.019	17.883 ± 6.326
CC_3	0.240 ± 0.007	15.210 ± 3.124
CC_4	0.260 ± 0.015	11.164 ± 1.037

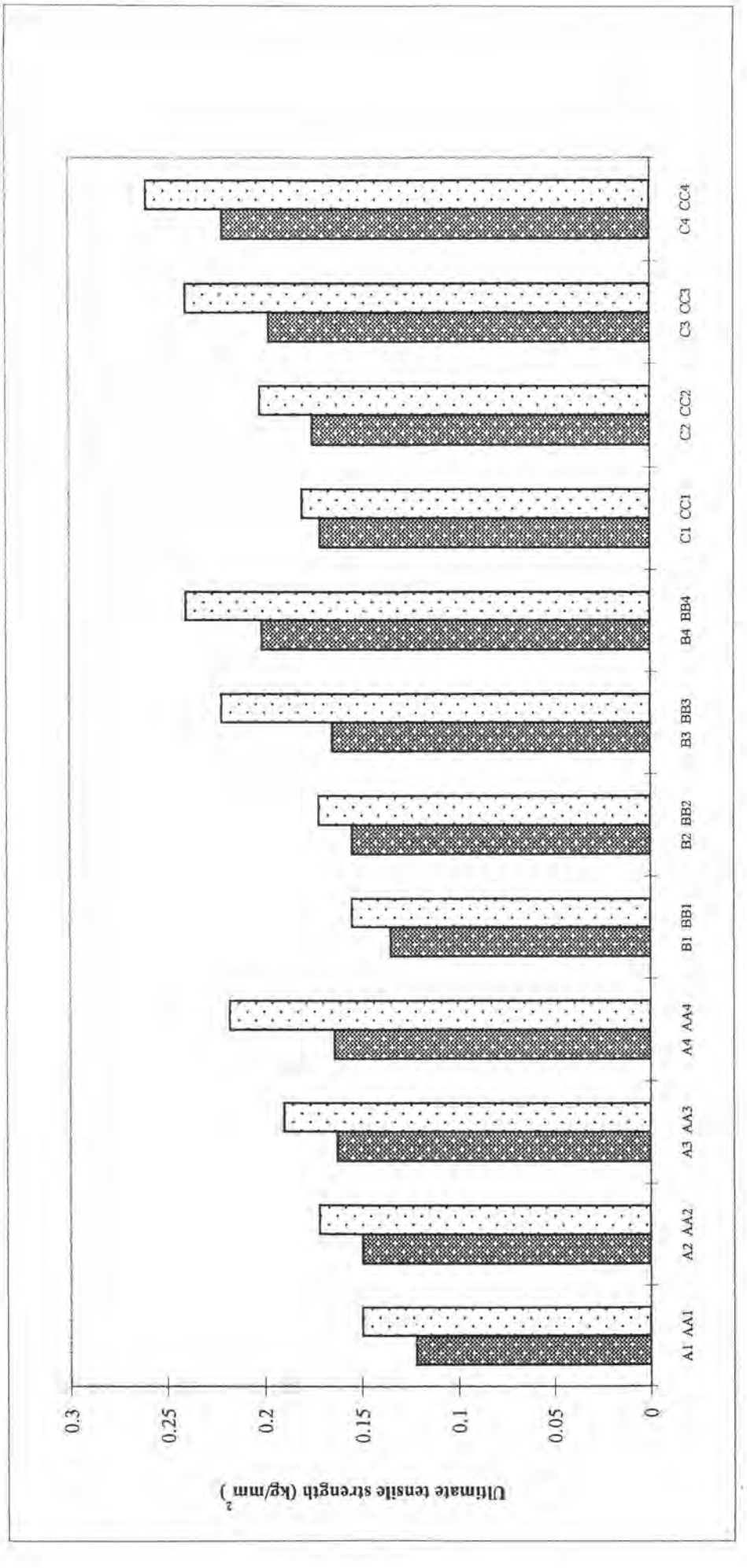

Figure 20 Ultimate tensile strength of terbutaline sulfate transdermal patches

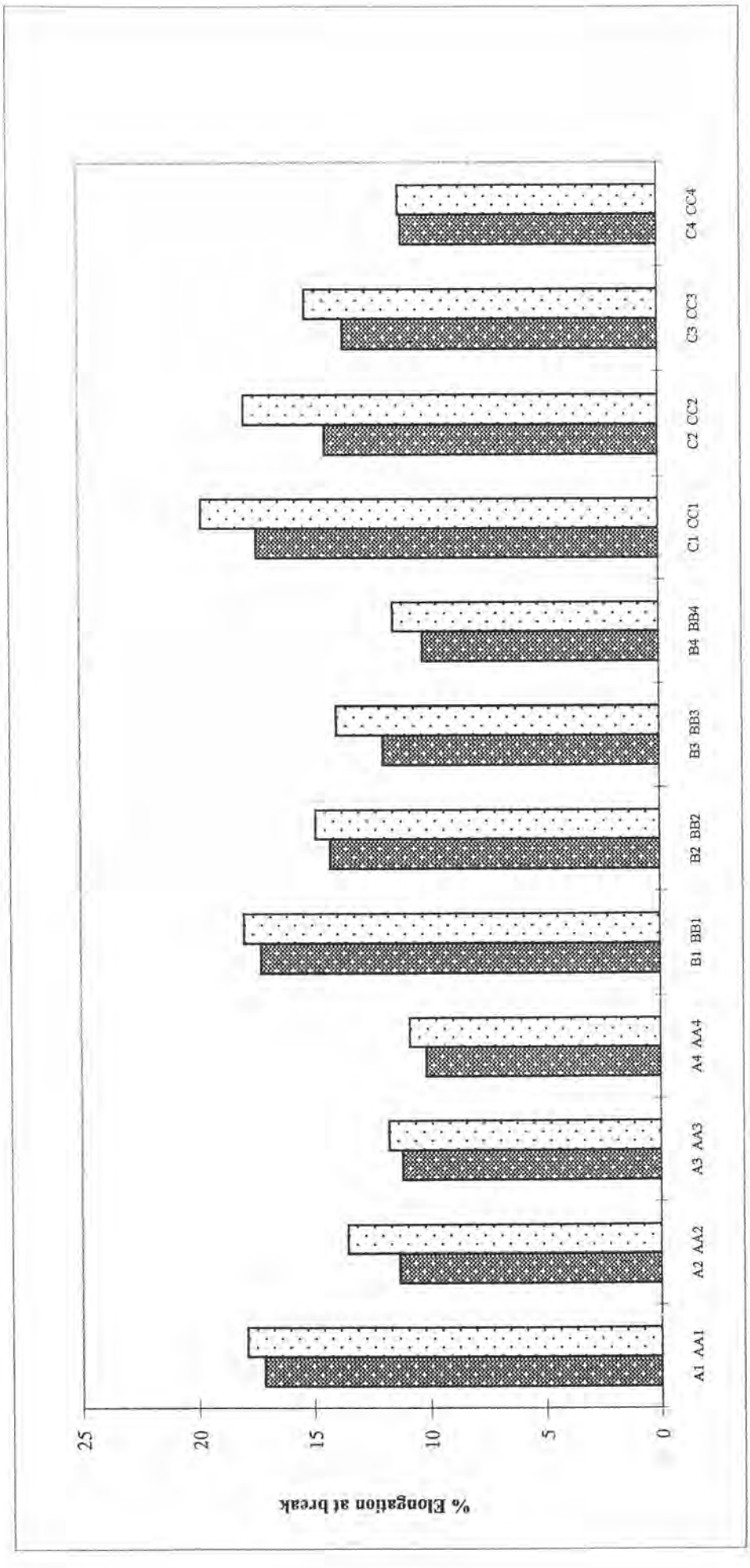

Figure 21 Percent elongation at break of terbutaline sulfate transdermal patches

Table 18 Peel adhesion property of terbutaline sulfate transdermal patches (n=6)

Formulation	Peel stress ± SD (g/mm)
A_1	22.470 ± 0.086
A_2	21.309 ± 0.116
A_3	19.219 ± 0.100
A_4	16.472 ± 0.195
B_1	30.583 ± 0.235
B_2	28.800 ± 0.112
B_3	24.370 ± 0.145
B_4	20.941 ± 0.282
C_1	35.241 ± 0.094
C_2	31.497 ± 0.341
C_3	27.380 ± 0.228
C_4	23.402 ± 0.250
AA_1	14.438 ± 0.334
AA_2	13.390 ± 0.170
AA_3	12.907 ± 0.150
AA_4	12.854 ± 0.195
BB_1	18.921 ± 0.424
BB_2	14.607 ± 0.316
BB_3	13.027 ± 0.306
BB_4	12.904 ± 0.296
CC_1	19.633 ± 0.159
CC_2	15.674 ± 0.346
CC_3	13.313 ± 0.187
CC_4	13.283 ± 0.204

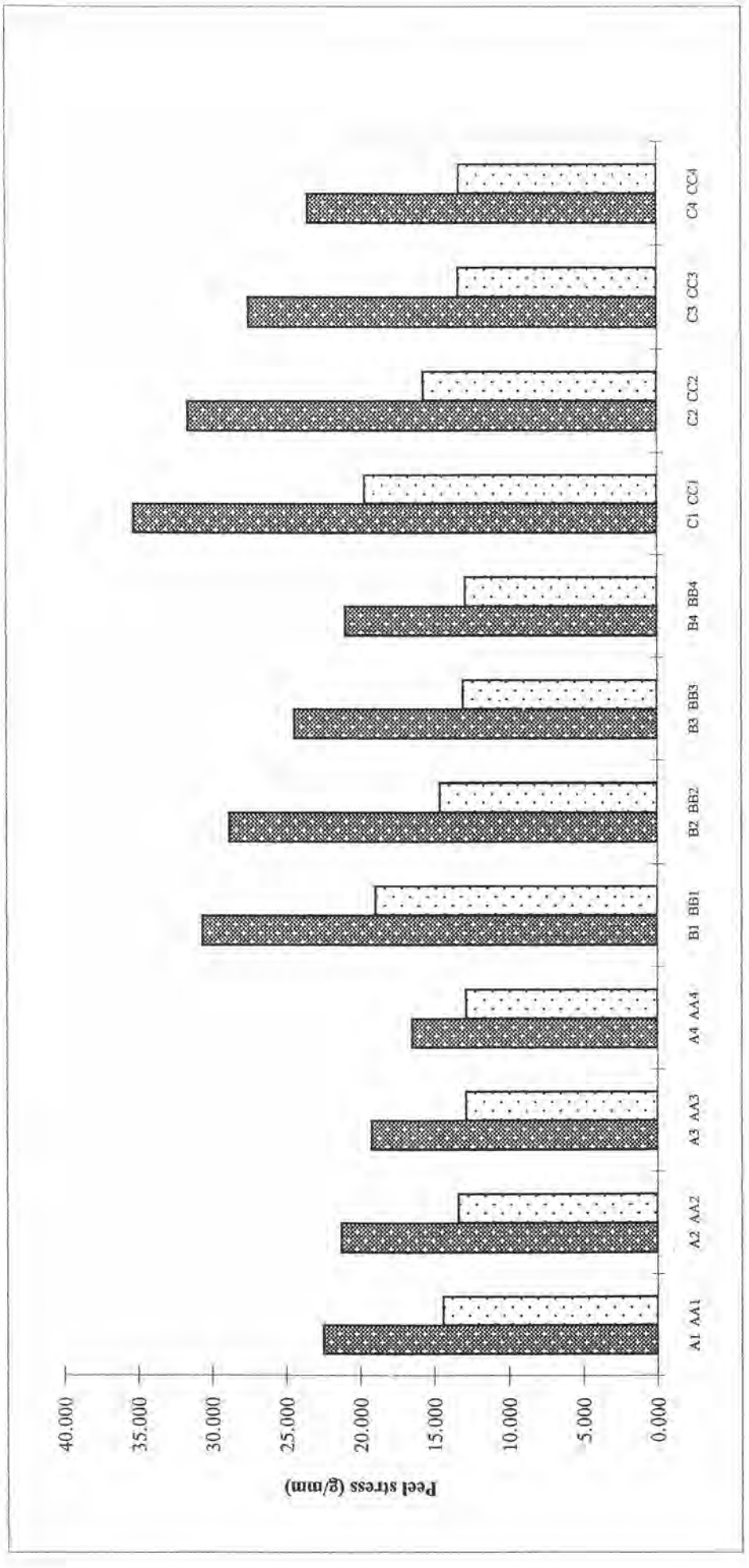

Figure 22 Peel stress of terbutaline sulfate transdermal patches

2.6 Surface Morphology

The surface photomicrograph of terbutaline sulfate transdermal patches was determined using scanning electron microscope (SEM) at x 200 magnification. The cross-section of films was also observed at x 300 and x 3000 magnifications.

The surface photomicrographs of terbutaline sulfate transdermal patches using different concentrations of SEACURE 143 and 10 %w/w PVP K-90 are shown in Figure 23. The surface topographs of films were uniform, smooth and non porous. The surface photomicrographs of films using different concentrations of SEACURE 243 or SEACURE 343 and 10 %w/w PVP K-90 were the same as Figure 23.

The surface photomicrographs of terbutaline sulfate transdermal patches using different concentrations of chitosan and 15 %w/w PVP K-90 are shown in Figures 24 to 26. The needle-shaped crystals were observed to form on the surface of films. Moreover, the results indicated that the films using lower concentration of chitosan exhibited higher amount of crystals than those using higher concentration of chitosan. The results were the same in all molecular weights of chitosan.

The cross-section photomicrographs of terbutaline sulfate transdermal patches are shown in Figures 27 to 34. The results indicated that all formulations showed uniform and smooth cross-section photomicrographs when observed at x 300 magnification. Further studies on x 3000 magnification did not show significant differences. The cross-section photomicrographs showed smooth surface and no porosity. The rough surface detected from SEM was the swelling of films when exposed to higher magnification.

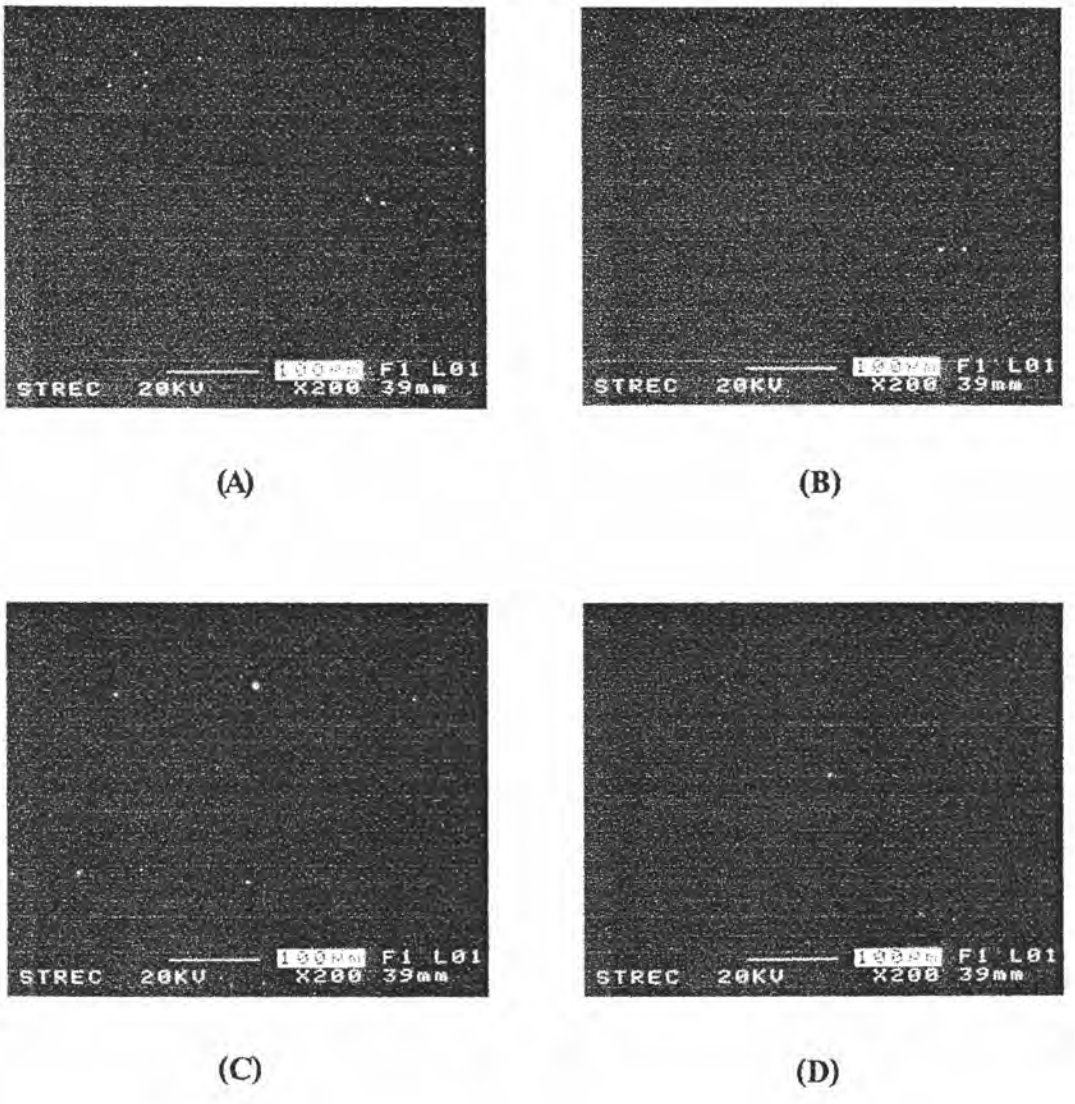

Figure 23 The surface photomicrographs of terbutaline sulfate transdermal patches with different concentrations of SEACURE 143 and 10 %w/w PVP K-90 at magnification of x 200 (A: 0.1 %w/w, B: 0.3 %w/w, C: 0.5 %w/w, D: 0.7 %w/w) Formulations A_1, A_2, A_3 and A_4 respectively

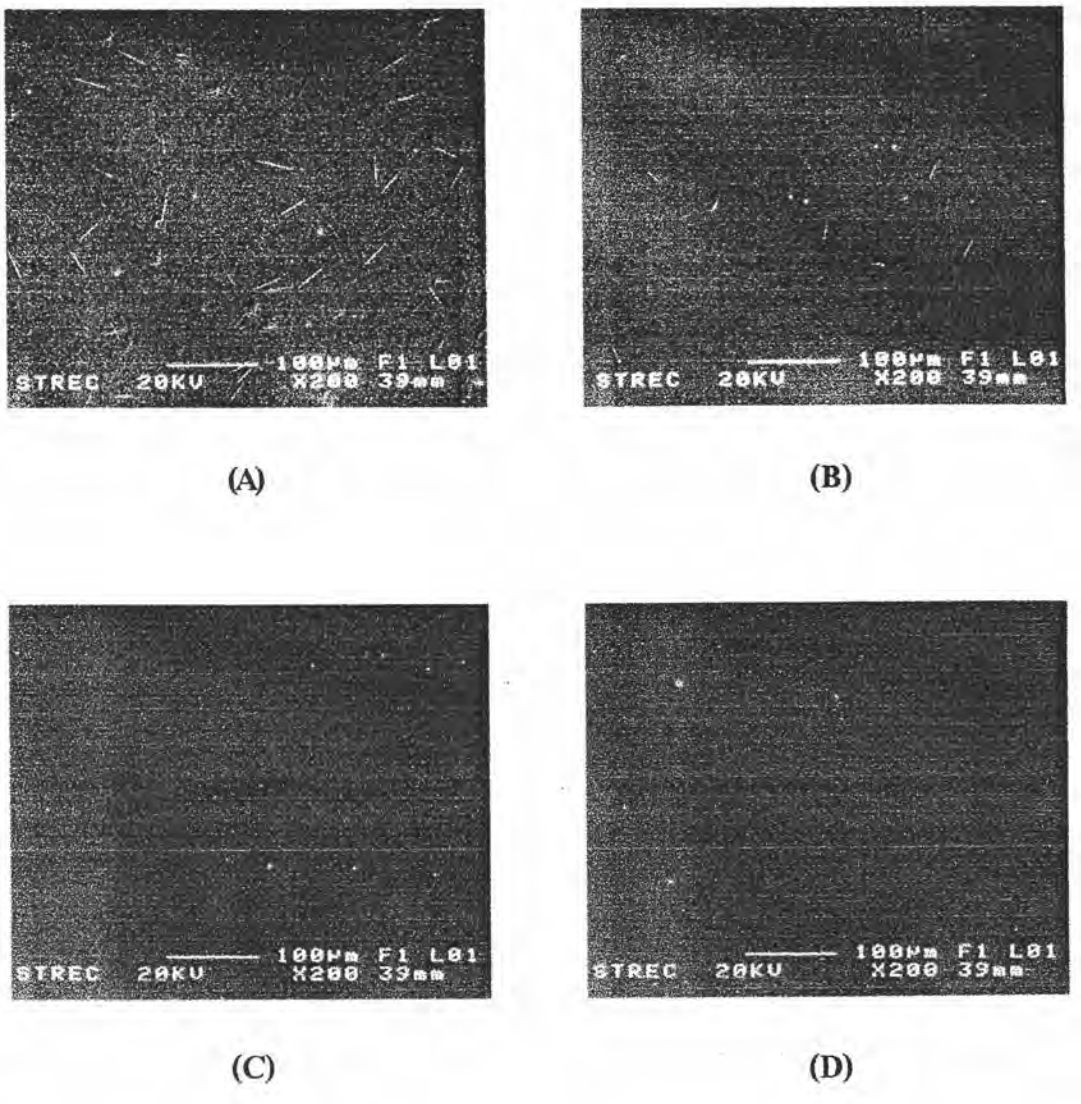

(A) (B)

(C) (D)

Figure 24 The surface photomicrographs of terbutaline sulfate transdermal patches with different concentrations of SEACURE 143 and 15 %w/w PVP K-90 at magnification of x 200 (A: 0.1 %w/w, B: 0.3 %w/w, C: 0.5 %w/w, D: 0.7 %w/w) Formulations AA_1, AA_2, AA_3 and AA_4 respectively

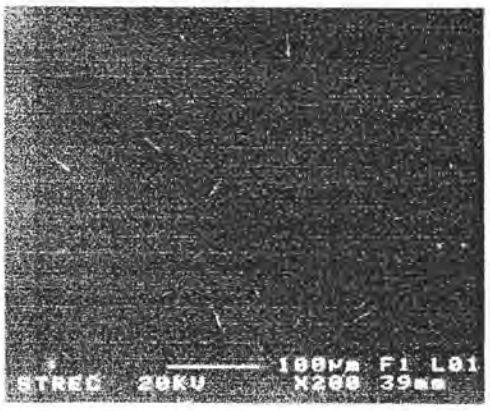

(A)

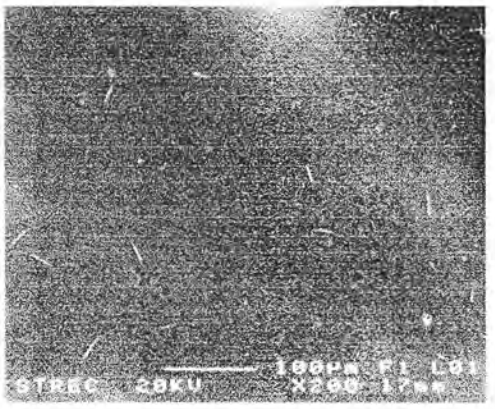

(B)

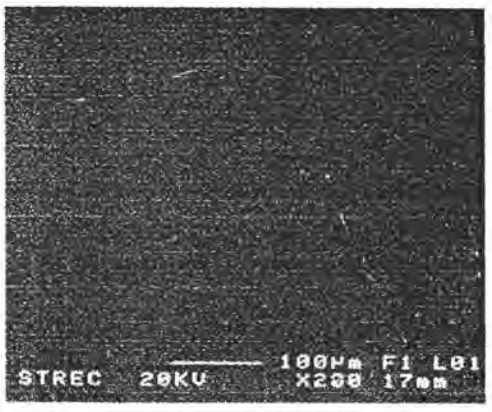

(C)

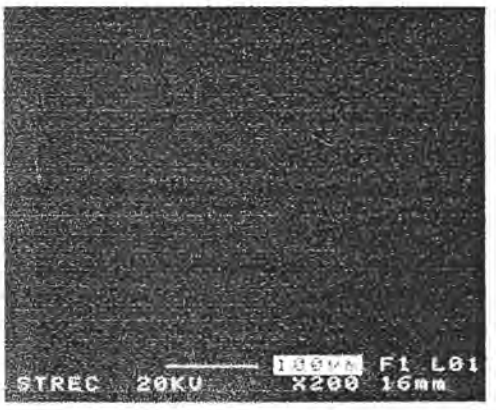

(D)

Figure 25 The surface photomicrographs of terbutaline sulfate transdermal patches with different concentrations of SEACURE 243 and 15 %w/w PVP K-90 at magnification of x 200 (A: 0.1 %w/w, B: 0.3 %w/w, C: 0.5 %w/w, D: 0.7 %w/w) Formulations BB_1, BB_2, BB_3 and BB_4 respectively

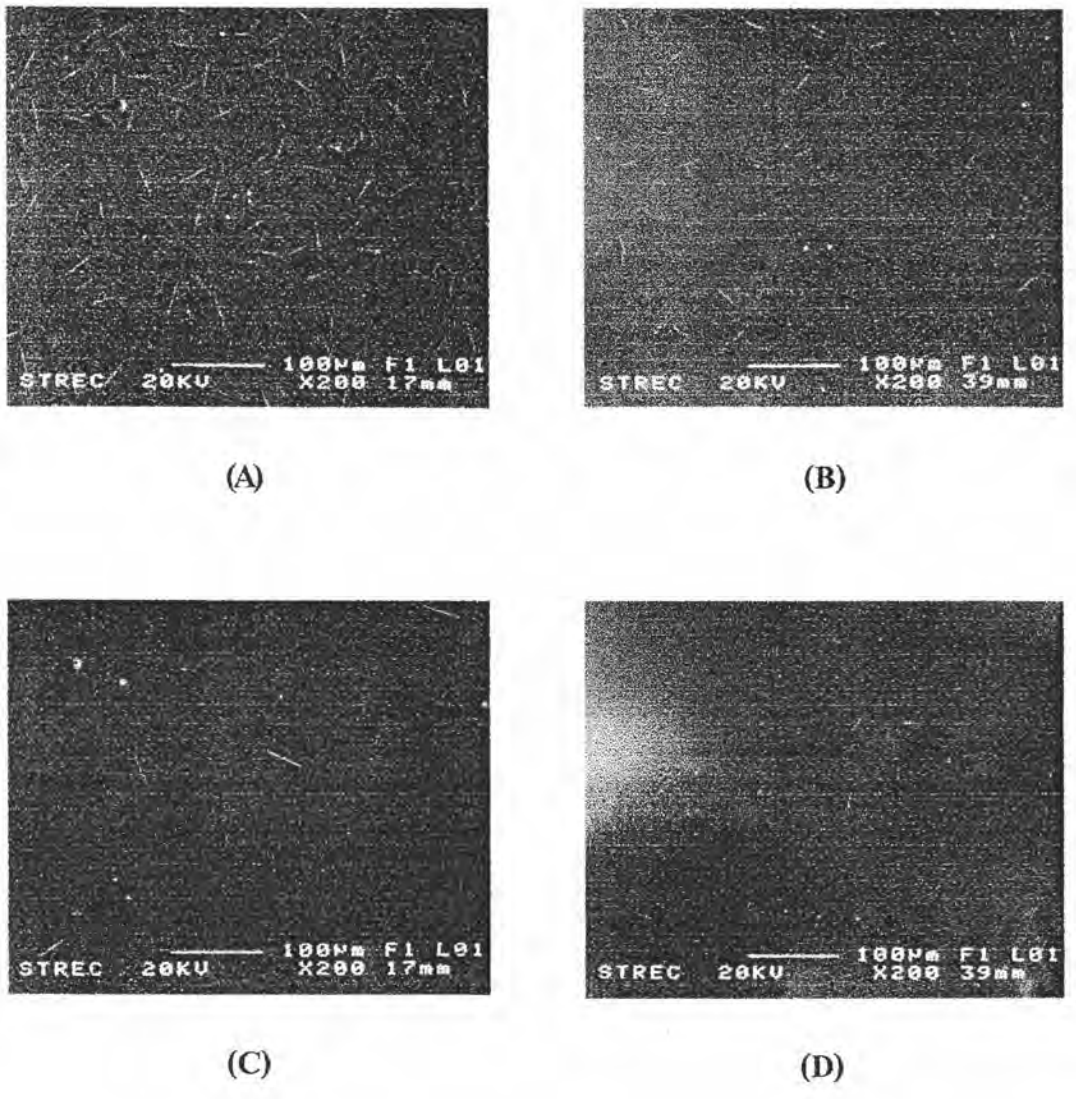

(A) (B)

(C) (D)

Figure 26 The surface photomicrographs of terbutaline sulfate transdermal patches with different concentrations of SEACURE 343 and 15 %w/w PVP K-90 at magnification of x 200 (A: 0.1 %w/w, B: 0.3 %w/w, C: 0.5 %w/w, D: 0.7 %w/w) Formulations CC_1, CC_2, CC_3 and CC_4 respectively

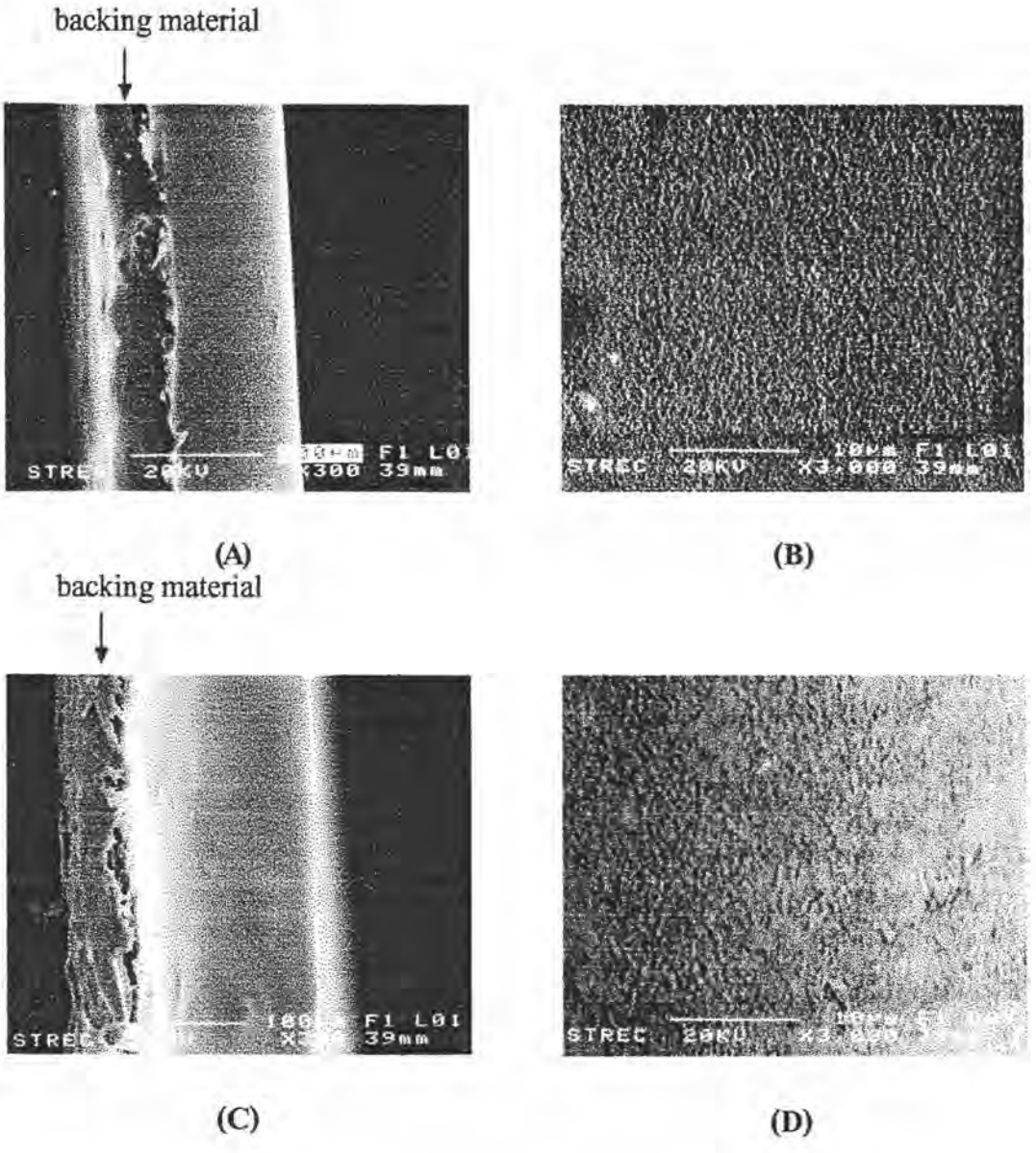

Figure 27 The cross-section photomicrographs of terbutaline sulfate transdermal patches with different concentrations of SEACURE 143 and 10 %w/w PVP K-90 at magnifications of x 300 and x 3000 (A: 0.1 %w/w x 300, B: 0.1 %w/w x 3000, C: 0.7 %w/w x 300, D: 0.7 %w/w x 3000) Formulations A_1 and A_4 respectively

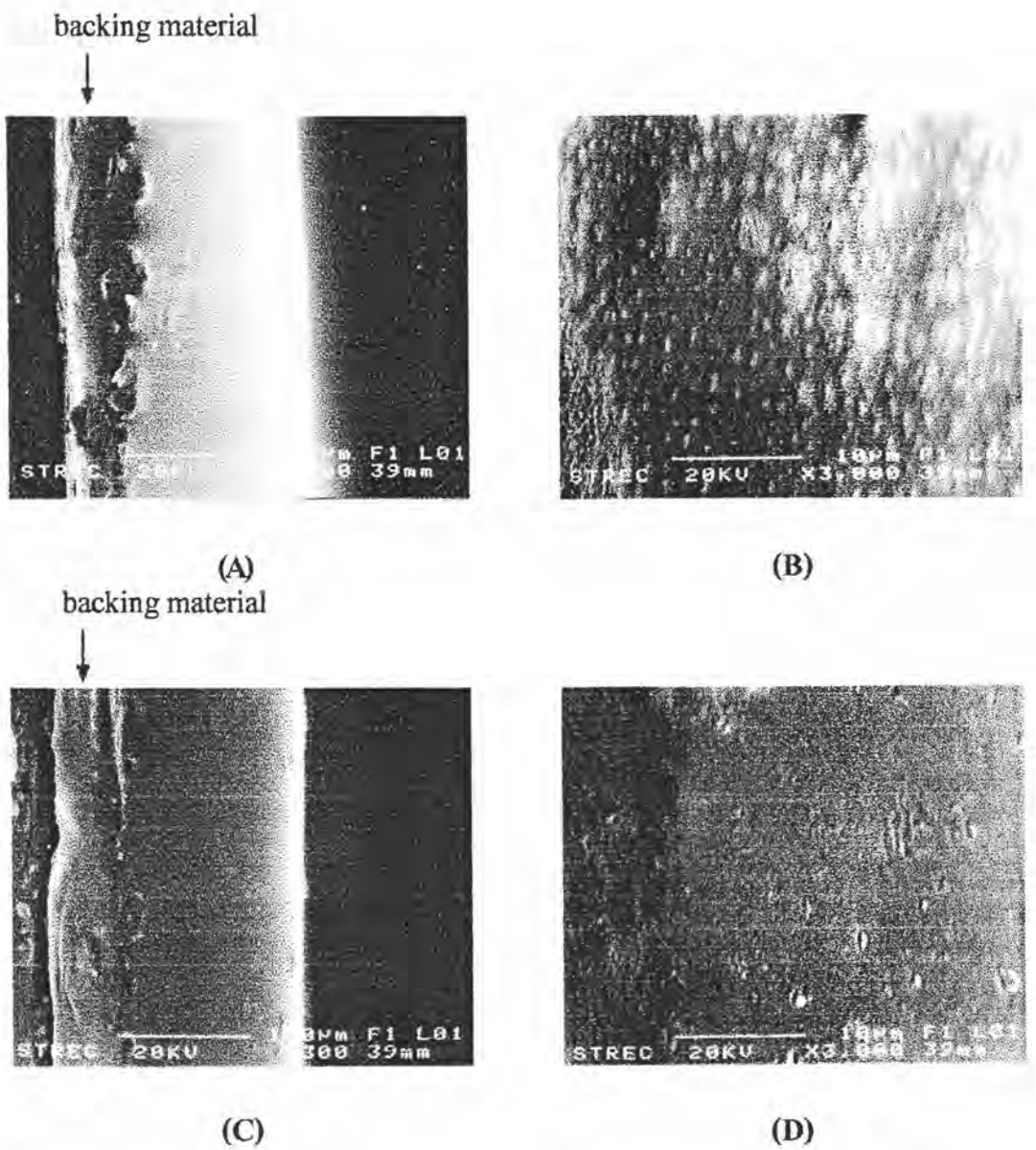

Figure 28 The cross-section photomicrographs of terbutaline sulfate transdermal patches with different concentrations of SEACURE 243 and 10 %w/w PVP K-90 at magnifications of x 300 and x 3000 (A: 0.1 %w/w x 300, B: 0.1 %w/w x 3000, C: 0.3 %w/w x 300, D: 0.3 %w/w x 3000) Formulations B_1 and B_2 respectively

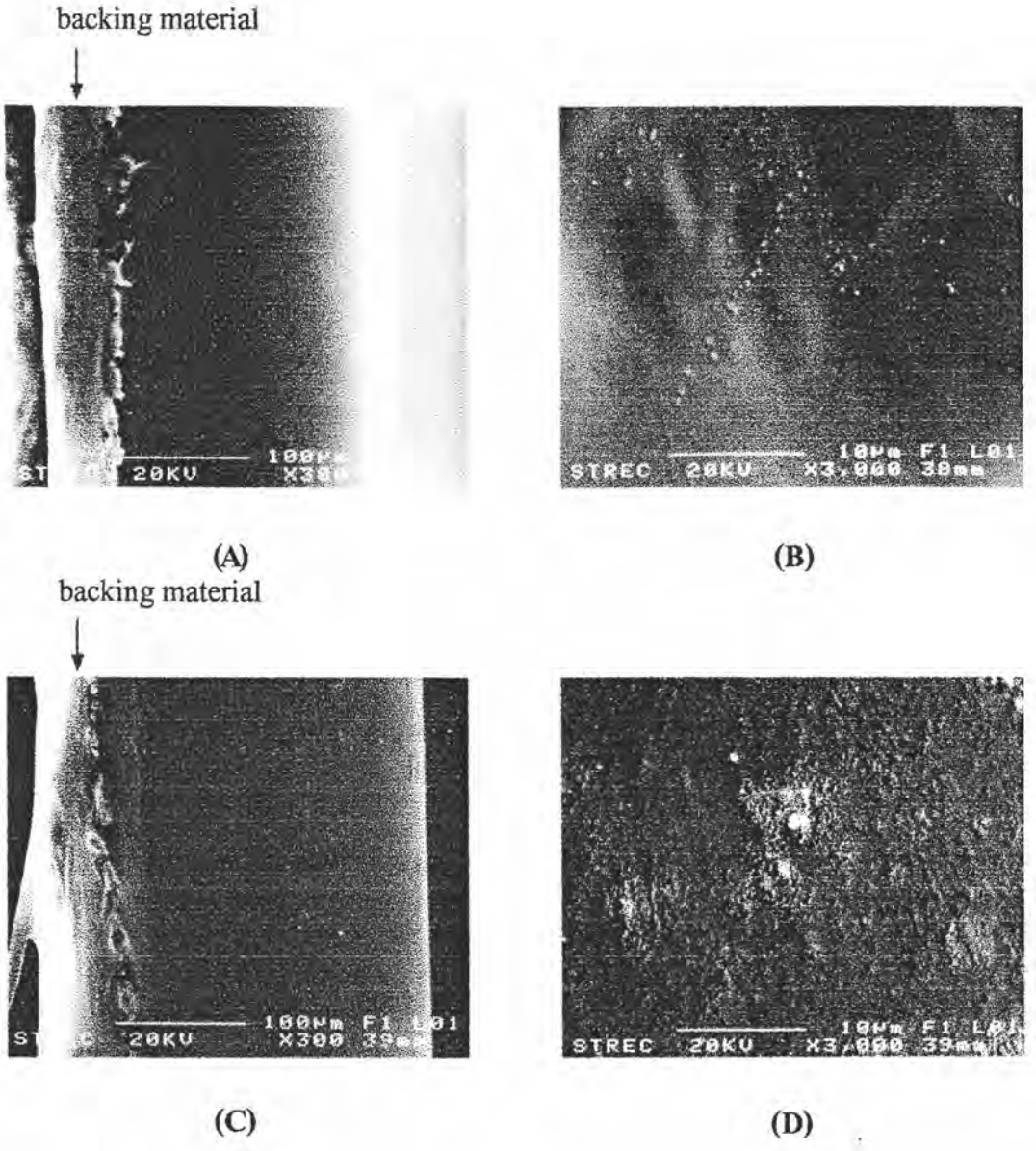

Figure 29 The cross-section photomicrographs of terbutaline sulfate transdermal patches with different concentrations of SEACURE 243 and 10 %w/w PVP K-90 at magnifications of x 300 and x 3000 (A: 0.5 %w/w x 300, B: 0.5 %w/w x 3000, C: 0.7 %w/w x 300, D: 0.7 %w/w x 3000) Formulations B_3 and B_4 respectively

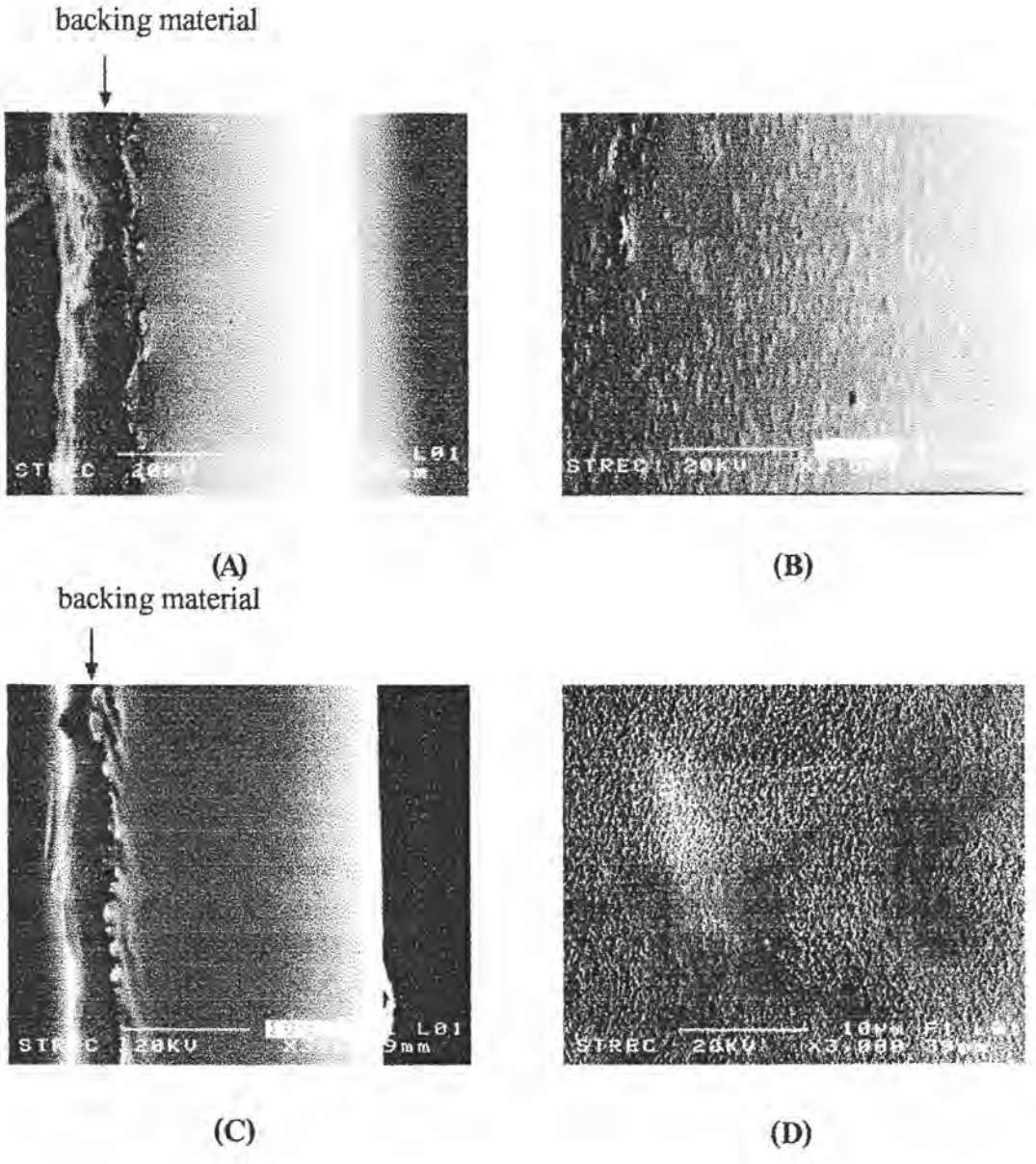

Figure 30 The cross-section photomicrographs of terbutaline sulfate transdermal patches with different concentrations of SEACURE 343 and 10 %w/w PVP K-90 at magnifications of x 300 and x 3000 (A: 0.1 %w/w x 300, B: 0.1 %w/w x 3000, C: 0.7 %w/w x 300, D: 0.7 %w/w x 3000) Formulations C_1 and C_4 respectively

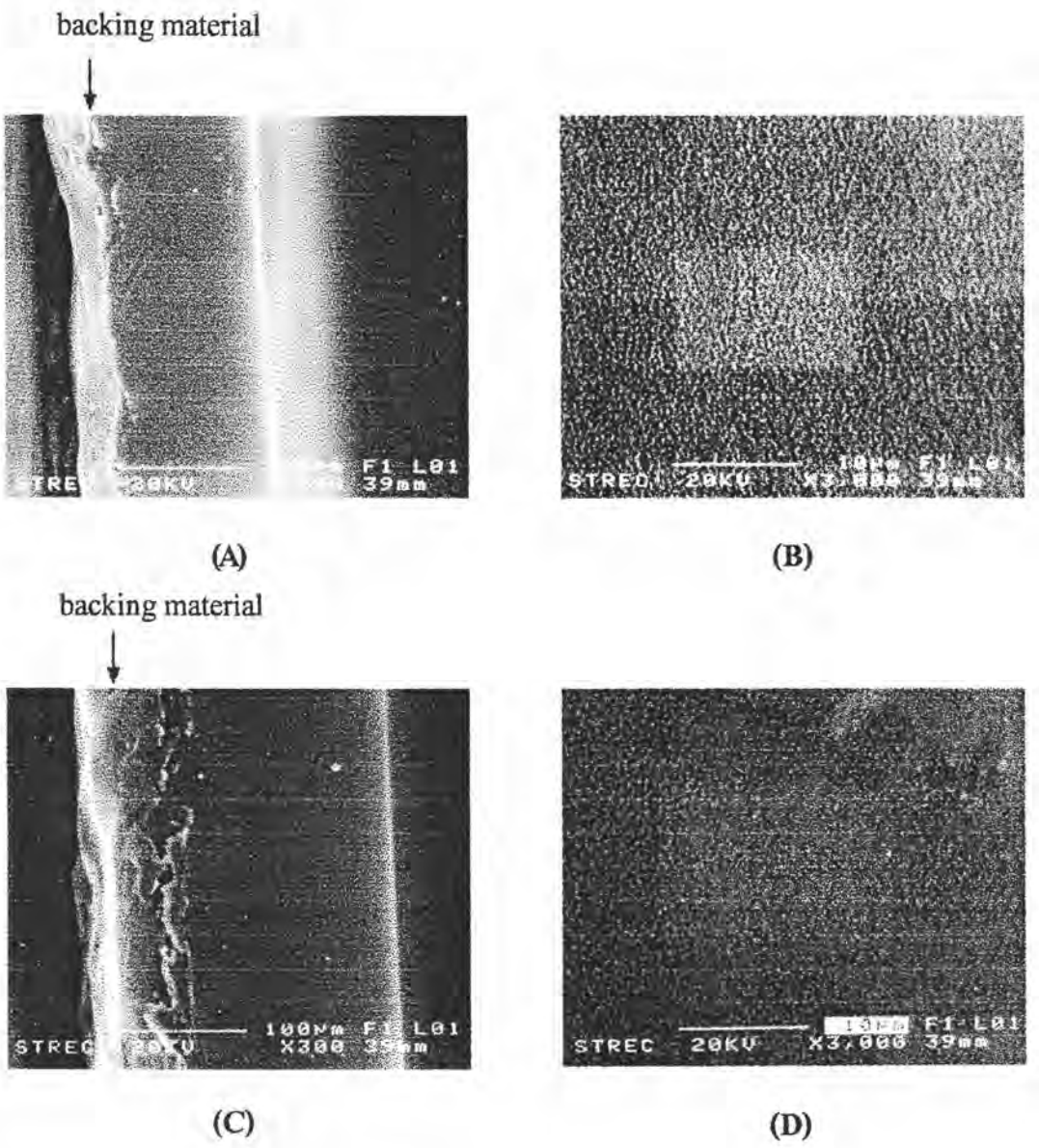

Figure 31 The cross-section photomicrographs of terbutaline sulfate transdermal patches with different concentrations of SEACURE 143 and 15 %w/w PVP K-90 at magnifications of x 300 and x 3000 (A: 0.1 %w/w x 300, B: 0.1 %w/w x 3000, C: 0.7 %w/w x 300, D: 0.7 %w/w x 3000) Formulations AA_1 and AA_4 respectively

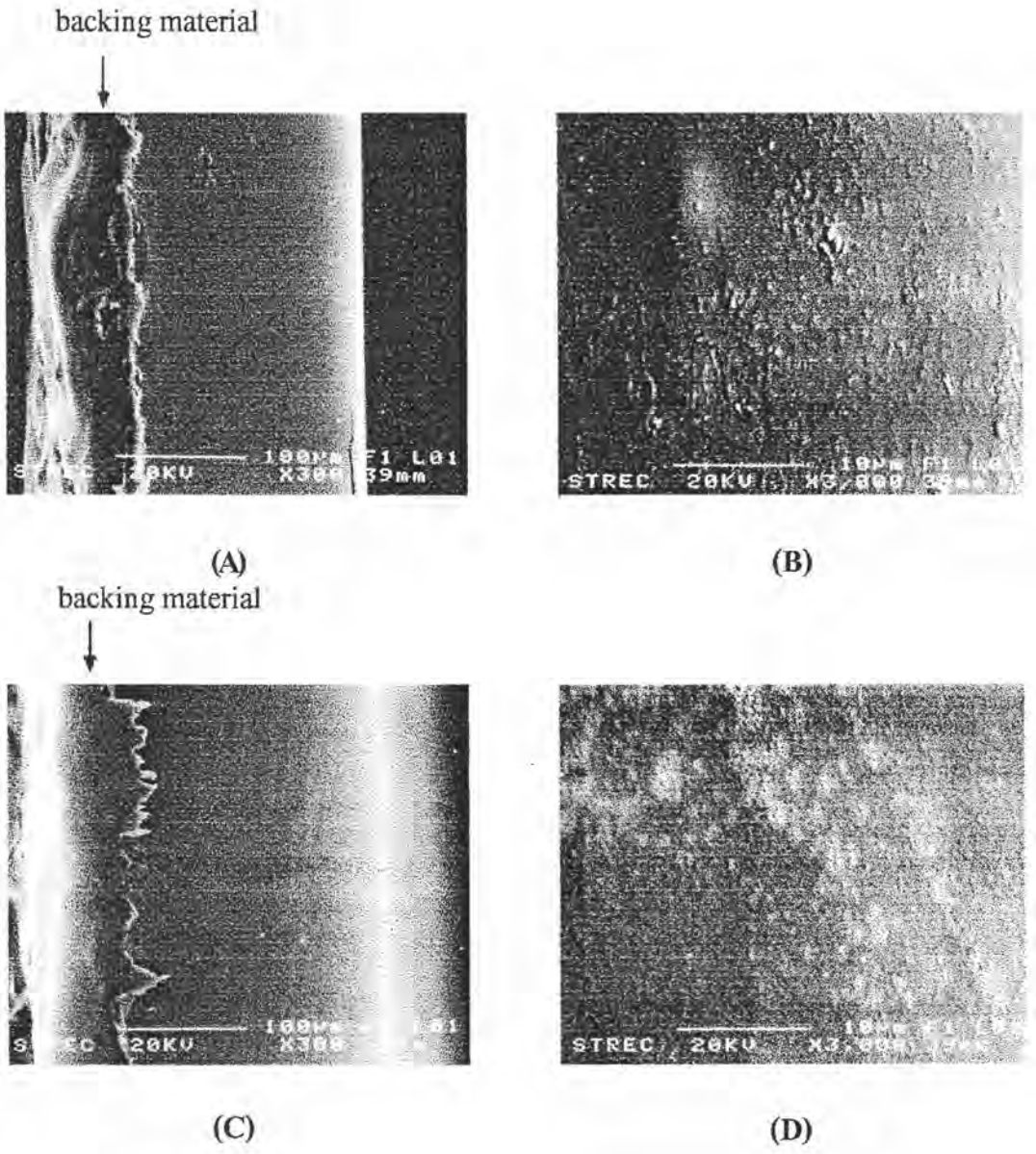

Figure 32 The cross-section photomicrographs of terbutaline sulfate transdermal patches with different concentrations of SEACURE 243 and 15 %w/w PVP K-90 at magnifications of x 300 and x 3000 (A: 0.1 %w/w x 300, B: 0.1 %w/w x 3000, C: 0.3 %w/w x 300, D: 0.3 %w/w x 3000) Formulations BB_1 and BB_2 respectively

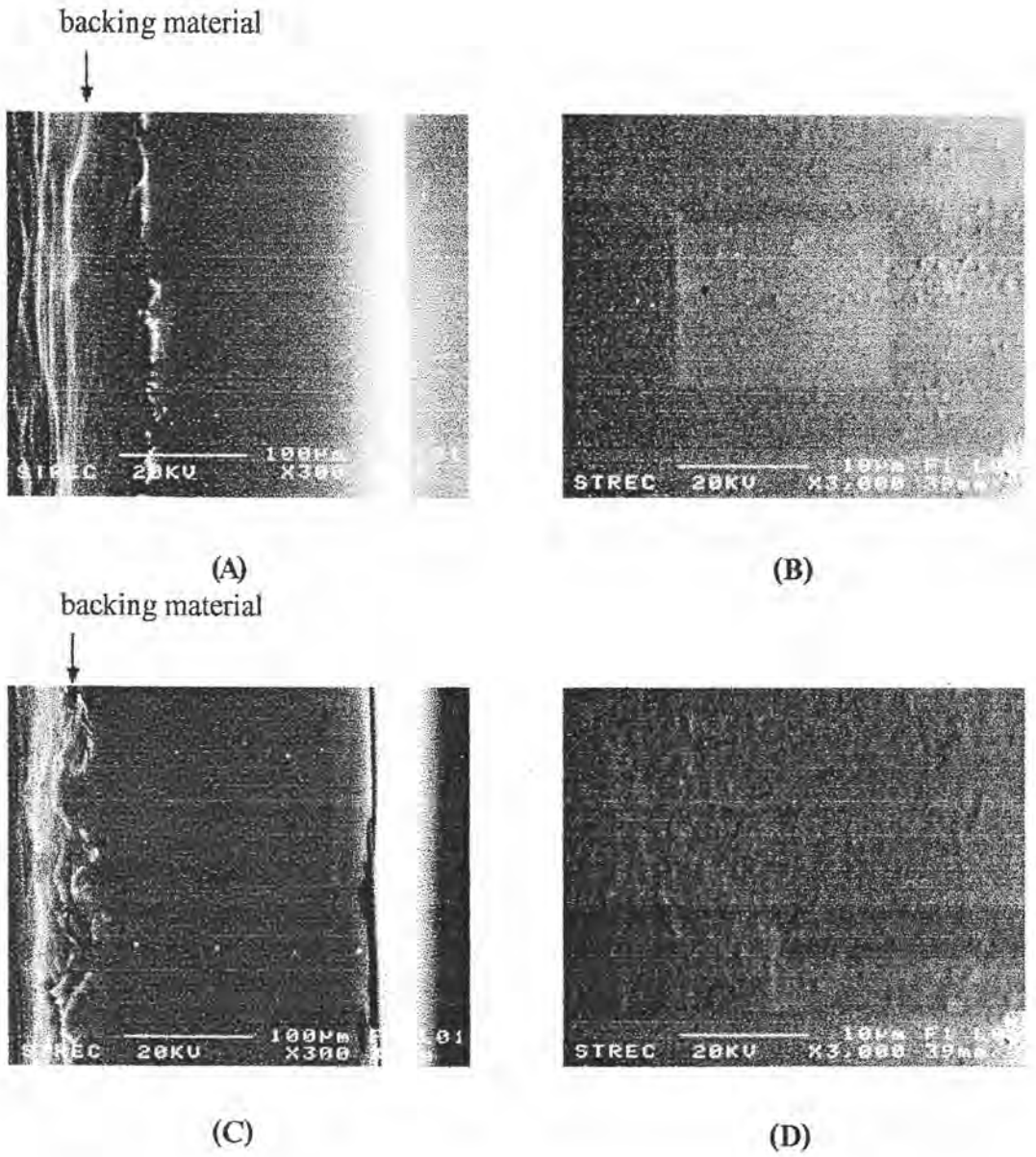

Figure 33 The cross-section photomicrographs of terbutaline sulfate transdermal patches with different concentrations of SEACURE 243 and 15 %w/w PVP K-90 at magnifications of x 300 and x 3000 (A: 0.5 %w/w x 300, B: 0.5 %w/w x 3000, C: 0.7 %w/w x 300, D: 0.7 %w/w x 3000) Formulations BB_3 and BB_4 respectively

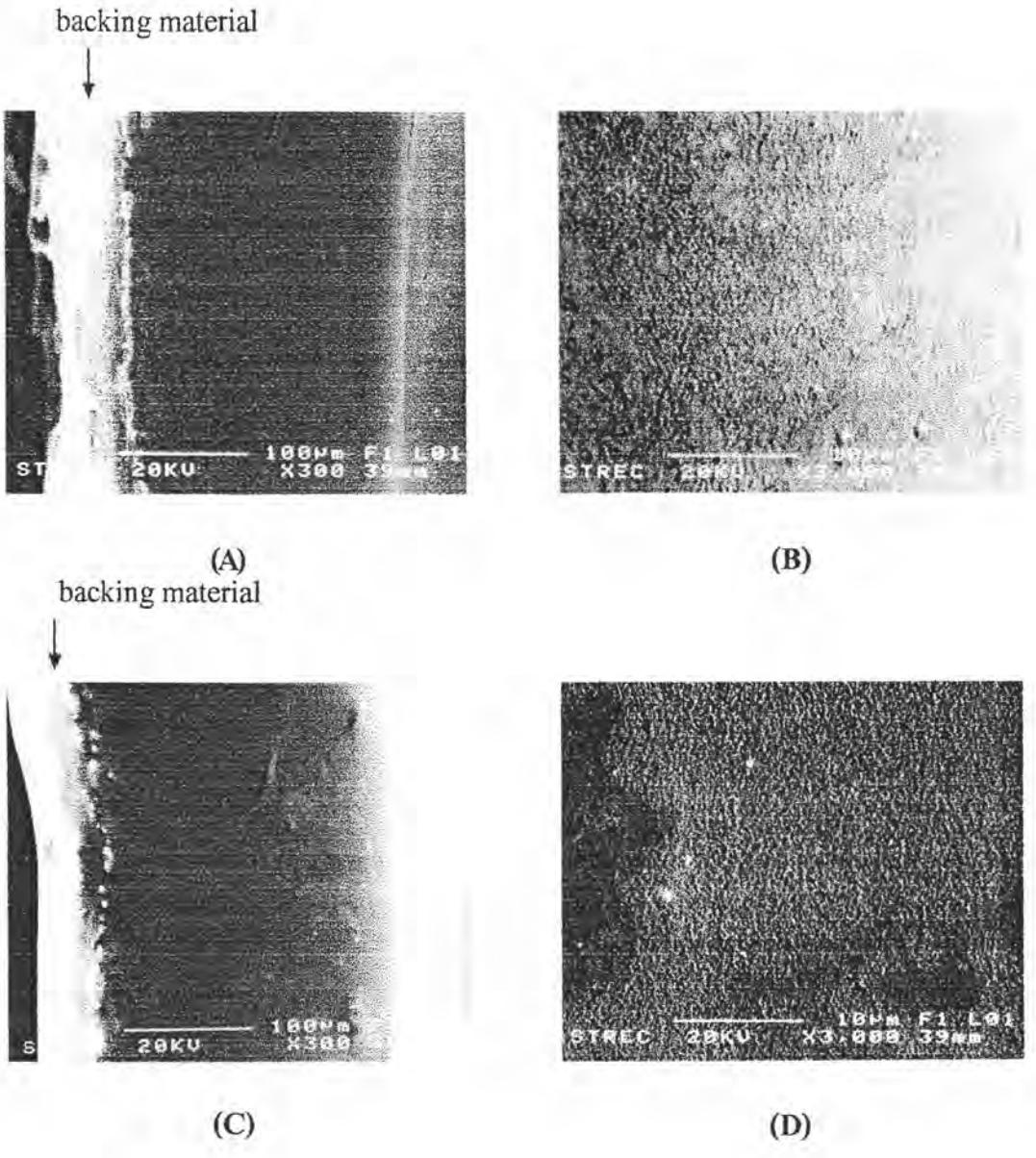

Figure 34 The cross-section photomicrographs of terbutaline sulfate transdermal patches with different concentrations of SEACURE 343 and 15 %w/w PVP K-90 at magnifications of x 300 and x 3000 (A: 0.1 %w/w x 300, B: 0.1 %w/w x 3000, C: 0.7 %w/w x 300, D: 0.7 %w/w x 3000) Formulations CC_1 and CC_4 respectively

2.7 Infrared Spectrometry

Infrared (IR) spectra of pure substances, polymers blend, drug-polymers blends and selected terbutaline sulfate transdermal patches are illustrated in Figures 35-39. IR spectrum of chitosan indicated the broad bands of O-H stretching and N-H stretching at 3432 cm^{-1}. The C=O stretching was shown at 1653 cm^{-1}. Peak at 1602 cm^{-1} resulted from the N-H bending of chitosan. The broad peak of C-O-C stretching was exhibited at 1092 cm^{-1}. In order to estimate the degree of acetylation, the peak intensity of C=O stretching at 1653 cm^{-1} compared to other peak, particularly peak intensity of O-H stretching at 3432 cm^{-1} was conducted. It was suggested that higher peak of C=O stretching at 1653 cm^{-1} when compared to peak of O-H stretching at 3432 cm^{-1} indicated higher degree of acetylation. From the IR spectra of three grades of chitosan (Figure 35), it could be stated that the degree of acetylation decreased in the following order: SEACURE 243 > SEACURE 143 > SEACURE 343. The ratio between peak intensity of C-O-C stretching at 1092 cm^{-1} and peak intensity of O-H stretching at 3432 cm^{-1} was used to estimate the polymer chain length of chitosan (Ritthidej et al., 1994). The higher ratio indicated longer chain length.

The IR spectrum of terbutaline sulfate showed O-H stretching at 3340 cm^{-1}; aromatic C-H stretching at 3058 cm^{-1}; secondary amine salt stretching at 2811, 2664 and 2501 cm^{-1}; aromatic ring stretching at 1612 and 1488 cm^{-1}; t-butyl symmetric bending at 1409 and 1380 cm^{-1}; phenolic C-O stretching at 1200; 1,3,5 trisubstituted benzene, out of plane bending at 853 and 693 cm^{-1}.

The IR spectrum of SEACURE 243 and PVP K-90 film ratio 1:1 is illustrated in Figure 37. The IR spectrum of blending film showed the combination of

SEACURE 243 peaks with those of PVP K-90 and the characteristic peaks of both polymers were also presented.

The IR spectrum of SEACURE 243 and terbutaline sulfate film ratio 1:1 is also illustrated in Figure 37. The IR spectrum of blending film showed the combination of SEACURE 243 peaks with those of terbutaline sulfate and the characteristic peaks of both SEACURE 243 and terbutaline sulfate were also revealed.

The effect of PVP K-90 and terbutaline sulfate blend is shown in Figure 37. The IR spectrum of blending film showed the combination of PVP K-90 peaks with those of terbutaline sulfate and the characteristic peaks of both PVP K-90 and terbutaline sulfate were also revealed.

The effect of SEACURE 243, PVP K-90 and terbutaline sulfate blend is also shown in Figure 37. The IR spectrum of blending film showed the combination of SEACURE 243, PVP K-90 and terbutaline sulfate peaks.

The terbutaline sulfate transdermal patches could not be directly ground with finely powder of potassium bromide when prepared the sample for IR study. Since the film had an adhesive property therefore it tended to adhere to potassium bromide and could not be tabletted into disc. Thus, in this study the terbutaline sulfate transdermal patch was directly used for observation in IR study. However, those patches did not show any peak of IR spectra. IR spectra of terbutaline sulfate transdermal patches are shown in Figures 38 and 39.

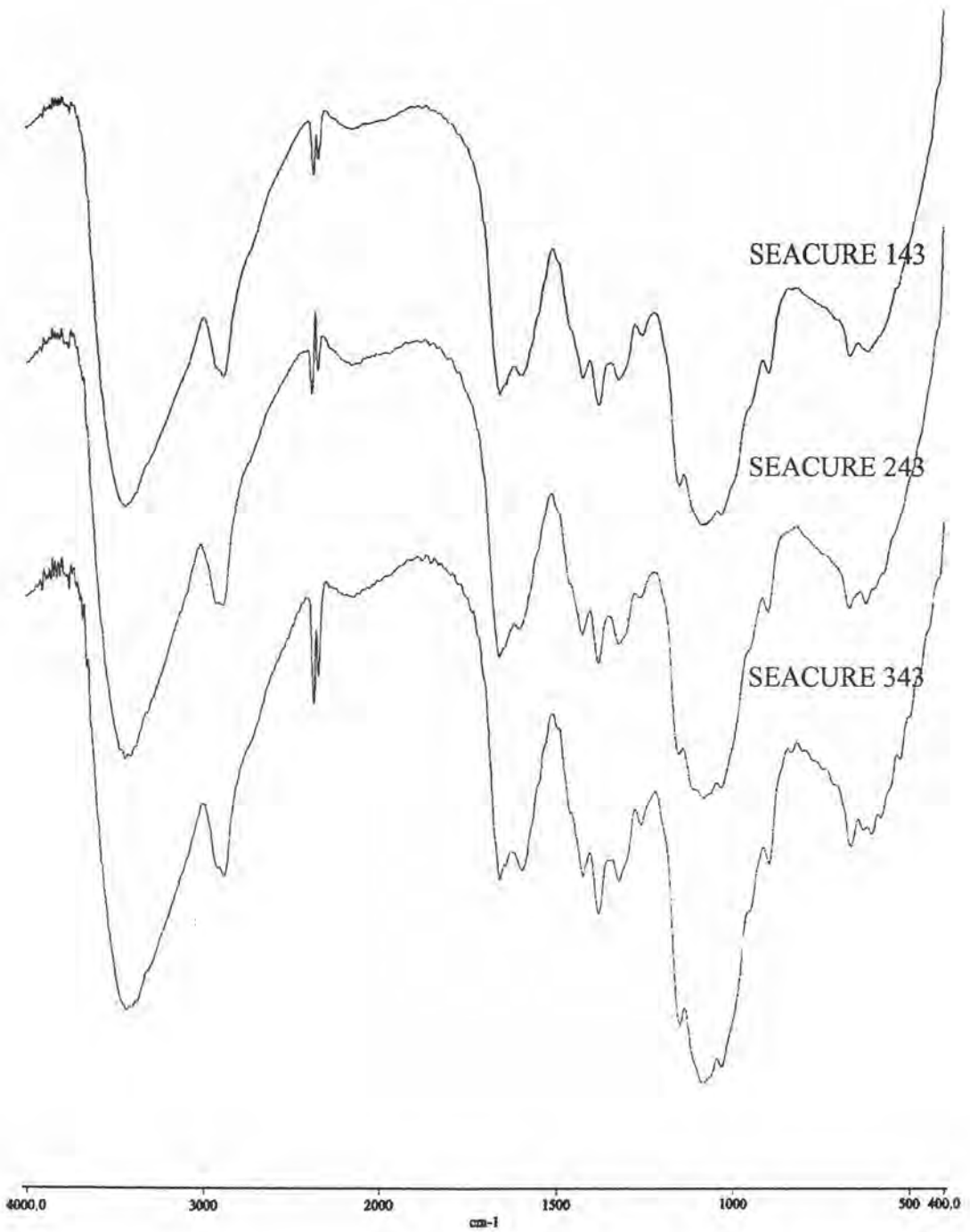

Figure 35 IR spectra of SEACURE 143, SEACURE 243 and SEACURE 343

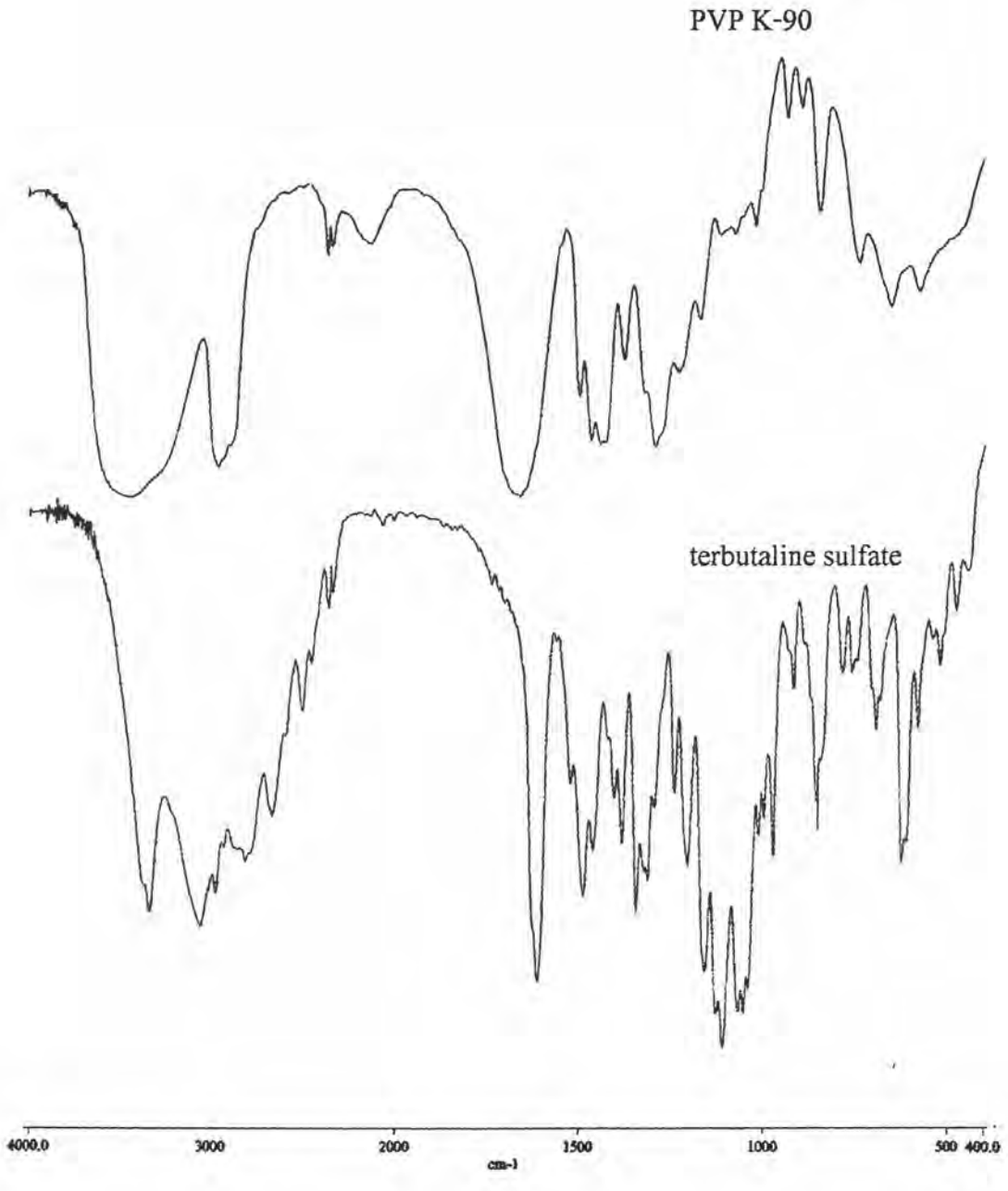

Figure 36 IR spectra of PVP K-90 and terbutaline sulfate

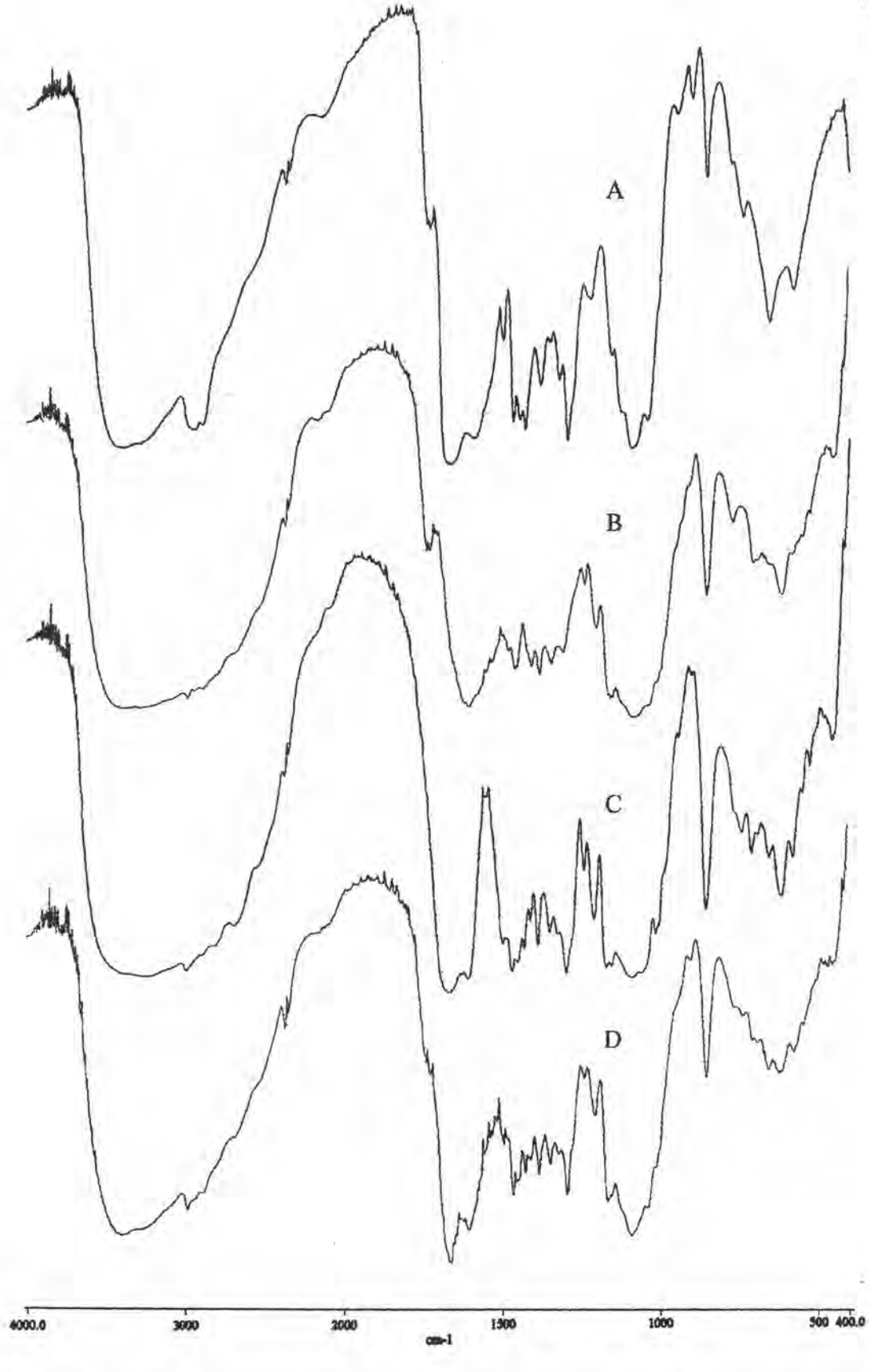

Figure 37 IR spectra of SEACURE 243 and PVP K-90 film (A); SEACURE 243 and terbutaline sulfate film (B); PVP K-90 and terbutaline sulfate film (C); SEACURE 243, PVP K-90 and terbutaline sulfate film (D)

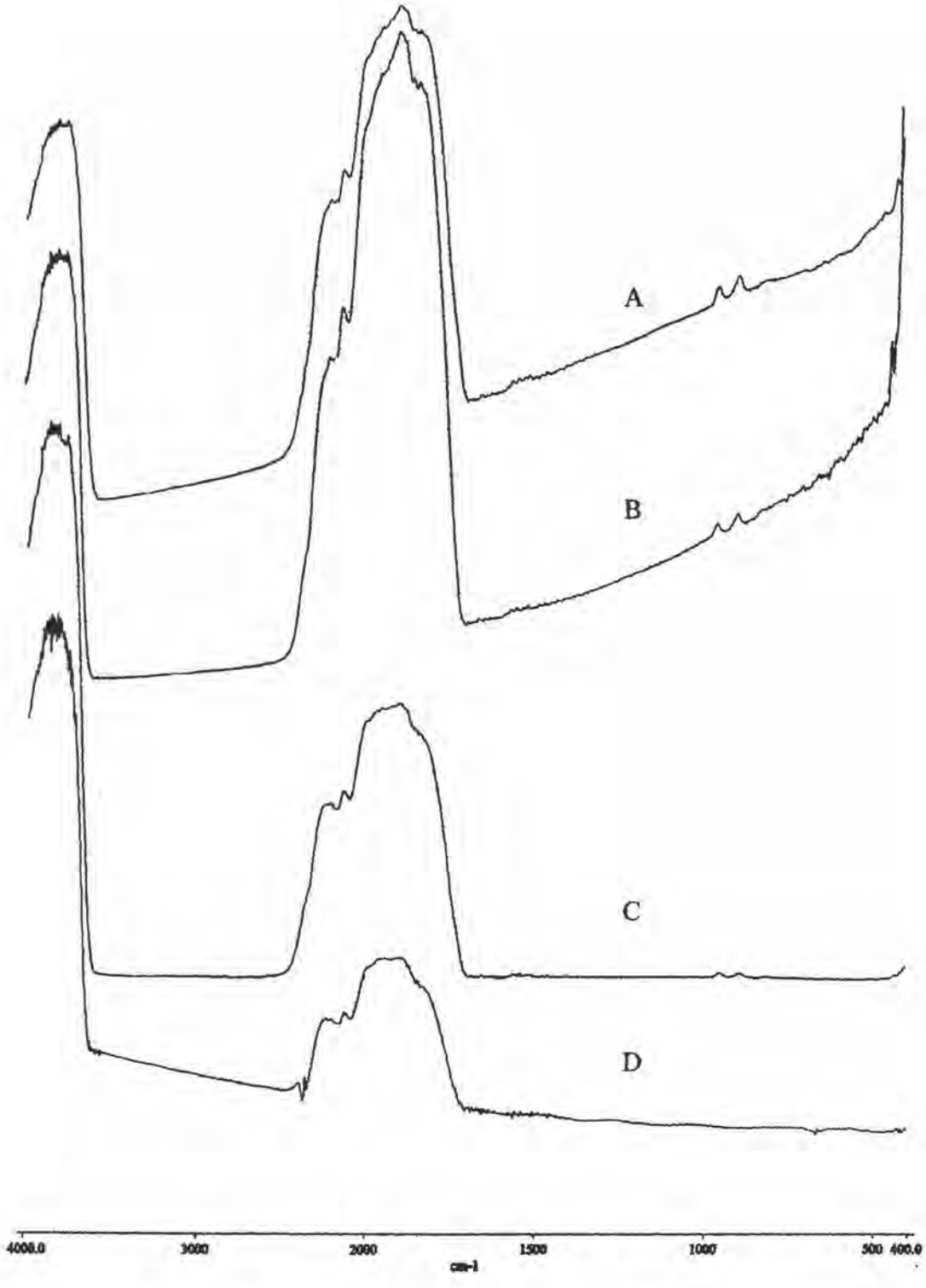

Figure 38 IR spectra of terbutaline sulfate transdermal patches; 10 %w/w PVP K-90 and 0.1 %w/w SEACURE 143 (A), 0.7 %w/w SEACURE 143 (B), 0.1 % w/w SEACURE 243(C) and 0.7 %w/w SEACURE 243(D) (Formulations A_1, A_4, B_1 and B_4 respectively)

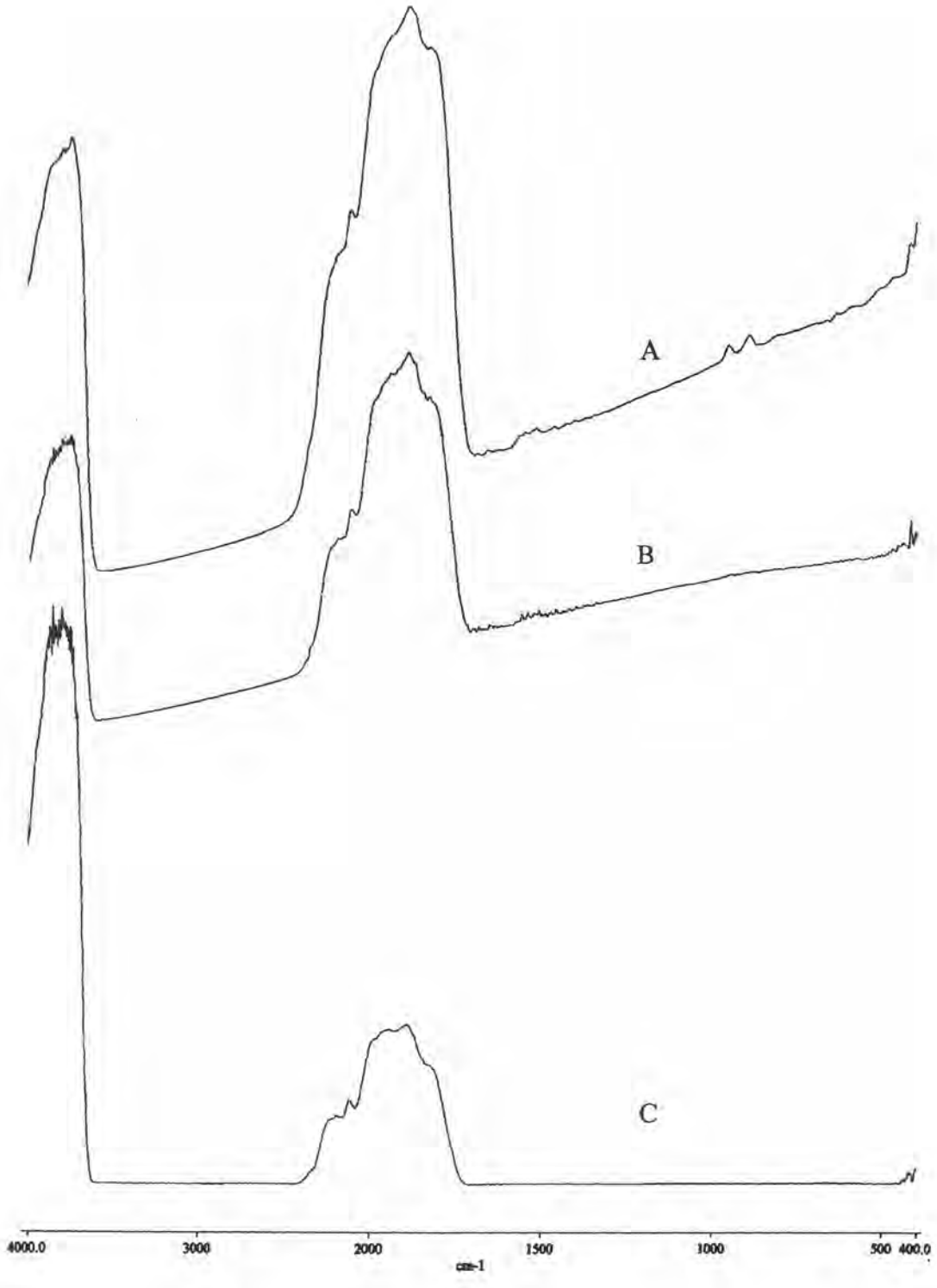

Figure 39 IR spectra of terbutaline sulfate transdermal patches; 15 %w/w PVP K-90 and 0.1 %w/w SEACURE 143 (A), 0.1 %w/w SEACURE 243 (B) and 0.1 %w/w SEACURE 343 (C) (Formulations AA_1, BB_1 and CC_1 respectively)

2.8 Powder X-ray Diffraction Analysis

The X-ray diffraction patterns of three grades of chitosan powders and films are illustrated in Figure 40. The X-ray diffractograms of chitosan powders showed a large diffraction peak at about 20° 2θ and a minor diffraction peak at 10.4° 2θ. Ogawa (1991) had proposed chitosan into three forms: non-crystalline, anhydrous crystalline and hydrated crystalline. The hydrated form showed a reflection at an angle of 10.4 ° 2θ, whereas the anhydrous form showed a reflection at an angle of 15 ° 2θ. The intensities of diffraction peak of hydrated form decreased in the following order: SEACURE 143 > SEACURE 243 > SEACURE 343 for chitosan powders. The X-ray diffraction patterns of all chitosan powders did not show the reflection at 15 ° 2θ of anhydrous form.

The X-ray diffractograms of chitosan films showed the same position of reflection as those of chitosan powders. However, the intensities of the diffraction peak of chitosan lactate films were weaker than those of chitosan powders, especially peak at about 20° 2θ. The result indicated that crystallinity of salt form of chitosan film was less than neutral form of chitosan powder. The intensities of hydrated form at 10.4° 2θ did not show distinct difference for all grades of chitosan films.

2.9 Differential Scanning Calorimetry

The DSC thermograms of pure polymers, terbutaline sulfate, drug-free films and selected terbutaline sulfate transdermal patches are exhibited in Figures 41 to 48 and summarized in Table 19.

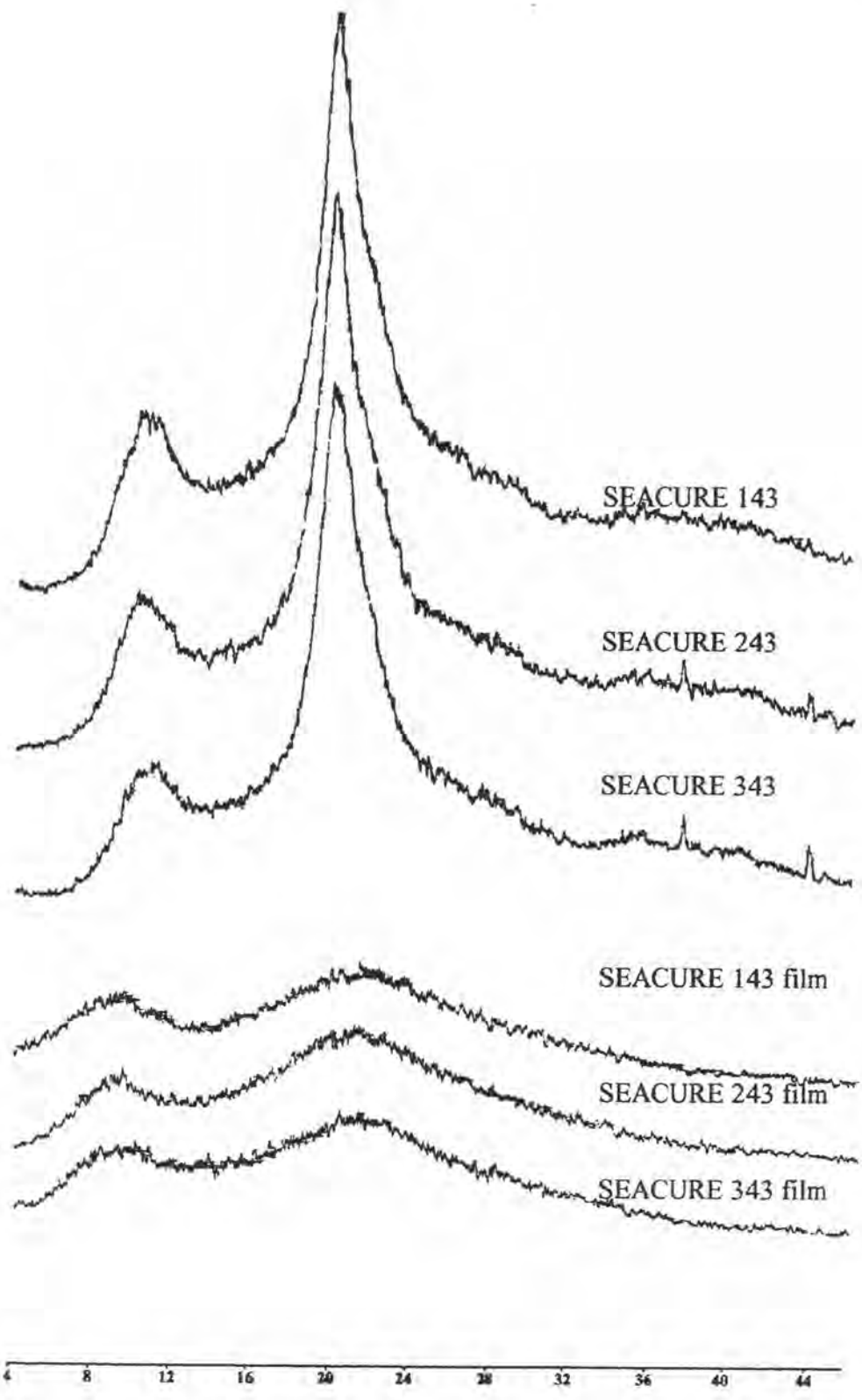

Figure 40 X-ray diffractograms of SEACURE 143, SEACURE 243, SEACURE 343, SEACURE 143 film, SEACURE 243 film and SEACURE 343 film

The DSC thermograms of pure polymer substances; SEACURE 143, 243 and 343 showed melting endotherm at 190.7, 211.7 and 216.0 °C respectively (Figure 41); PVP K-90 showed melting endotherm at 138.6 °C. Terbutaline sulfate showed melting endotherm at 267.4 °C (Figure 42). Ahuja and Ashman (1990) reported that terbutaline sulfate melted with decomposition. Melting points determined by DSC for batches of terbutaline sulfate identified as crystal form A and crystal form B ranged from 264.0 to 271.0 °C and 258.0 to 260.0 °C respectively. Thus in this experiment, terbutaline sulfate should be identified as crystal form A.

All obtained drug-free films and terbutaline sulfate transdermal patches thermograms did not show any separation peak of pure polymer. The DSC thermograms of all films were different in pattern and endothermic temperature.

DSC thermograms of 0.7 %w/w SEACURE 243 film, plasticized 0.7 %w/w SEACURE 243 film and plasticized 15 %w/w PVP K-90 film showed endothermic peaks at 139.5, 166.3 and 138.2 °C respectively (Figure 43).

DSC thermograms of polymer-polymer blend and drug-polymers blends are shown in Figure 44. SEACURE 243 and PVP K-90 film (ratio 1:1) exhibited melting endotherm at 146.6 °C. DSC thermograms of drug-polymers blends showed two endothermic peaks. The melting endotherm of SEACURE 243 and terbutaline sulfate film (ratio 1:1) was exhibited at 136.7 °C and 252.9 °C. PVP K-90 and terbutaline sulfate film (ratio 1:1) showed endothermic peak at 150.7 and 270.0 °C. SEACURE 243, PVP K-90 and terbutaline sulfate film (ratio 1:1:1) showed endothermic peak at 126.6 and 252.7 °C. The second melting endotherm of drug-polymers blends was different in pattern. SEACURE 243 and terbutaline sulfate blend film showed sharp peak, the others showed small and broad peak.

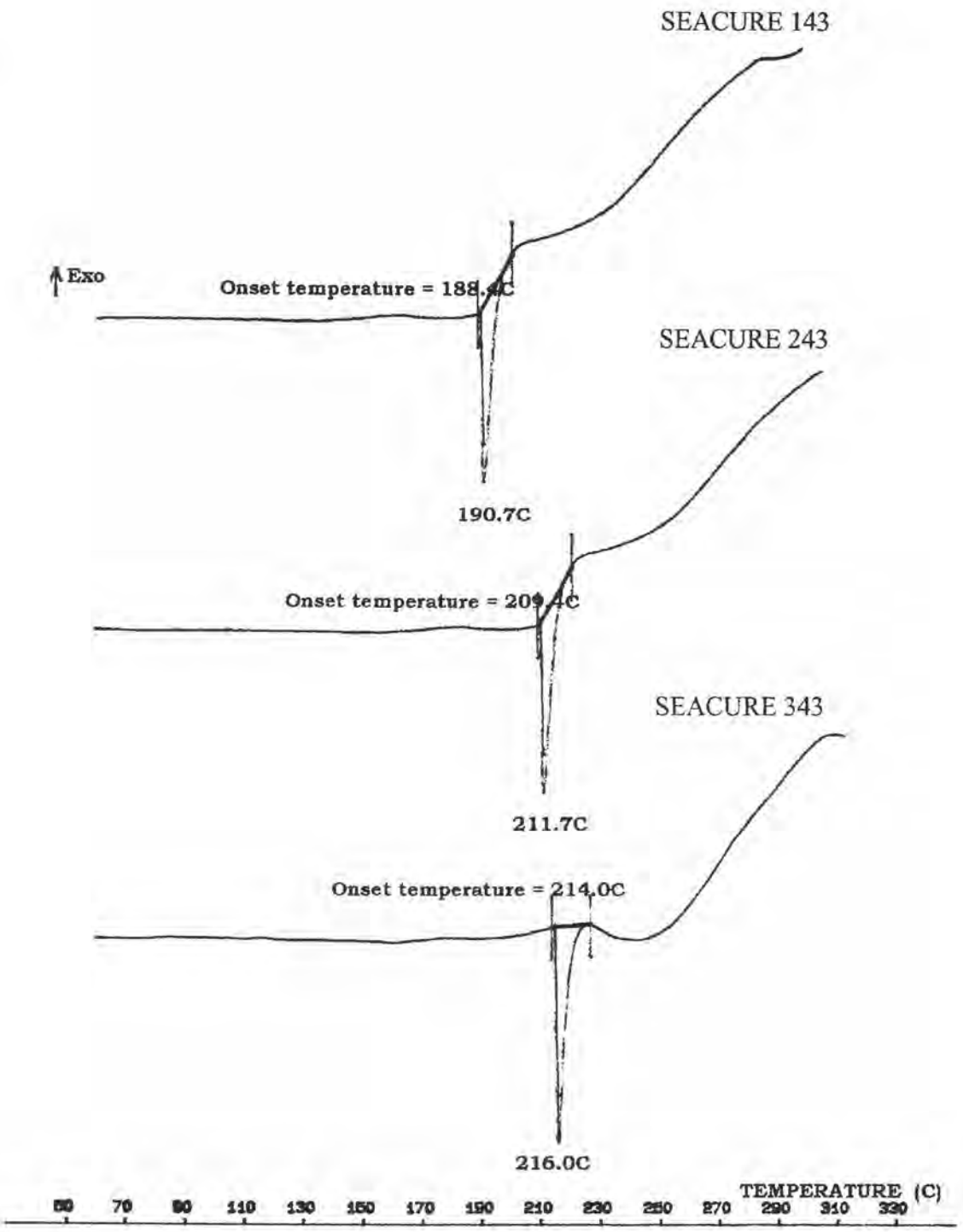

Figure 41 DSC thermograms of SEACURE 143, SEACURE 243 and SEACURE 343

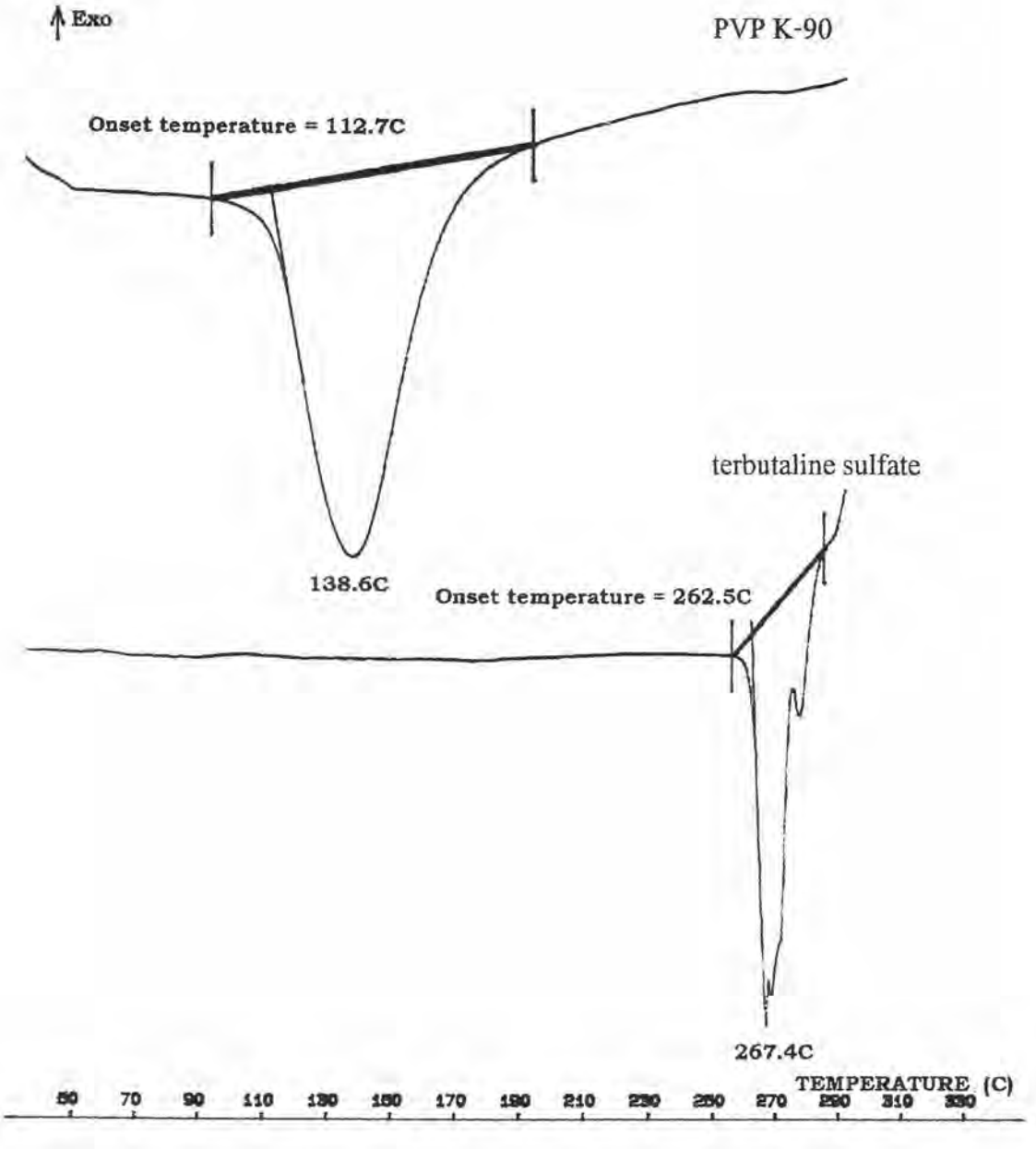

Figure 42 DSC thermograms of PVP K-90 and terbutaline sulfate

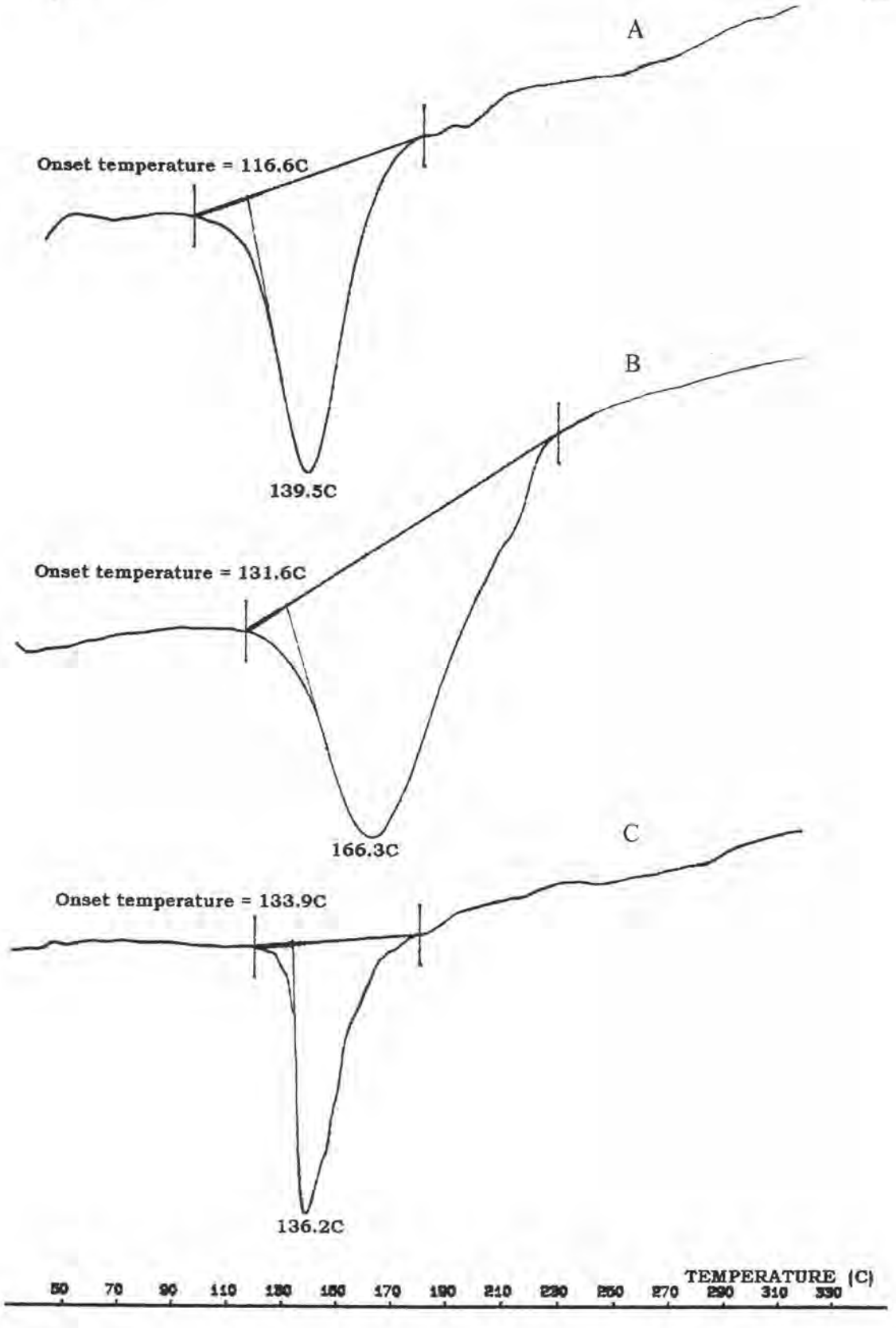

Figure 43 DSC thermograms of 0.7 %w/w SEACURE 243 film (A), plasticized 0.7 %w/w SEACURE 243 film (B) and plasticized 15 %w/w PVP K-90 film (C)

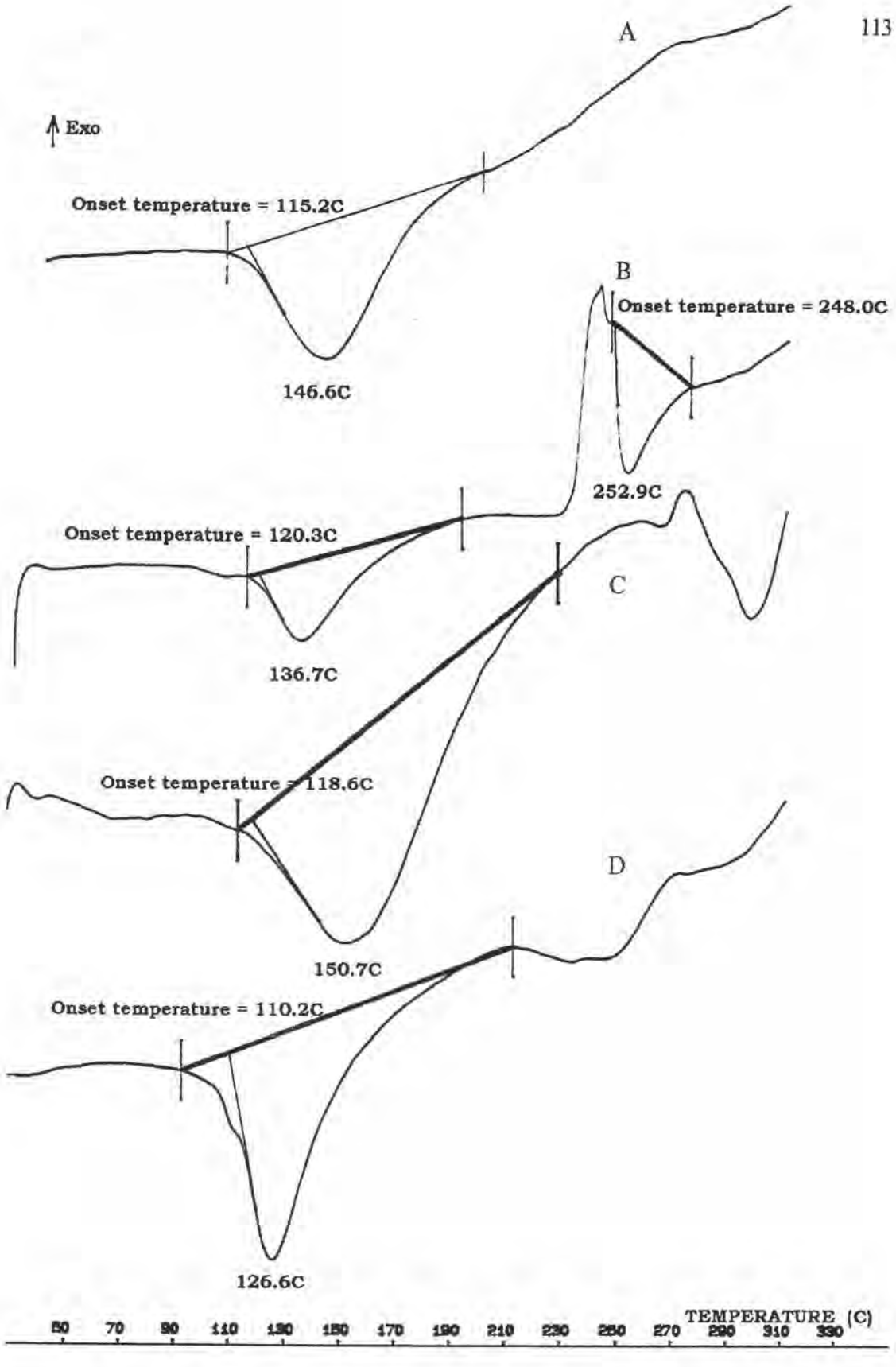

Figure 44 DSC thermograms of SEACURE 243 and PVP K-90 film (ratio1:1) (A); SEACURE 243 and terbutaline sulfate film (ratio1:1) (B); PVP K-90 and terbutaline sulfate film (ratio1:1) (C); SEACURE 243, PVP K-90 and terbutaline sulfate film (ratio1:1:1) (D)

Terbutaline sulfate transdermal patches prepared by using 10%w/w PVP K-90 and 0.1 %w/w SEACURE 143 (A_1) exhibited the first melting endotherm at 169.3 °C and the second melting endotherm at 276.7 °C. The onset temperature of terbutaline sulfate was 254.0 °C (Figure 45).

The obtained thermogram of 10 %w/w PVP K-90 and 0.1 %w/w SEACURE 243 (B_1) showed the higher first melting endotherm at 202.3 °C and the second melting endotherm at 276.8 °C. The first endothermic peak was sharp (Figure 45).

DSC thermogram of 10 %w/w PVP K-90 and 0.1 %w/w SEACURE 343 (C_1) showed the first melting endotherm at 139.2 °C lower than from films prepared using SEACURE 143 and 243. The pattern of endotherm showed broader peak than from film prepared using SEACURE 243. Melting endotherm of terbutaline sulfate was shown at 276.4 °C (Figure 45).

The effect of chitosan concentration on DSC thermogram was examined. DSC thermograms of film prepared by using 15 %w/w of PVP K-90 with 0.1 and 0.7 %w/w SEACURE 143 (AA_1 and AA_4 respectively) showed first endotherm at 142.4 and 162.2 °C respectively (Figure 46). The higher chitosan concentration led to the higher melting endothermic temperature and broader endothermic peak.

DSC thermogram of film prepared by using 15 %w/w of PVP K-90 and 0.7 %w/w SEACURE 243 (BB_4) showed first endotherm at 146.8 °C which was higher than that of film prepared by using 0.1 %w/w SEACURE 243 (BB_1) (Figure 47).

The effect of PVP K-90 concentration was shown in lower first melting endotherm and broader peak width when higher concentration was used. The first

melting endotherm was exhibited at 202.3 and 136.6 °C (Figures 45 and 47 respectively) for film prepared using 0.1 %w/w SEACURE 243 with 10 and 15 %w/w PVP K-90 respectively (B_1 and BB_1).

DSC thermograms of drug-free BB_1 and BB_4 showed the same melting endotherm at 156.2 °C (Figure 48) whereas DSC thermograms of BB_1 and BB_4 showed melting endotherm at 136.6 and 146.8 °C respectively (Figure 47).

2.9 Terbutaline Sulfate Content

A transdermal patch with a contact surface area of 1.77 cm^2 and a total terbutaline sulfate content of 15 mg was prepared in this study. Content of terbutaline sulfate in transdermal patches is presented in Table 20. The transdermal patches contained not less than 90.0 percent (13.5 mg) and not more than 110.0 percent (16.5 mg) of the labeled amount of terbutaline sulfate. The results indicated that terbutaline sulfate content was in the range of 13.5-16.5 mg.

3. *In-vitro* Evaluation

3.1 The Permeability of Terbutaline Sulfate through Shed Snake Skin

The average cumulative amount of terbutaline sulfate skin permeation per surface area from terbutaline sulfate saturated solution is shown in Table 21 and Figure 49.

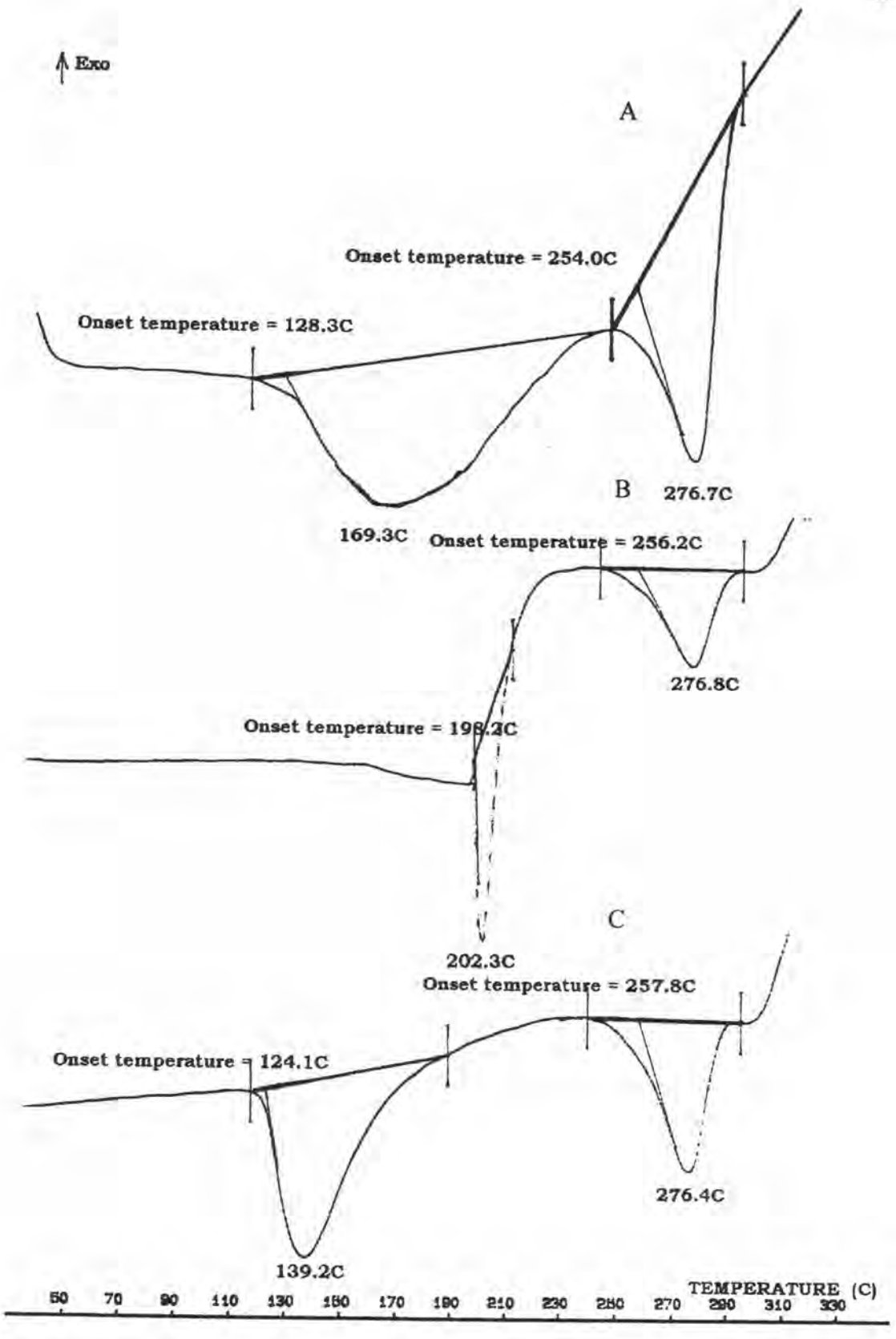

Figure 45 DSC thermograms of terbutaline sulfate transdermal patches 10 %w/w PVP K-90 and 0.1%w/w SEACURE 143 (A); 0.1 %w/w SEACURE 243 (B); 0.1 %w/w SEACURE 343 (C) (Formulations A_1, B_1 and C_1 respectively)

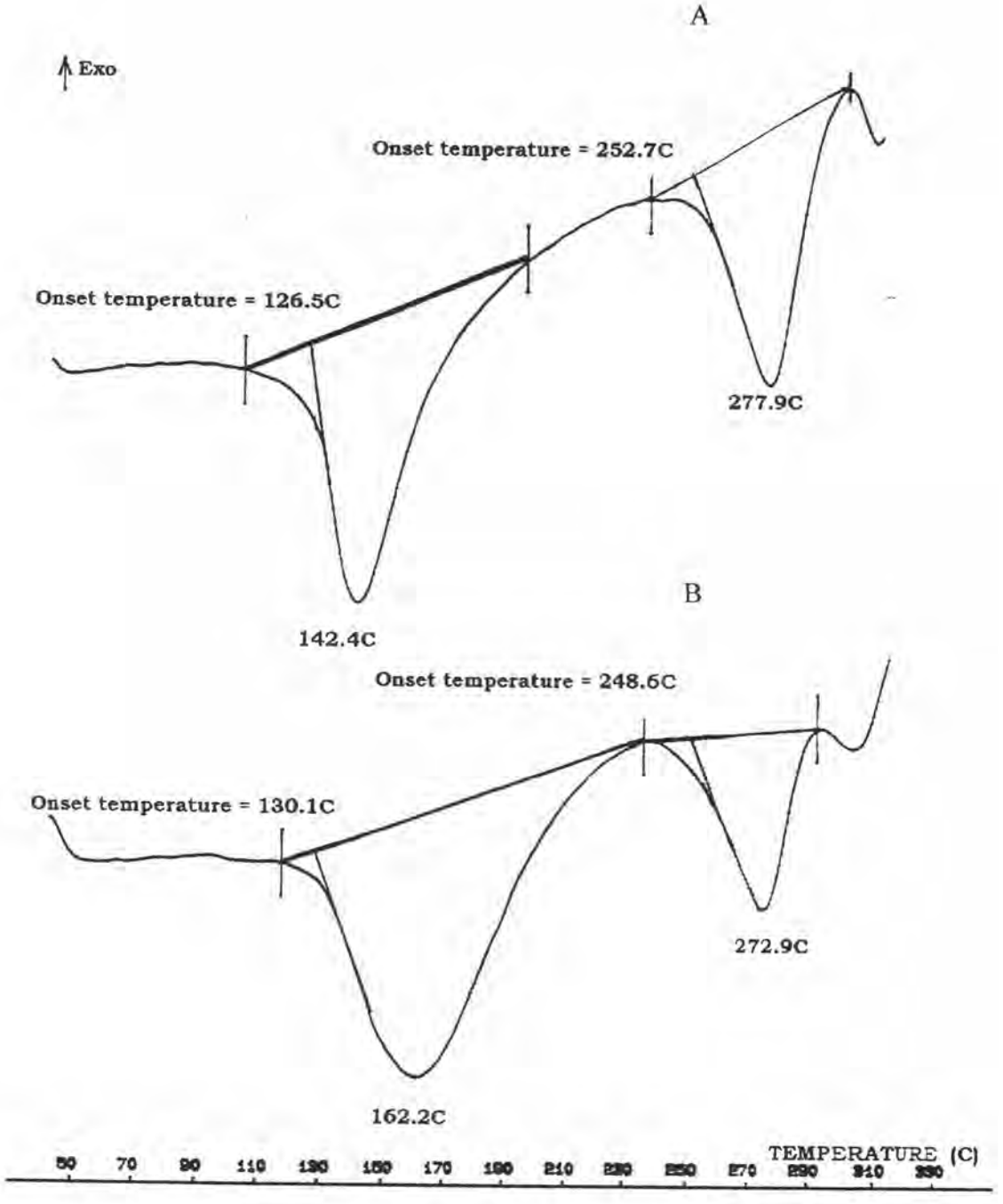

Figure 46 DSC thermograms of terbutaline sulfate transdermal patches 15 %w/w PVP K-90 and 0.1 %w/w SEACURE 143 (A); 0.7 %w/w SEACURE 143 (B) (Formulations AA_1 and AA_2 respectively)

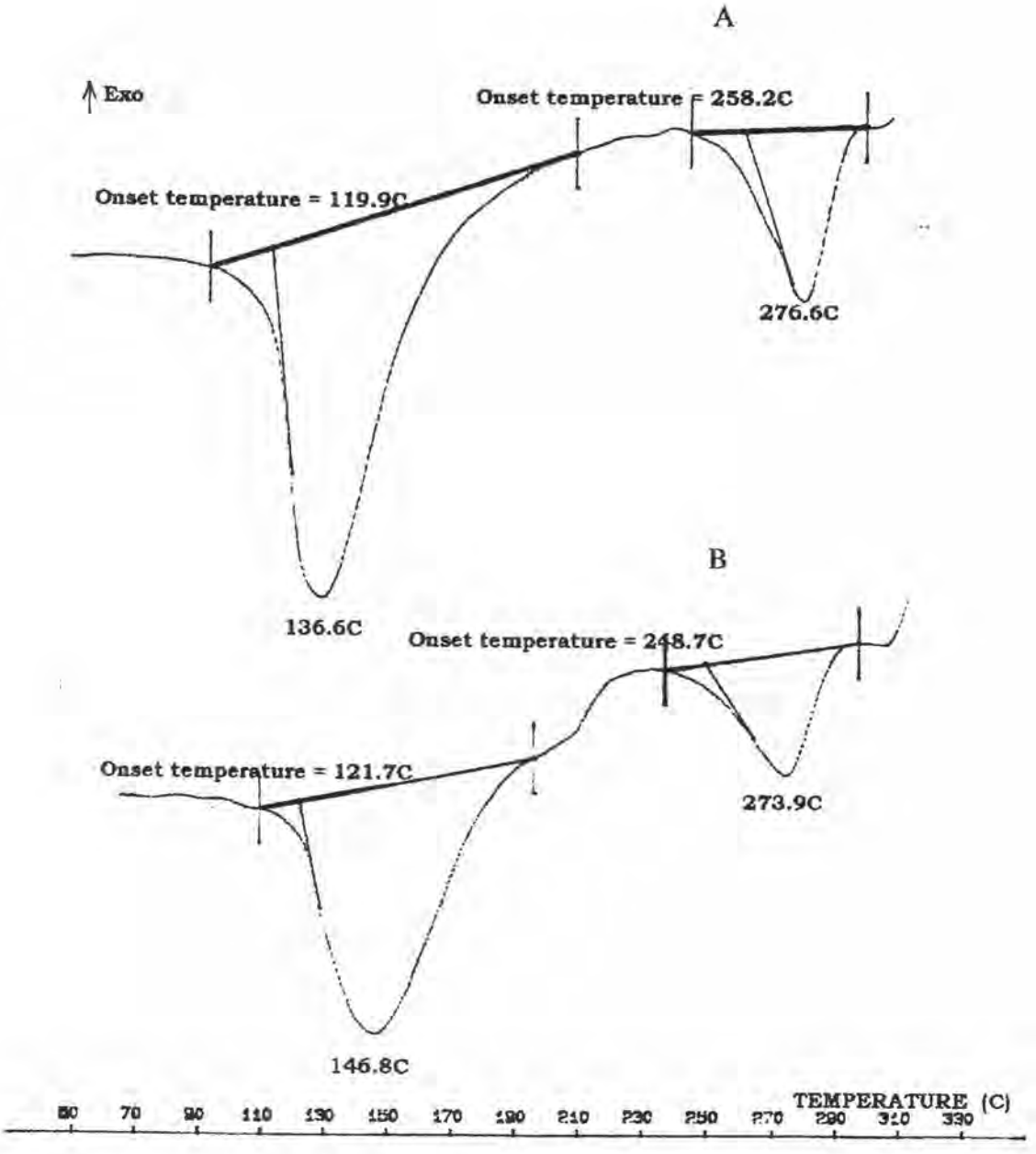

Figure 47 DSC thermograms of terbutaline sulfate transdermal patches 15 %w/w PVP K-90 and 0.1 %w/w SEACURE 243 (A): 0.7 %w/w SEACURE 243 (B) (Formulations BB_1 and BB_4 respectively)

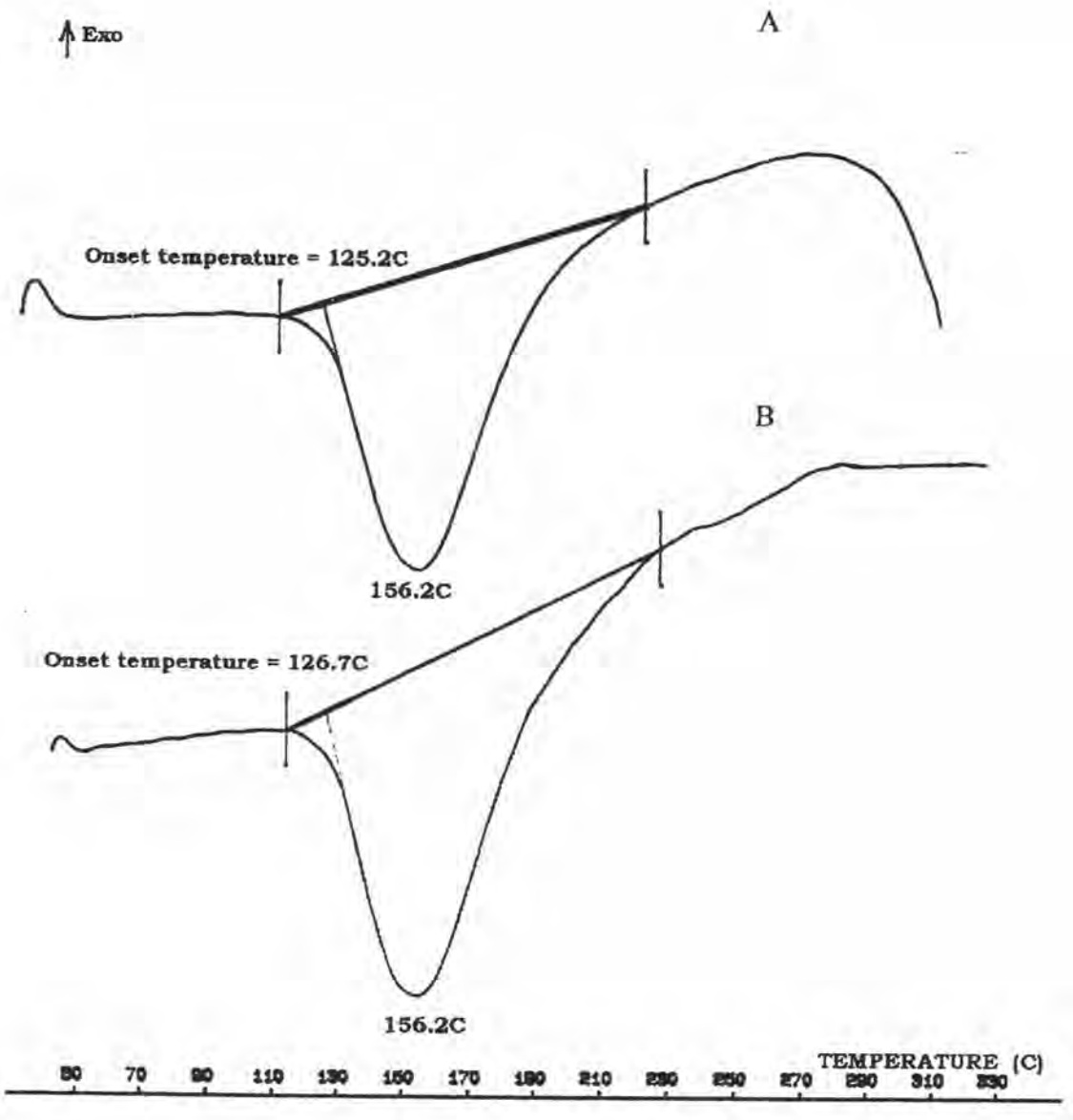

Figure 48 DSC thermograms of plasticized 0.1 %w/w SEACURE 243 and 15 %w/w PVP K-90 film (A); 0.7 %w/w SEACURE 243 and 15 %w/w PVP K-90 film(B)(Formulations BB_1 without drug and BB_4 without drug respectively)

Table 19 DSC peak temperature of pure substances, drug-free films and terbutaline sulfate transdermal patches

Sample	Order of DSC peak temperature (°C)	
	1	2
SEACURE 143	190.7	-
SEACURE 243	211.7	-
SEACURE 343	216.0	-
PVP K-90	138.6	-
Terbutaline sulfate	267.4	-
0.7 %w/w SEACURE 243 film	139.5	-
Plasticized 0.7 %w/w SEACURE 243 film	166.3	-
Plasticized 15 %w/w PVP K-90 film	138.2	-
SEACURE 243 and PVP K-90 film (1:1)	146.6	-
SEACURE 243 and terbutaline sulfate film(1:1)	136.7	252.9
PVP K-90 and terbutaline sulfate film (1:1)	150.7	270.0
SEACURE 243, PVP K-90 film and terbutaline sulfate film (1:1:1)	126.6	252.7
A_1	169.3	276.7
B_1	202.3	276.8
C_1	139.2	276.4
AA_1	142.4	277.9
AA_4	162.2	272.9
BB_1	136.6	276.6
BB_4	146.8	273.9
Drug-free BB_1	156.2	-
Drug-free BB_4	156.2	-

Table 20 Content of terbutaline sulfate in transdermal patches

Formulation	Content of terbutaline sulfate (mg)			Average	SD
	Sample 1	Sample 2	Sample 3		
A_1	14.354	14.477	13.468	14.100	0.551
A_2	14.477	13.509	13.901	13.962	0.487
A_3	14.313	13.674	14.725	14.237	0.529
A_4	14.004	14.045	14.766	14.271	0.429
B_1	13.509	13.406	13.653	13.523	0.124
B_2	13.447	13.756	13.736	13.646	0.173
B_3	15.075	13.674	13.880	14.210	0.756
B_4	16.517	14.416	15.508	15.480	1.051
C_1	14.004	13.489	14.704	14.065	0.610
C_2	14.148	13.468	15.611	14.409	1.095
C_3	13.777	15.425	15.384	14.862	0.940
C_4	15.260	14.766	14.951	14.993	0.250
AA_1	14.127	14.498	14.416	14.347	0.195
AA_2	13.241	13.489	15.096	13.942	1.007
AA_3	14.313	15.384	14.931	14.876	0.538
AA_4	13.921	13.282	14.725	13.976	0.723
BB_1	14.972	14.148	14.766	14.629	0.429
BB_2	14.890	14.498	14.581	14.656	0.206
BB_3	13.509	14.354	14.601	14.155	0.573
BB_4	14.457	13.839	14.622	14.306	0.413
CC_1	13.612	13.468	14.704	13.928	0.676
CC_2	15.549	13.921	14.766	14.745	0.814
CC_3	14.477	13.612	14.416	14.168	0.483
CC_4	14.766	13.736	15.075	14.526	0.701

Table 21 The average cumulative amount of terbutaline sulfate skin permeation per surface area ($\mu g/cm^2$) from terbutaline sulfate saturated solution (n=3)

Time (hrs)	Cumulative drug permeation ($\mu g/cm^2$)
0	0
1	6.806
2	13.776
4	37.961
6	77.834
8	125.544
12	161.316
16	219.140
20	305.911
24	395.972

Correlation coefficient = 0.9887

Regression equation y = 16.475 x - 20.877

where: x = time (hours)

y = cumulative amount of terbutaline sulfate per surface area ($\mu g/cm^2$)

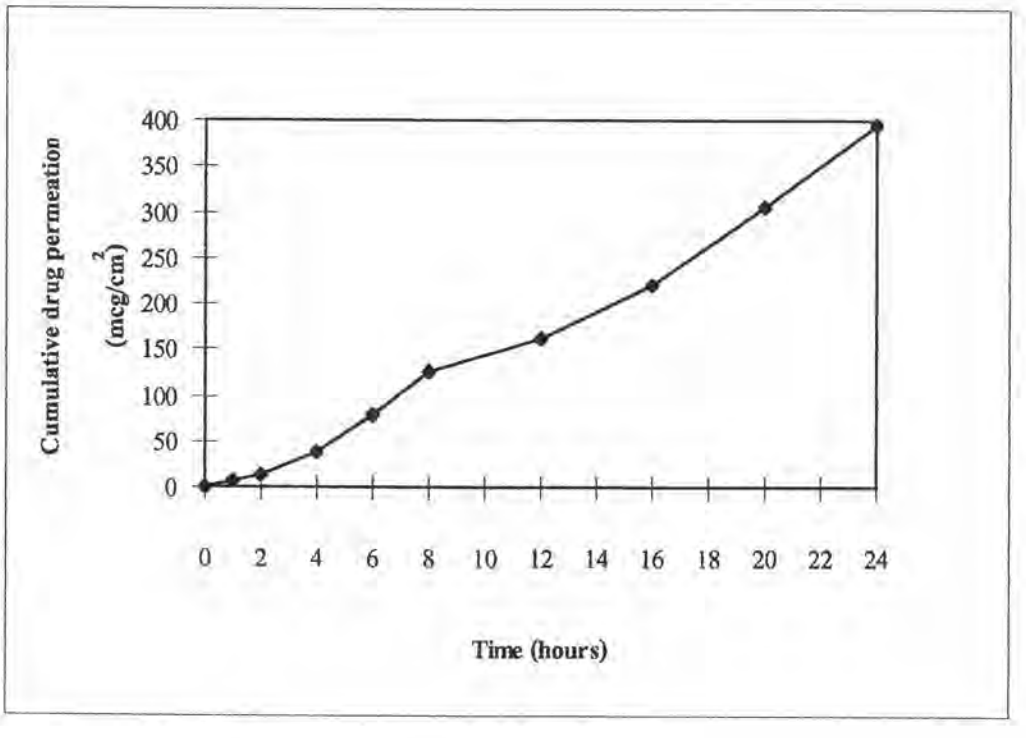

Figure 49 Skin permeation-time profile of terbutaline sulfate per surface area from terbutaline sulfate saturated solution

3.2 The *In-vitro* Permeation Study of Terbutaline Sulfate Transdermal Patches

In this study, selected terbutaline sulfate transdermal patches were examined for *in-vitro* permeation study. The results of skin permeation data of terbutaline sulfate transdermal patches are summarized in Appendix F. The average cumulative amount of terbutaline sulfate skin permeation per surface area ($\mu g/cm^2$) from various terbutaline sulfate transdermal patches are shown in Table 22. Figures 50 to 69 illustrate the skin permeation profiles of terbutaline sulfate transdermal patches. All data were presented as average cumulative permeation of terbutaline sulfate through skin. All preparations sustained permeation of terbutaline sulfate over 24 hours.

From the result, it could be seen that using 0.1 %w/w SEACURE 143 and 10% w/w PVP K-90 (A_1) as adhesive matrix gave the highest cumulative drug permeation through shed snake skin. The effect of chitosan concentration is shown in Figures 50 to 53. The results indicated that using lower concentration of chitosan led to higher drug permeated. The results were the same for all grades of chitosan. However, it could be seen that when using 15 %w/w of PVP K-90 in formulations BB_1 to BB_4 increasing chitosan concentration did not affect the amount of drug permeated.

The effect of molecular weight of chitosan was also examined. Figures 54 to 57 show the skin permeation profiles of terbutaline sulfate transdermal patches using the same concentrations of chitosan and PVP K-90 but varying the molecular weight of chitosan. The obtained results indicated that the higher molecular weight of chitosan led to lower amount of drug permeated.

To study the effect of concentration of PVP K-90 on the skin permeation profiles of terbutaline sulfate transdermal patches. PVP K-90 was used in a concentrations of 10 and 15 % w/w respectively. Figures 58 to 61 illustrate the skin permeation profiles of terbutaline sulfate transdermal patches which were prepared with SEACURE 243 in concentrations of 0.1, 0.3, 0.5 and 0.7 %w/w respectively. The results indicated that higher concentration of PVP K-90 decreased the amount of drug permeated. However, when using high concentration of chitosan the result indicated that the amount of drug permeated from higher concentration of PVP K-90 was not obviously different from that of drug permeated from lower concentration of PVP K-90.

Correlation coefficient and regression equation of the relationships between average cumulative amount of terbutaline sulfate permeation per surface area versus

time, average cumulative amount of terbutaline sulfate permeation per surface area versus square root time and log terbutaline sulfate remained per surface area versus time are shown in Table 23. The skin permeation profiles of average cumulative amount of drug per surface area versus square root time are presented in Figures 62 to 65. The skin permeation profiles of log drug remained per surface area versus time are illustrated in Figures 66-69. From all correlation coefficients, it could lead to the controlled release pattern. The correlation coefficients of relationships between cumulative amount of permeated drug against time and log drug remained against time were higher than the correlation coefficient of relationship between cumulative amount of permeated drug against square root time. However, the obtained results from analysis of variances of correlation coefficients from three kinetic patterns indicated that there was no significant difference in correlation coefficients from three kinetic patterns (Table 40 Appendix F). Thus, the drug permeation kinetic of all terbutaline sulfate transdermal patches seemed to follow the zero order, Higuchi's or first order pattern.

Table 22 The average cumulative amount of terbutaline sulfate skin permeation per surface area ($\mu g/cm^2$) from terbutaline sulfate transdermal patches (n=3)

Time	Cumulative drug permeation ($\mu g/cm^2$)							
(hrs)	A_1	A_2	A_3	A_4	B_1	B_2	B_3	B_4
0	0	0	0	0	0	0	0	0
1	8.619	6.905	5.109	3.012	7.612	6.957	3.012	0.000
2	11.402	8.875	7.063	4.030	9.756	8.050	4.597	3.045
4	14.908	11.447	8.902	5.163	12.154	10.315	6.541	4.419
6	18.423	14.482	12.184	7.672	14.925	12.714	8.664	7.340
8	20.452	16.529	14.398	10.082	17.908	15.949	11.701	8.306
12	23.835	20.566	16.835	12.701	22.194	19.162	15.481	11.312
16	27.788	24.130	20.171	16.487	25.607	22.759	19.551	13.703
20	32.377	27.420	22.433	19.450	29.656	25.691	22.985	15.355
24	38.891	31.747	27.977	22.585	33.444	29.673	25.828	19.489
Time	Cumulative drug permeation ($\mu g/cm^2$)							
(hrs)	C_1	C_2	C_3	C_4	BB_1	BB_2	BB_3	BB_4
0	0	0	0	0	0	0	0	0
1	7.095	5.094	0.000	0.000	0.000	0.000	0.000	0.000
2	8.724	6.905	3.012	0.000	4.284	3.986	4.199	4.014
4	10.956	8.938	4.634	3.987	4.676	4.504	4.634	4.527
6	14.351	11.770	6.932	6.574	7.372	7.129	6.932	6.730
8	15.538	13.811	10.238	7.273	9.081	7.975	7.618	7.789
12	20.117	17.122	13.759	9.465	11.491	11.359	11.571	10.587
16	22.761	21.143	17.061	10.650	13.975	12.936	12.651	12.554
20	26.359	24.382	21.516	12.823	17.104	15.508	15.015	15.501
24	30.583	27.346	23.832	14.526	18.235	17.792	16.956	16.247

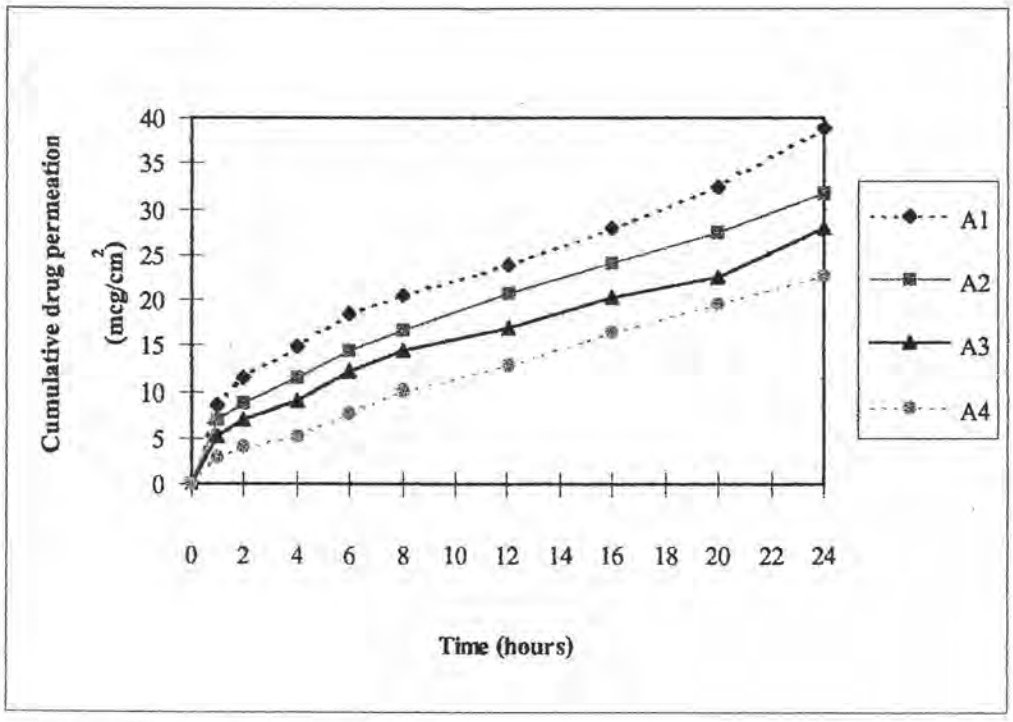

Figure 50 Effect of SEACURE 143 concentrations on skin permeation-time profiles of terbutaline sulfate transdermal patches (Formulations A_1-A_4)

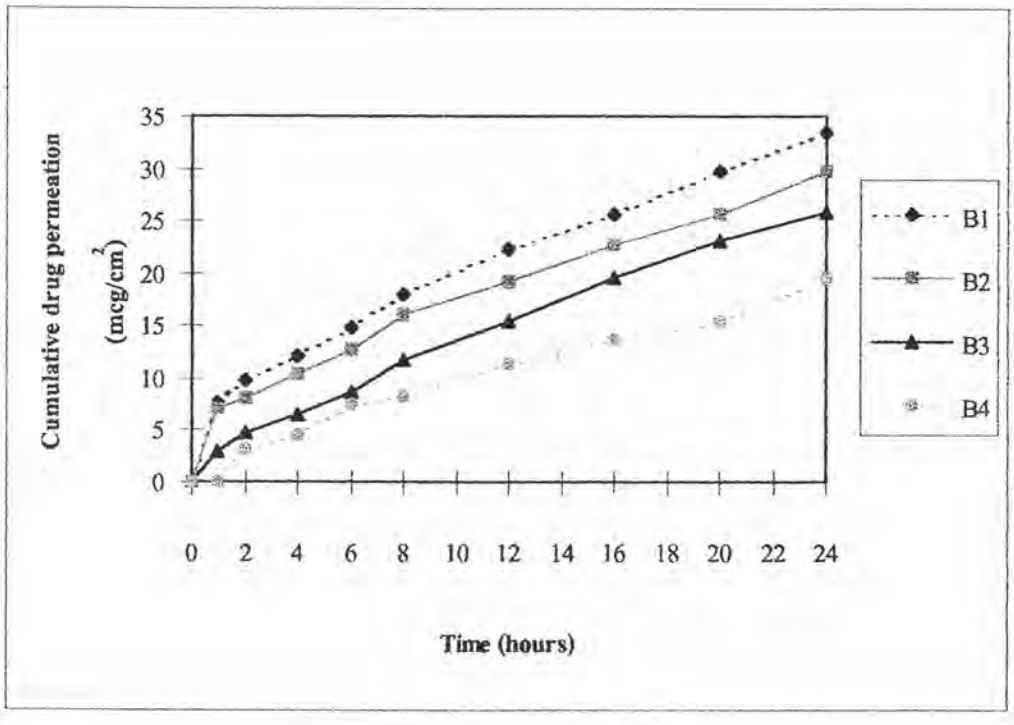

Figure 51 Effect of SEACURE 243 concentrations on skin permeation-time profiles of terbutaline sulfate transdermal patches (Formulations B_1-B_4)

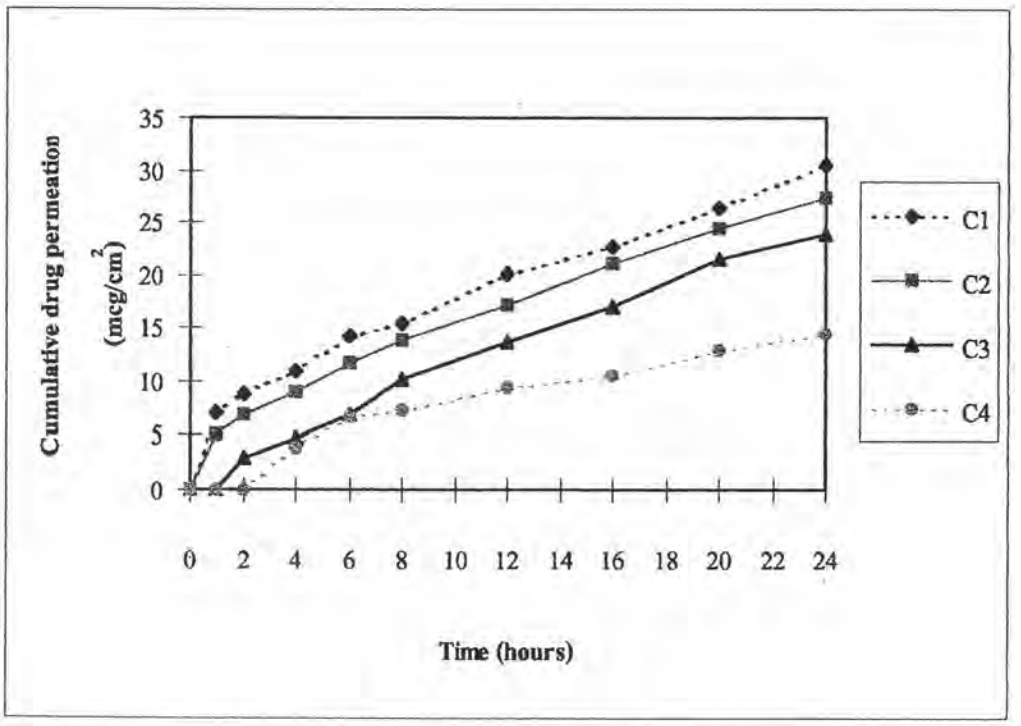

Figure 52 Effect of SEACURE 343 concentrations on skin permeation-time profiles of terbutaline sulfate transdermal patches (Formulations C_1-C_4)

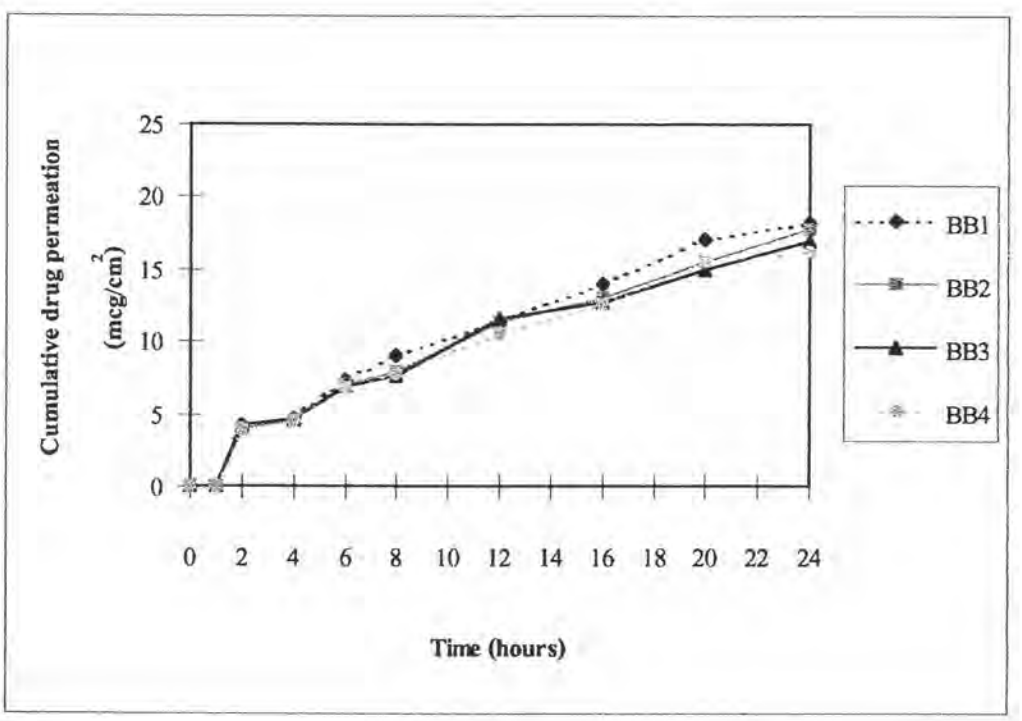

Figure 53 Effect of SEACURE 243 concentrations on skin permeation-time profiles of terbutaline sulfate transdermal patches (Formulations BB_1-BB_4)

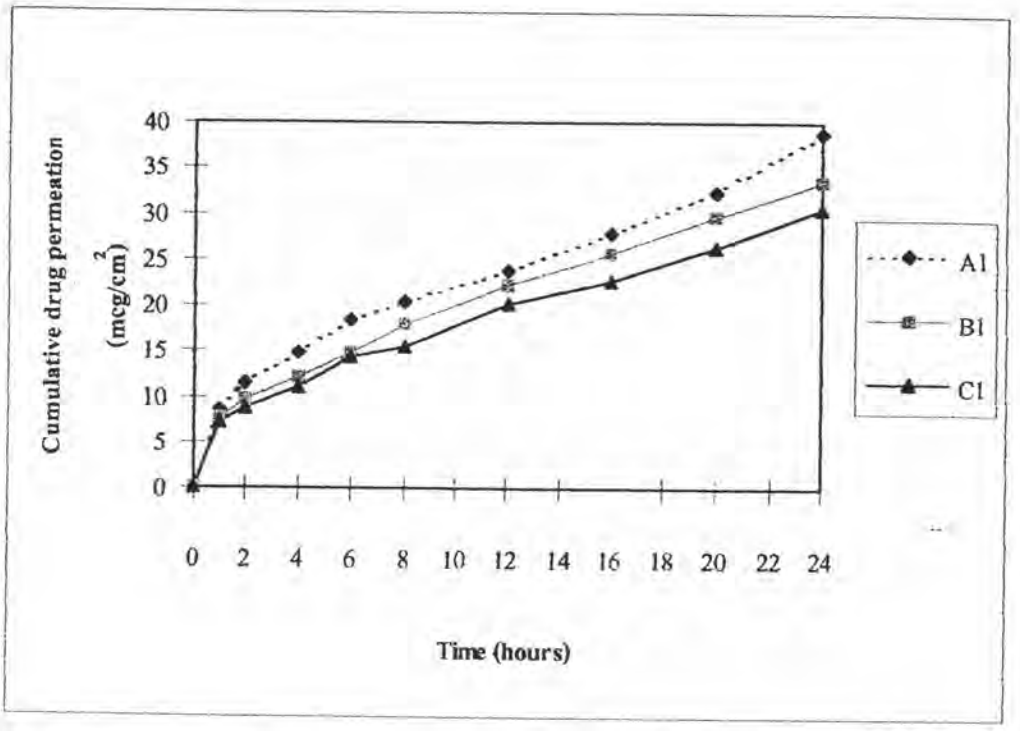

Figure 54 Effect of molecular weights of chitosan on skin permeation-time profiles of terbutaline sulfate transdermal patches (Formulations A_1, B_1 and C_1)

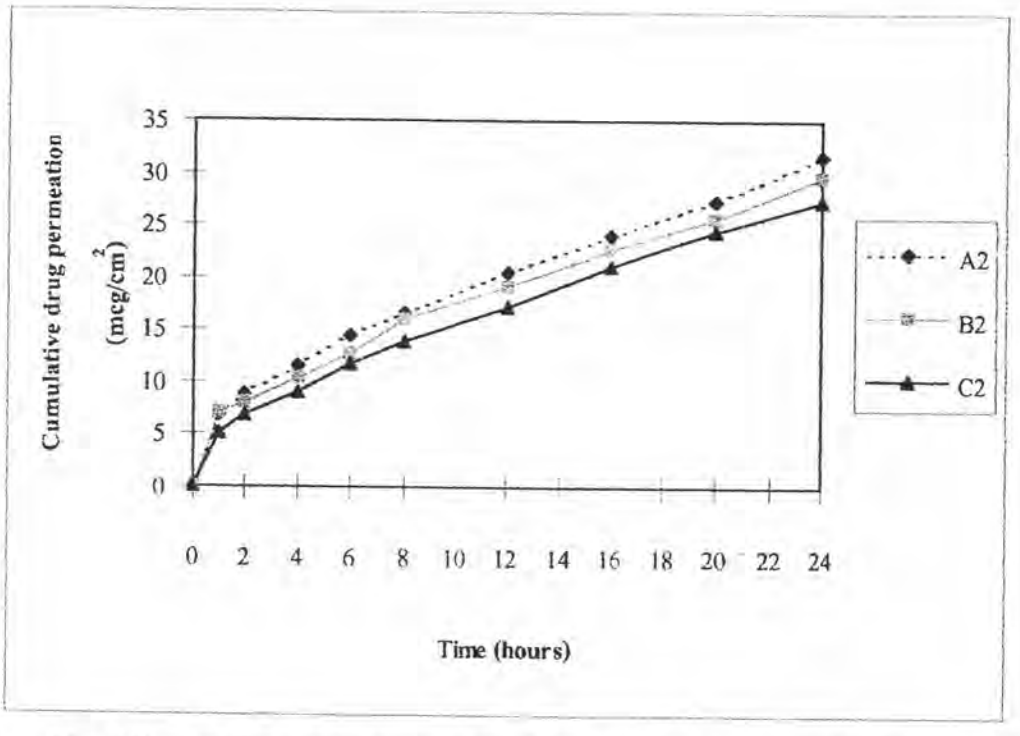

Figure 55 Effect of molecular weights of chitosan on skin permeation-time profiles of terbutaline sulfate transdermal patches (Formulations A_2, B_2 and C_2)

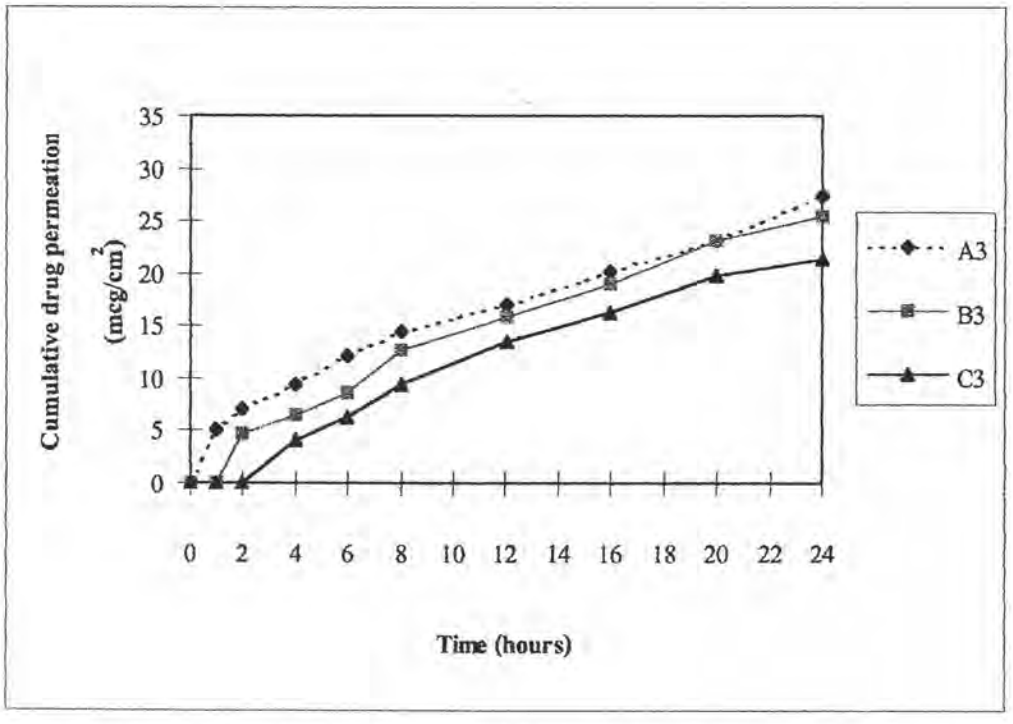

Figure 56 Effect of molecular weights of chitosan on skin permeation-time profiles of terbutaline sulfate transdermal patches (Formulations A_3, B_3 and C_3)

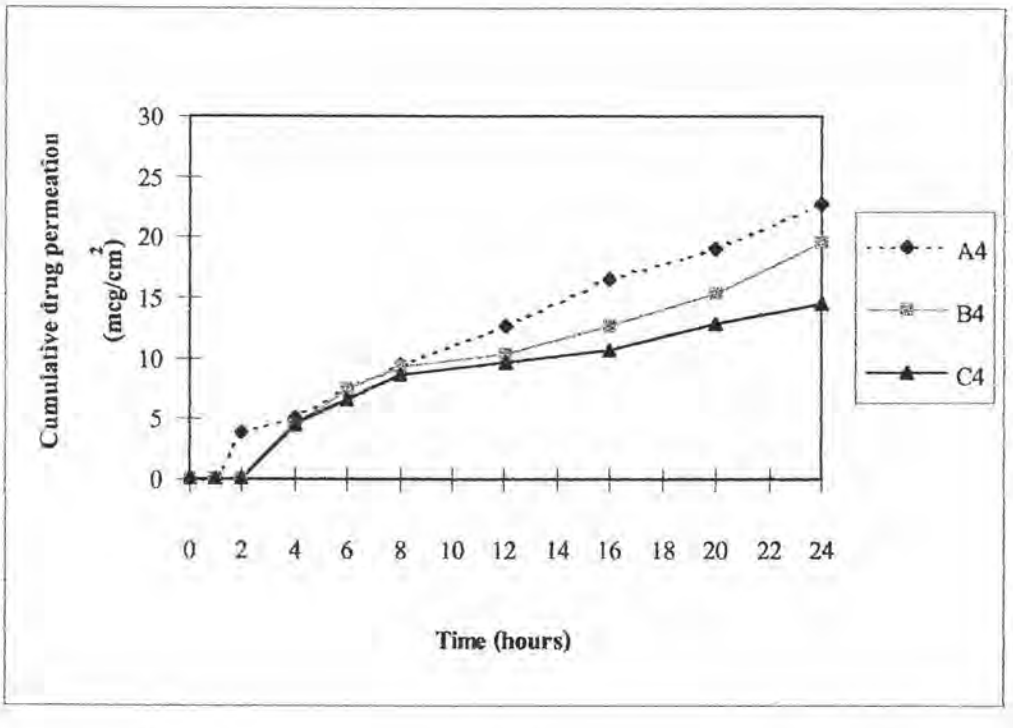

Figure 57 Effect of molecular weights of chitosan on skin permeation-time profiles of terbutaline sulfate transdermal patches (Formulations A_4, B_4 and C_4)

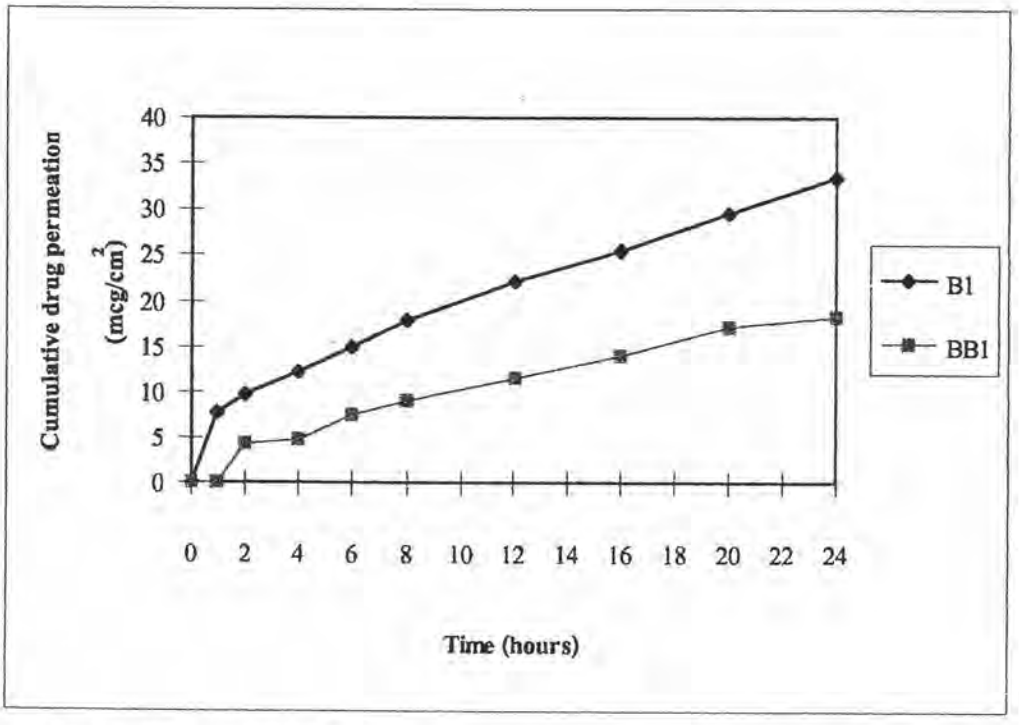

Figure 58 Effect of PVP K-90 concentrations on skin permeation-time profiles of terbutaline sulfate transdermal patches (Formulations B_1 and BB_1)

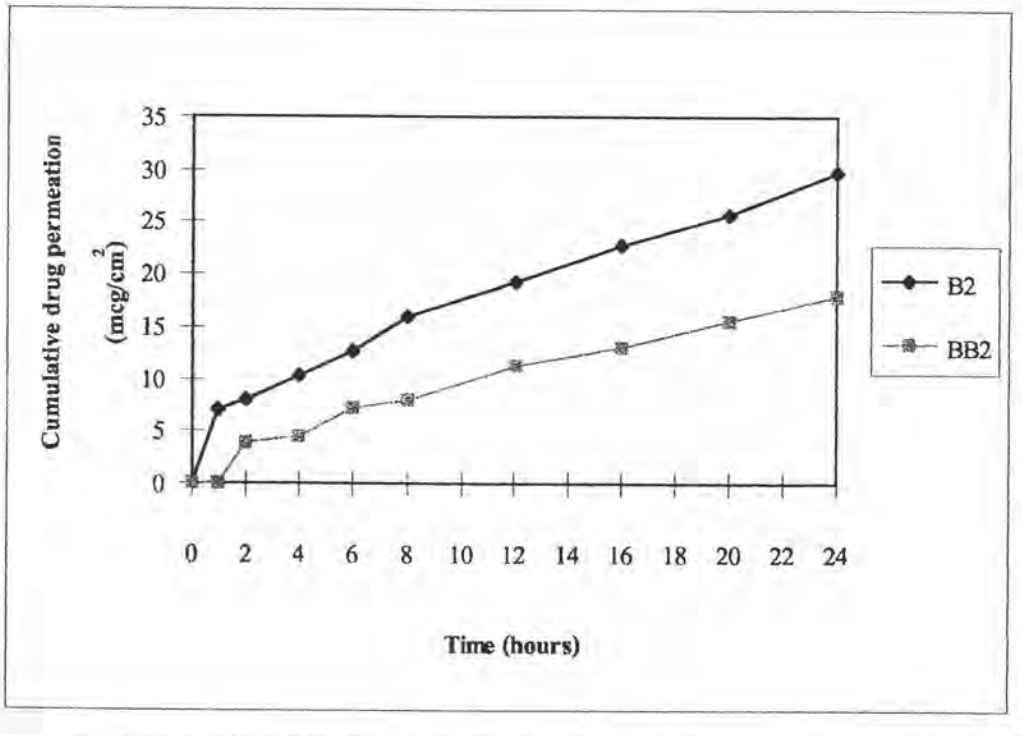

Figure 59 Effect of PVP K-90 concentrations on skin permeation-time profiles of terbutaline sulfate transdermal patches (Formulations B_2 and BB_2)

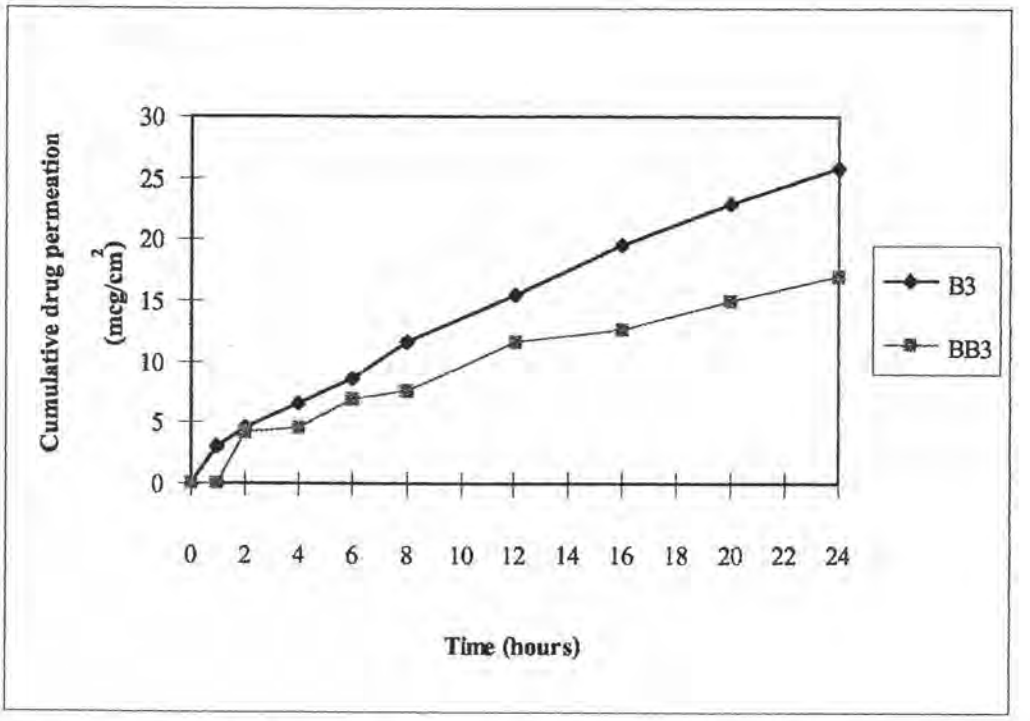

Figure 60 Effect of PVP K-90 concentrations on skin permeation-time profiles of terbutaline sulfate transdermal patches (Formulations B_3 and BB_3)

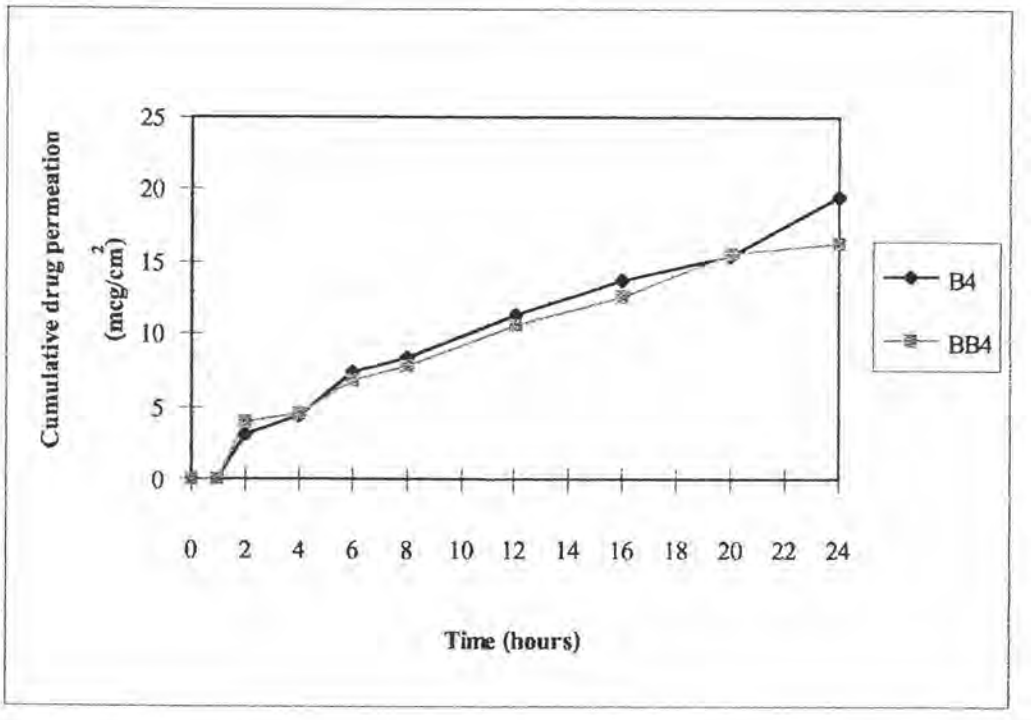

Figure 61 Effect of PVP K-90 concentrations on skin permeation-time profiles of terbutaline sulfate transdermal patches (Formulations B_4 and BB_4)

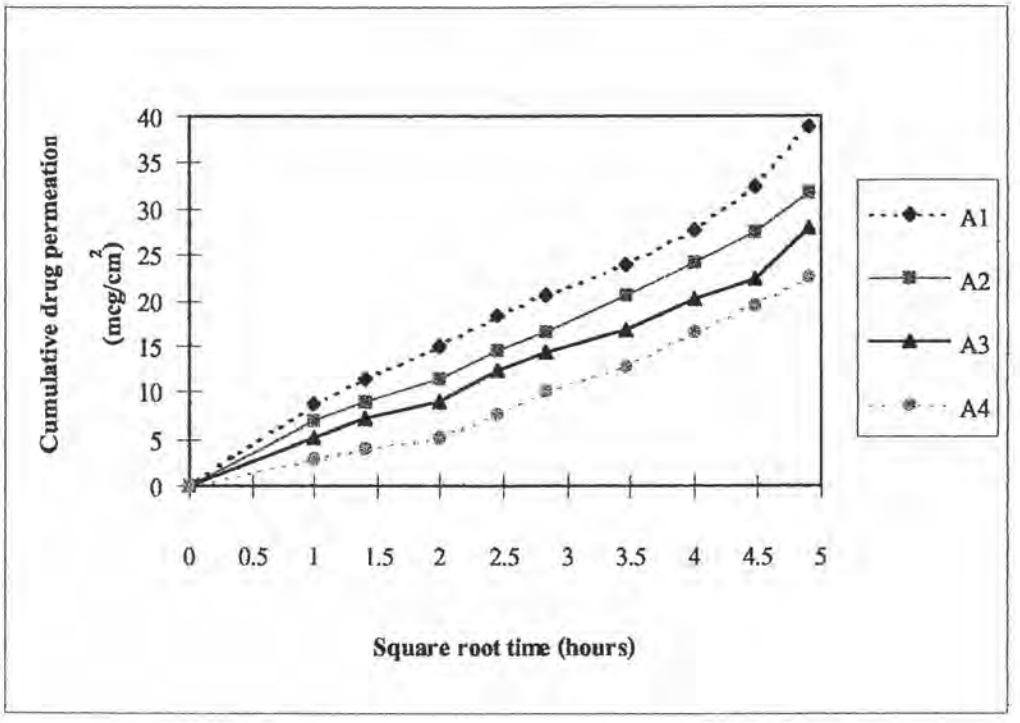

Figure 62 Higuchi's plot of skin permeation-square root of time profiles of terbutaline sulfate transdermal patches (Formulations A_1-A_4)

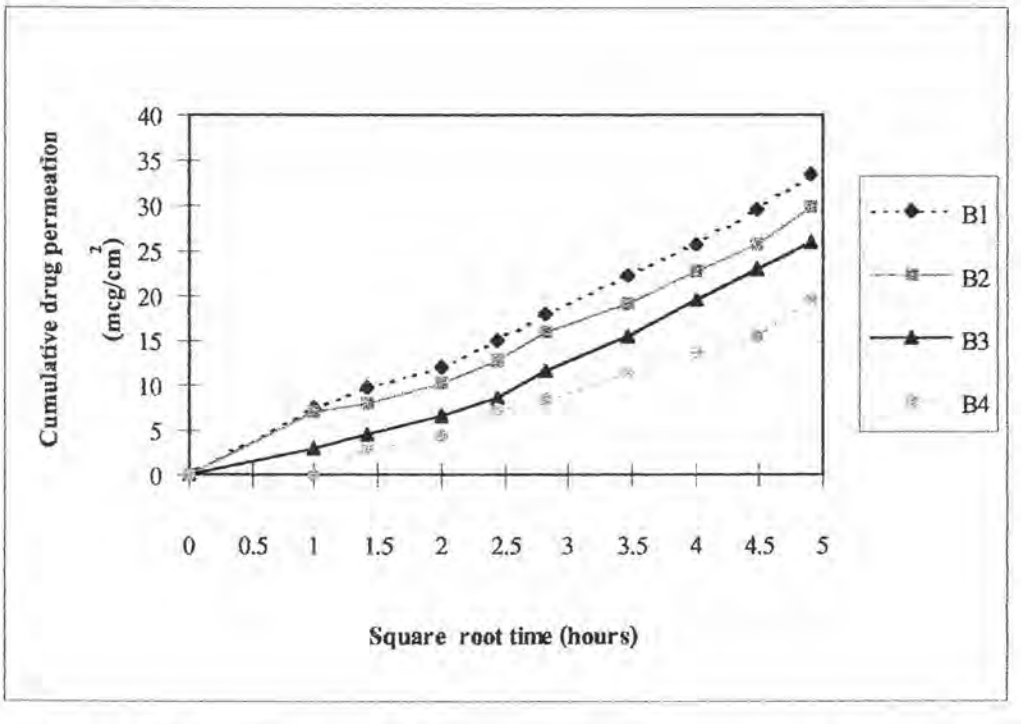

Figure 63 Higuchi's plot of skin permeation-square root of time profiles of terbutaline sulfate transdermal patches (Formulations B_1-B_4)

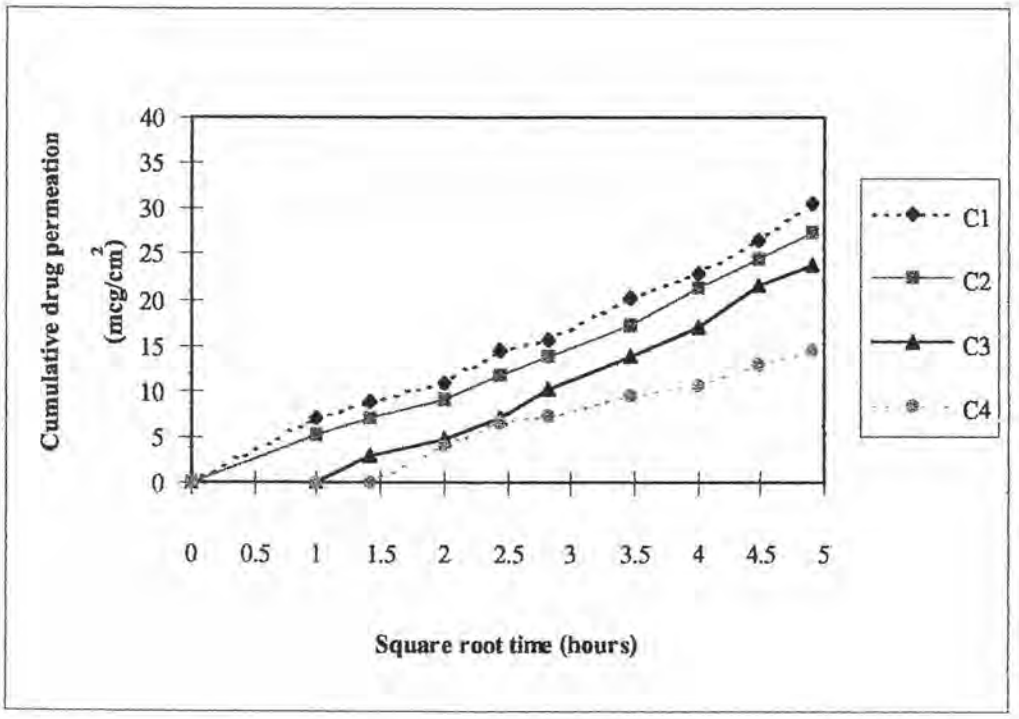

Figure 64 Higuchi's plot of skin permeation-square root of time profiles of terbutaline sulfate transdermal patches (Formulations C_1-C_4)

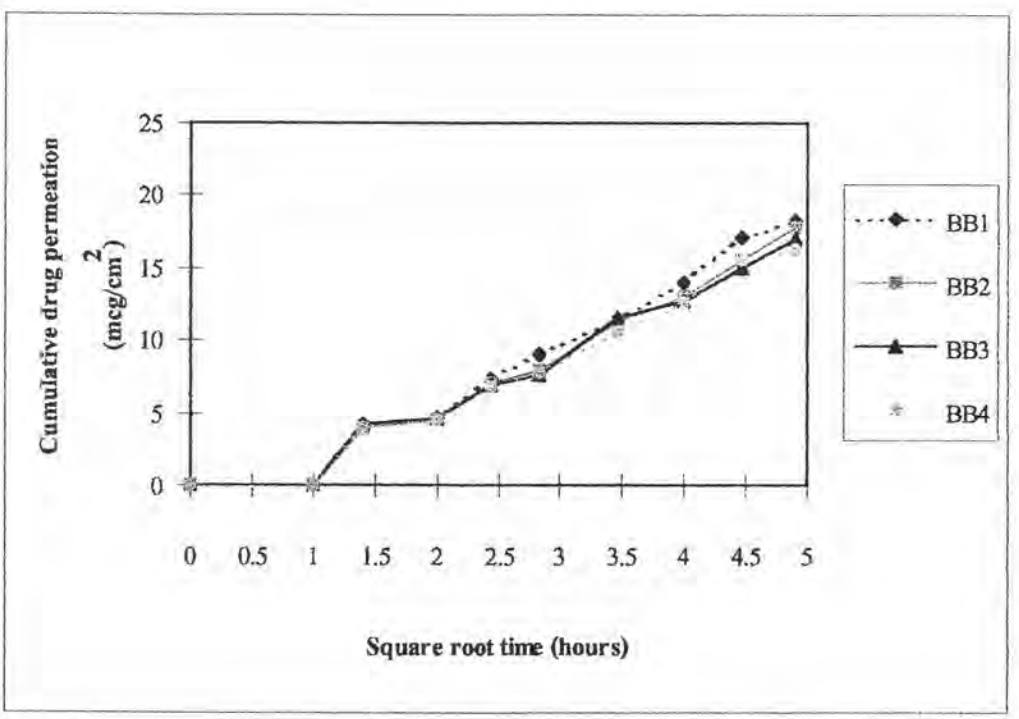

Figure 65 Higuchi's plot of skin permeation-square root of time profiles of terbutaline sulfate transdermal patches (Formulations BB_1-BB_4)

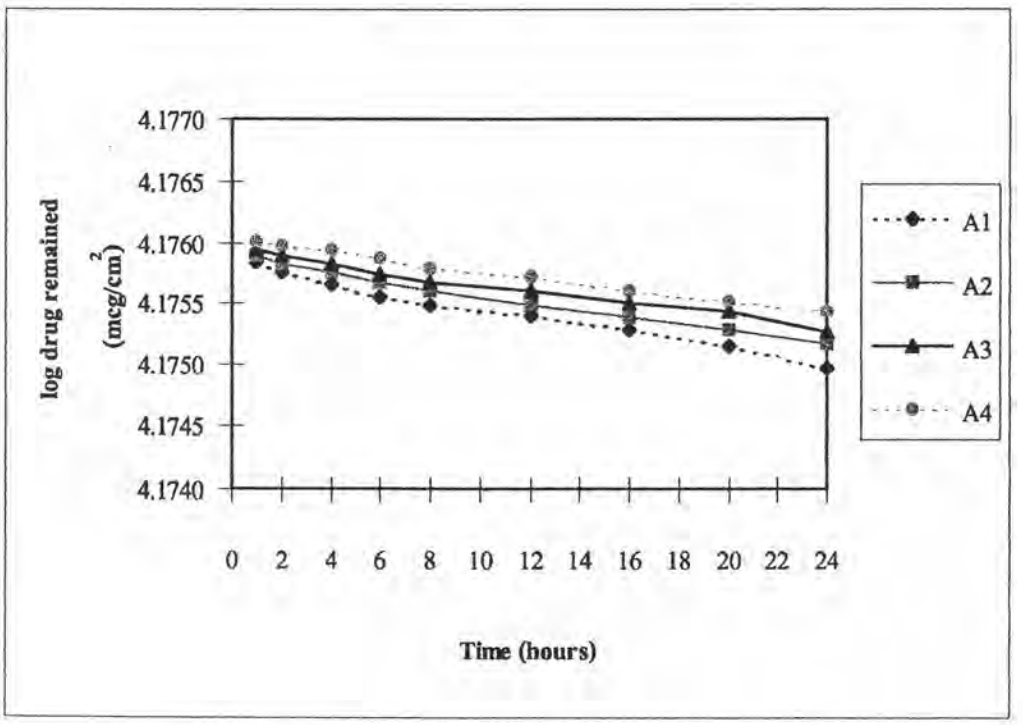

Figure 66 First order plot of log drug remained-time profiles of terbutaline sulfate transdermal patches (Formulations A_1-A_4)

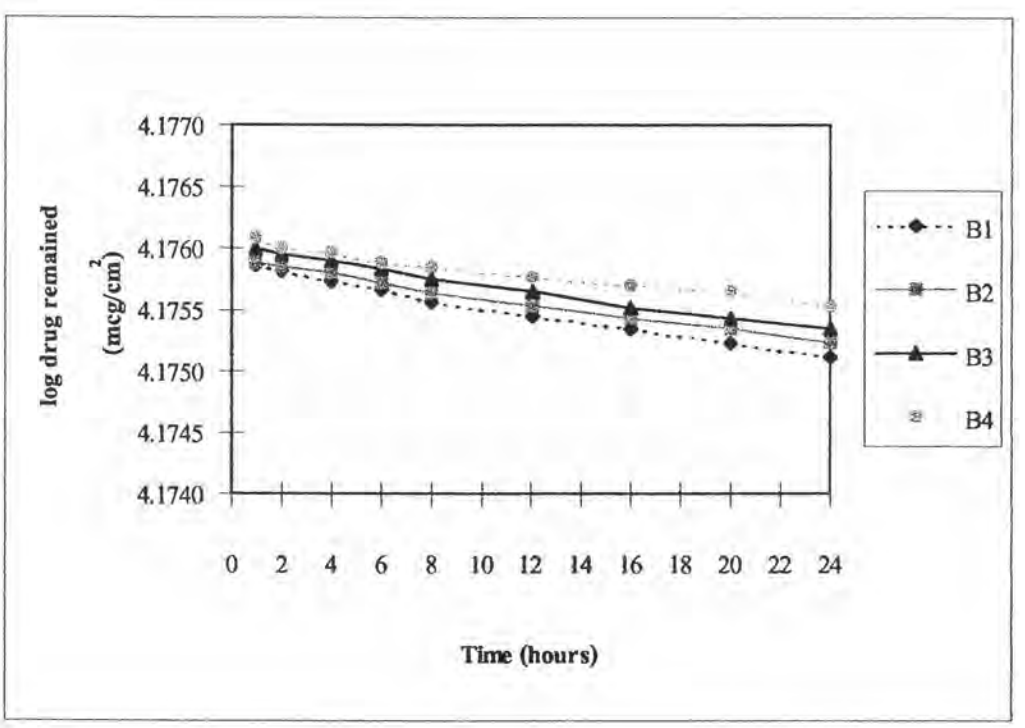

Figure 67 First order plot of log drug remained-time profiles of terbutaline sulfate transdermal patches (Formulations B_1-B_4)

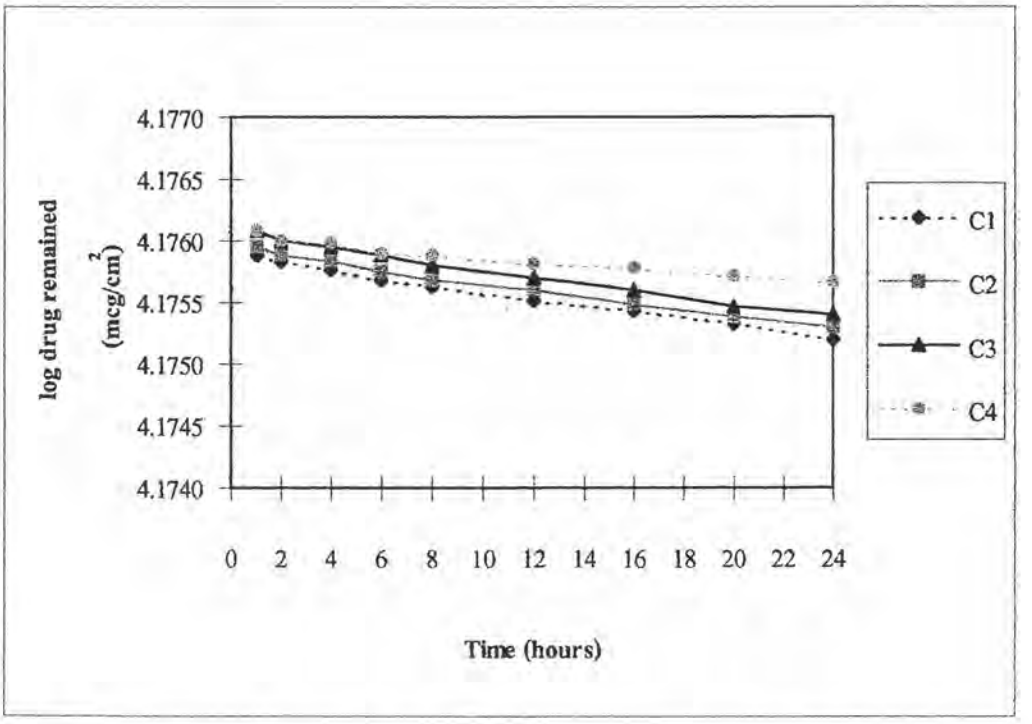

Figure 68 First order plot of log drug remained-time profiles of terbutaline sulfate transdermal patches (Formulations C_1-C_4)

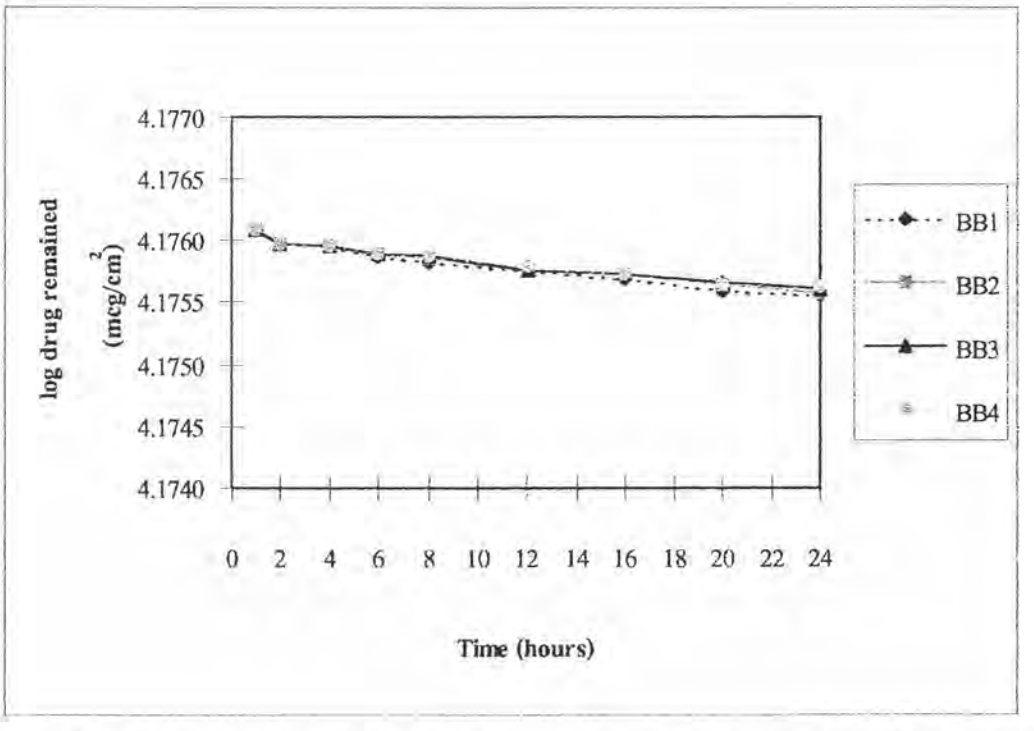

Figure 69 First order plot of log drug remained-time profiles of terbutaline sulfate transdermal patches (Formulations BB_1-BB_4)

Table 23 Correlation coefficient and regression equation of the relationships between cumulative permeated terbutaline sulfate against time (A), cumulative permeated terbutaline sulfate against square root time (B) and log terbutaline sulfate remained against time (C)

Formulation	A		B		C	
	Correlation coefficient	Regression equation	Correlation coefficient	Regression equation	Correlation coefficient	Regression equation
A_1	0.9845	y=1.2020x+9.4348	0.9795	y=7.2119x+0.5993	0.9846	$y=-3x10^{-5}x+4.1758$
A_2	0.9908	y=1.0405x+7.2591	0.9906	y=6.2588x-0.4355	0.9908	$y=-3x10^{-5}x+4.1759$
A_3	0.9826	y=0.9184x+5.5181	0.9803	y=5.5181x-1.2558	0.9827	$y=-3x10^{-5}x+4.1759$
A_4	0.9962	y=0.8584x+2.3722	0.9755	y=5.1100x-3.8184	0.9962	$y=-2x10^{-5}x+4.1760$
B_1	0.9913	y=1.1009x+7.8752	0.9903	y=6.6189x-0.2575	0.9913	$y=-3x10^{-5}x+4.1759$
B_2	0.9917	y=0.9797x+6.6840	0.9859	y=5.8762x-0.5115	0.9918	$y=-3x10^{-5}x+4.1759$
B_3	0.9935	y=1.0057x+2.7586	0.9845	y=6.0226x-4.5996	0.9935	$y=-3x10^{-5}x+4.1760$
B_4	0.9856	y=0.7076x+2.2335	0.9825	y=4.5531x-4.1568	0.9857	$y=-2x10^{-5}x+4.1760$
C_1	0.9909	y=0.9861x+7.1978	0.9862	y=5.9177x-0.0543	0.9910	$y=-3x10^{-5}x+4.1759$
C_2	0.9919	y=0.9568x+5.2809	0.9898	y=5.7494x-1.7775	0.9920	$y=-3x10^{-5}x+4.1759$
C_3	0.9917	y=0.9751x+1.4089	0.9871	y=6.2698x-7.3822	0.9917	$y=-3x10^{-5}x+4.1761$
C_4	0.9769	y=0.4871x+3.0661	0.9724	y=3.8106x-3.9966	0.9766	$y=-1x10^{-5}x+4.1760$
BB_1	0.9846	y=0.6709x+3.0618	0.9835	y=4.3213x-3.0110	0.9846	$y=-2x10^{-5}+4.1760$
BB_2	0.9894	y=0.6378x+2.8143	0.9832	y=4.0973x-2.9248	0.9894	$y=-2x10^{-5}x+4.1760$
BB_3	0.9826	y=0.6001x+3.0455	0.9793	y=3.8612x-2.3730	0.9826	$y=-2x10^{-5}x+4.1760$
BB_4	0.9851	y=0.5942x+2.9100	0.9823	y=3.8240x-2.4578	0.9851	$y=-2x10^{-5}x+4.1760$